Evolutionary palaeobiology of deep-water conodonts

Caroline J. Smith

University of Durham

Evolutionary Palaeobiology of Deep-water Conodonts

PART II

GROWTH & PALAEOECOLOGY OF DEEP-WATER CONODONTS

By

Caroline J. Smith

A thesis submitted in partial fulfilment of
the requirements for the degree of Doctor of Philosophy

Department of Geological Sciences
University of Durham
October 1999

PART II CONTENTS

1. GROWTH AND PALAEOECOLOGY OF DEEP-WATER CONODONTS.

2. GROWTH ANALYSIS OF DEEP-WATER CONODONT GENERA.

3. GROWTH OF CONODONT ELEMENTS.

4. CONCLUSIONS

REFERENCES

APPENDIX 2A

Table of Text-Figures PART II

Chapter 1

Chapter 2

Text-Figure 2.5.2. Shows the biometric plot of dimension a (mm) against dimension b (mm) of the Pa elements of *Periodon aculeatus*. A line has been fitted to the data and the R^2 value is indicated top left.

Text-Figure 2.5.3. The biometric plot of Periodon aculeatus M elements showing dimension a (mm) on the x-axis against b (mm) on the y-axis.

Text-Figure 2.6.1. Element of *Parapachycladina* showing the 3 major incremental breaks and minor incremental patters between, in the crown (drawn from Zhang *et al.*, 1997)

Text -Figure 2.8.1. Basic structure of a coniform conodont element showing the relationship of the crown, basal body and white matter and demonstrating the simple 'cone-in-cone' style structure of simple conodont elements (drawn from Sansom, 1992).

Text-Figure 2.9.1. Shows a scanning electron microscope image of the basal cavity of *Drepanodus* (specimen 692/14) and the incremental lines in the crown. MaI shows the positions of major incremental lines (scale bar botttom left = 100µm).

Text-Figure 2.9.2. High magnification SEM image of *Drepanodus* (specimen 692/14) shown by boxed area in Figure X. MaI = major increment and MiI = minor increment (Scale bar = 20µm).

Text-Figure 2.10.1. Fischer plot constructed from the minor increment width as observed in *Drepanodus*. N.B. Cycle number 1 represent the first formed increment, successively higher numbers represent later additions. Cumulative thickness values (y-axis) are in microns. Vertical lines delimit major increments.

Text-Figure 2.11.1. Plot of raw thickness against increment number in *Drepanodus* where 1 is the oldest increment and 16 is the youngest or last formed.

Text-Figure 2.12.1. SEM image of *Protopanderodus* pf element (specimen 667/21) showing growth increments at the basal cavity (scale bar = 200 µm). Boxed area represents the position of the image for Text Figure Y.

Text-Figure 2.12.2. High magnification SEM image of *Protopanderodus* element showing the nature of the major and minor lamellae sets (scale bar = 50µm)

Text-Figure 2.13.1. Fischer plot of the minor increment widths of *Protopanderodus* (667/21). Vertical lines show major incremental lines.

Text-Figure 2.14.1. Growth curve for *Protopanderodus* (667/21) using raw thickness of major increments plotted against each individual increment.

Text-Figure 2.15.1. Tracing of the enamel microstructure in *Protopanderodus* (specimen 979912D). The specimen is orientated with the inner edge down. Increment thickness measured for both the inner and outer sets from the midline (dashed line) of the element to the edge.

Text-Figure 2.16.1. Top. Fischer plot for the inner minor increments of specimen (979912D) Bottom. Fischer plot of outer minor increments in *Protopanderodus* specimen (979912D).

Text-Figure 2.17.1. Major increments in *Protopanderoudus* specimen 979912D. Major increment dicontinuities were interpreted from axially compressed images.

Text-Figure 2.17.2. The growth curves based upon the outer (btm) and inner (top) major increment thickness for specimen 979912D figured in Text-Figure 2.15.1.

Text-Figure 2.19.1. Shows the various data sets (authors named) from the growth bands in corals and the extrapolated day length data based on the assumption that the present tidal lag has remained constant throughout the past half-billion years (drawn from Goldreich, 1982)

Text-Figure 2.20.1 Variations in productivity occurring in the central oceans at different latitudinal positions (adapted from Stowe, 1986).

Text-Figure 2.20.2 Calibrated growth plots for *Drepanodus* (specimen 692/14). Dotted vertical lines mark the major increments. The upper diagram shows the proposed correlation between peaks of growth and the marine productivity blooms. The lower diagram shows the inferred positions of the months represented by each major incremental break.

Text-Figure 2.20.3 Calibrated growth plots for *Protopanderodus* (specimen 668/21). The upper shows the inferred position of the spring and autumn bloom which correspond to the peaks of growth.

Text-Figure 2.20.4 Alternative interpretation of the *Protopanderodus* major increment plot.

Text-Figure 2.20.5. Calibrated growth plot for *Protopanderodus* (specimen 979912D) outer major increments

Text-Figure 2.23.1. Photomicrograph illustrating the whole *Periodon* M (110996D) element showing growth increments in both the basal cavity and across the recessive basal margin. Scale bar = 50µm

Text-Figure 2.23.2. Photomicrograph of increments in the basal cavity of the *Periodon* element (110996D) shown in Text-figure 2.23.1. Scale bar = 10µm.

Text-Figure 2.24.1. Fischer plot of the increment thickness data for *Periodon* specimen 110996D (top). Simple growth curve for *Periodon* specimen 110996D. Increment number (first formed =1) on the x-axis plotted against the thickness of the increment on the y-axis (btm.)

Text-Figure 2.25.1. Shows the complete data set for growth increment width of six *Periodon* samples (all M elements) plotted against the increment number (increment 1 is first formed, or youngest increment, increment 10 is the oldest or last formed increment). This figure assumes that growth was initiated at the same time in all elements.

Text-Figure 2.25.2. Growth curves for the incremental thickness of several specimens of the M element of *Periodon aculeatus* listed in Table 2.25. 1 is the first formed (youngest increment).

Text-Figure 2.25.3. The hypotheses for growth –functional cycles in *Periodon*.

Text-Figure 2.26.1. Calibrated *Periodon aculeatus* (specimen 110996D) growth curve.

Text-Figure 2.27.1. Shows the body plan of the benthopelagic Viperfish. Scale bar = ~10 cm (drawn from Stowe, 1986).

Text-Figure 2.27.2. The body plan of the Gulper eel showing the reduced body size but enlarged jaws. Scale bar = ~10 cm (drawn from Stowe, 1986).

Chapter 3

Text-Figure 3.2.1 The components and structure of vertebrate teeth (drawn from Carlson, 1992). A. Shows the lamella structure of the dentine and its relationship to the cementum (left) and the pulp (right). B. Shows the lamella micro-and ultrastructure of the crown enamel and its relationship to dentine.

Text-Figure 3.2.2. The developmental stages of a mammalian tooth (drawn from Carlson, 1992)

Text-Figure 3.3.1. Shows the elements of the dermo-skeleton, both odontodes and the odontocomplex. A. Odontodes from *Plecostomus commersonii*, B. Scales from *Latimeria chalumnae* with odontodes, C. Isolated odontode of a *Latimeria* scale. Shows an osseous basal plate, a pulpar cavity lined by dentine and its thin covering of enamel (or enameloid), D. Vertical section of a scale from *Latimeria* with two successive odontodes, E. Odontocomplex, with three odontodes and F. Three successive stages of development of a dogfish placoid scale (from right to left). Redrawn from Francillon-Vieillot *et al.* (1992).

Text-Figure 3.5.1. The Paraconodont elements a. *Prooneotodus gallatini* with short lamellae progressively added to the base of the element and, c. *Problematoconites* sp. where lamellae are interrupted on the outer side (like 2&3) but continuous on the inner side. The proposed position of the secreting tissue (dashed line) required to build a Paraconodont element (adapted from Szaniawski & Bengtson , 1993).

Text-Figure 3.7.1. The proposed relationship (after Bengtson, 1976) of the conodont element and the secreting tissue.

Text-Figure 3.8.1. Macrostructure of *Cordylodus* showing the relationship between the basal tissue and the crown. Scale bar = 200µm (from Sansom *et al.*, 1992)

Text-Figure 3.8.2. *Microstructure* – SEM image of the lamellar structure of the crown in *Cordylodus* Pander also showing the *ultrastructure* in the form of prismatic crystallites orthogonal to the growth lamellae which run right to left across the picture as shown by the arrow (drawn from Sansom, 1992). Scale bar = 5µm

Text-Figure 3.8.3. *Microstructure* - Globular structure of the basal tissues in *Cordylodus* Pander (drawn from Sansom, 1992). Scale bar = 20 µm

Text-Figure 3.8.4. A. *Macrostructure* of *Panderodus* element showing the relationship between the lamellae tissue, white matter and basal cavity. Scale bar = 200µm. B. *Micro- and ultrastructure* 'Fish-tail' alignment of crystallites in the crown lamellae. Lamellae are shown by the dark lines running diagonally top left to bottom right of the image as shown by the arrow (drawn from Sansom, 1992). Scale bar = 2µm

Text-Figure 3.8.5. The four 'types' of conodont formational patterns *sensu* Donoghue (1998). Drawn from Donoghue (1998)

Text-Figure 3.9.1. Diagram of *Panderodus* element showing the relationship between the crown white matter and basal body and the oblique growth lamellae in the crown tissue.

Text-Figure 3.10.1. The proposed growth stages in an element of *Protopanderodus* showing the initial phase of growth producing the "Proto-element" and the subsequent alternation of growth and

functional phases producing the adult element. Shaded grey areas indicate the epithelium or enamel secreting tissue.

Text-Figure 3.13.1. The general relationship between the hard tissues of a coniform conodont element.

Text-Figure 3.13.2. The proposed tissue association necessary to produce a conodont element with 'cone-in-cone' lamellar crown tissue, a core of white matter and lamellar/spherultic basal tissue.

Text-Figure 3.13.3. Formation of conodont elements in a differentiated mesodermal dental papilla. The cells producing the conodont element components (grey = epidermal tissue, upper and lower mesodermal \components are indicated). Arrows show direction of mineralisation of all three component tissues. The initial formation of the lamellar hard tissues of the conodont element so the crown builds up by outward accretion and the white matter forms a continuous core. The basal body grows in an opposing direction to the crown.

Text-Figure 3.13.4. Function, non-growth and growth non- function in conodont elements. 1. The element is surrounded and enveloped by epidermal tissue as formation continues 2. The epidermal tissue starts to sink and the element is functional. The cellular contacts are maintained with the mesodermal tissue. 3. Element is fully functional. 4. Envelopment by epidermal tissues and subsequent periodic enamel secretion.

Chapter 4

Text-figure 4.1. The conceptual model for conodont life strategies.

List of Tables Part II

Chapter 2

Chapter 3

Part II – Chapter 1

1. Growth and palaeoecology of Deep-water conodonts.

1.1 Structure

Part II, Chapter 1 forms the introduction to Part II and provides a brief review of the modern deep-sea conditions in order to assess the environmental factors affecting this environment and the subsequent effect these factors have on deep-sea organisms.

Part II, Chapter 2 reports the data collected from the analysis of growth in middle Ordovician deep-water conodont genera, *Drepanodus*, *Protopanderodus* and *Periodon* and, further discusses the initial implications and conclusions that this data set provides.

Part II, Chapter 3 reviews the studies of growth models in vertebrate teeth, odontodes, scales and conodonts and further acts to synthesise a model for conodont element growth and function (to include both rate and timing as assessed from the results in Chapter 2).

1.2 Aims

The majority of studies in conodont palaeobiology have, to date, been undertaken on shallow-water taxa. The following chapters focus on the Middle Ordovician deeper water conodonts of the North Atlantic Realm. Part II therefore has the following aims: -

1. To review the physical characteristics of the deep-sea environment in order to highlight the environmental processes acting on deep-sea conodonts.
2. To compare deep-sea conodont growth with previous growth studies and evaluate the differing effects of ecology on growth.
3. To review conodont growth studies; particularly the rate, timing and mechanisms of conodont element growth.

1.3 Introduction

During the Ordovician, conodonts were markedly provincial and ecologically diverse, ranging from shallow to abyssal depths (e.g. Sweet, 1988, Sweet & Bergström, 1984). The fossil record of deep-water conodonts thus provides an opportunity to study physiological and evolutionary processes operating in the oceanic realm. Conodonts were the first vertebrates to produce a mineralised skeleton and genera such as *Protopanderodus* and *Periodon* (as will be discussed in Part II) were some of the first animals to inhabit the deep-sea environment.

Global oceanography shows responses to variations in climate (Armstrong, 1996). A number of models for Early Palaeozoic oceans have been proposed which demonstrate a link through the carbon-cycle between ocean-state and global climate (Aldridge *et al.* 1993b, Jeppsson, 1990, Armstrong, 1996).

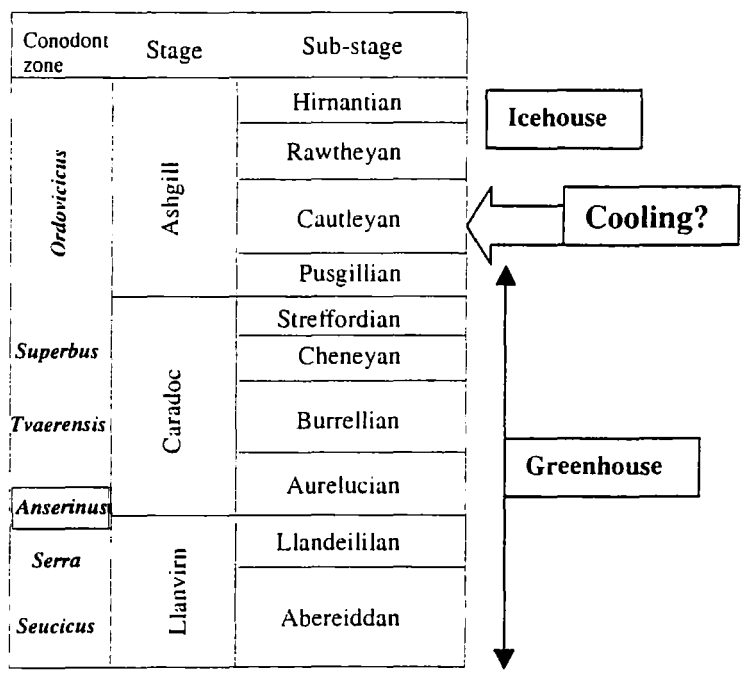

Text-Figure 1.3.1. Stratigraphy of part of the Ordovician (Llanvirn – Ashgill) showing the proposed stratigraphical position of the *anserinus* zone fauna and the positions of warm and cold phases as referred to in the text. The *Protopanderodus*, *Drepanodus* and *Periodon* samples analysed are from this middle Ordovician conodont zone (stratigraphy based on Fortey *et al.*, 1995)

Frakes *et al.* (1992) indicated the Earth reverted to a warm mode following termination of the end-Precambrian glaciation. This lasted to the end of the Ordovician being terminated by the return of thermohaline circulation and the onset of glaciation in the Late Ordovician (Frakes *et al.*, 1992, Armstrong, 1996, Text-figure 1.3.1.).

The middle Ordovician deeper-water conodonts inhabited a warm-mode or greenhouse state ocean significantly different from those of the present day. Part I of this thesis demonstrates a strong link between changes in ocean conditions and the behaviour of conodont biofacies. Part II is focussed on the growth of deep-water conodonts in a greenhouse setting.

1.4 The deep-sea

The deep-sea is the most typical environment on the Earth and 92% of the water surface on the earth extends beyond the shallow margins of the continents. Most of the Earth's surface is therefore under two or more kilometres of water. The deep-sea environment has long been of interest to marine biologists, although its remote nature has led to difficulties in sampling its inhabitants. Equally, the physical and chemical conditions of the deep ocean are poorly known.

To understand fully the controlling factors on the growth of deep-sea conodonts it is fundamental to document how the physical characteristics of the deep-water environment may affect the biological responses of the animal. Work, mainly on invertebrates, has shown animals record environmental rhythms in their hard tissues during their ontogeny (see Scrutton, 1973 for a full review). Different organisms will respond differently to environmental fluctuations depending on the habitat, rate of growth and detailed skeletal structure (Scrutton, 1973).

The shallow-marine environment is highly variable so shallow-water organisms are subject to large variations in light, temperature, tides, seasonality, sea-level and nutrient availability (Scrutton, 1973). It is fundamental when studying shallow-marine faunas to consider the variables that may affect whole organism growth in this environment. As a result of superimposed environmental variables, it can be difficult to make interpretations about the primary controls on growth in

shallow-water conodonts or other organisms. The deep-sea, in contrast provides a relatively stable environment that is not influenced by lunar affects, temperature, salinity, and pressure fluctuations. Consequently, the complex interactions of environmental variables found in shallow water should be minimised and the ecological controls on growth more easily elucidated.

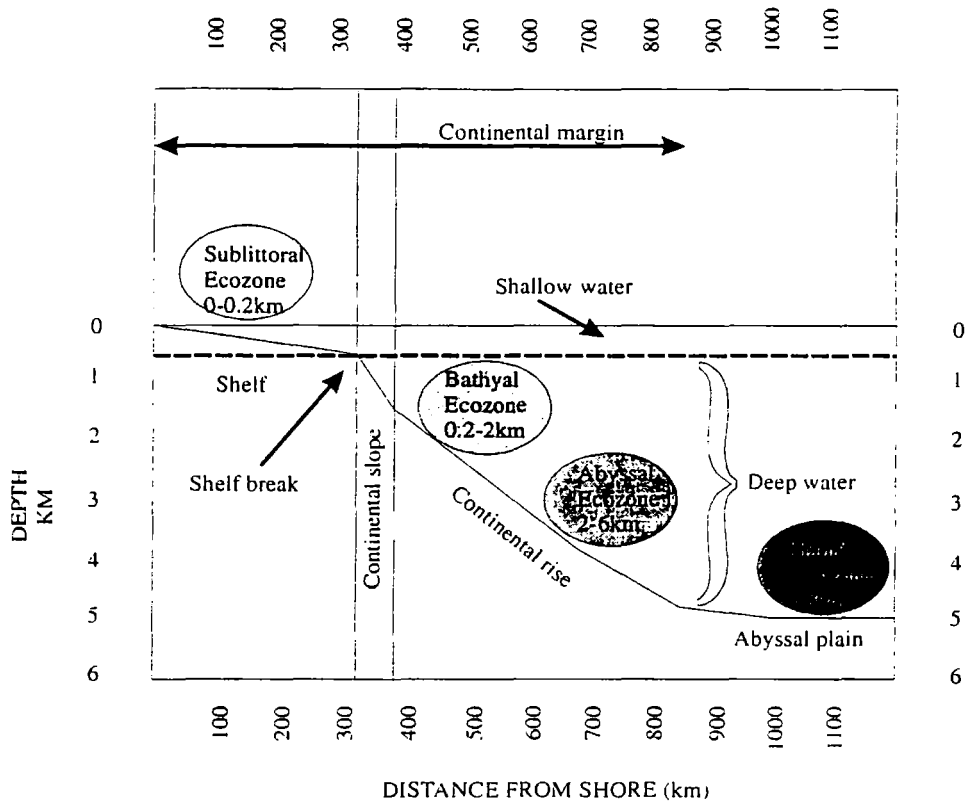

Text-Figure 1.4.1. Schematic cross section across a typical continental shelf to deep-sea profile. Boxed, shaded text shows the ecological zones into which the oceans can be divided (redrawn from Gage & Tyler, 1991).

In terms of hydrography the deep-sea is usually considered to be the region lying below 200metres water depth. However, in topographical terms, the deep-sea starts at the edge of the continental shelf (Text-figure 1.4.1.). Furthermore, the marine environment can be divided into a number of distinct ecological zones. These are described on the basis of the depths at which they occur. The sublittoral or intertidal ecozone describes the area in the water column up to approximately 0.2km

in depth. Deeper zones include the bathyal ecozone (0.2km – 2km), the abyssal ecozone (2-6km) and the hadal ecozone (>6km). The positions of these 'ecozones' are shown on Text-figure 1.4.1.

The permanent thermocline describes the transitional layer within the water column where the water temperature decreases rapidly as the depth increases. The temperature decreases rapidly until it reaches a value below 4° C. From this level downwards the temperature gradient becomes very small (see Text-figure 1.4.2). In most of the worlds oceans today, this more stable temperature regime is at 0.8-1.3km depth. This can vary, for example, in the North Atlantic where the Mediterranean outflow at intermediate depths depresses the 4° C isotherm to a depth of approximately 4km. As a result, the waters above the thermocline are heated and mixed and the permanent thermocline forms a barrier between the deep and surface waters. The deep ocean is, in effect, now isolated from the direct effect of surface parameters. At mid-latitudes, the upper mixed layer is deeper (as a result of mixing by increased wind stresses) and the position of the permanent thermocline is deeper in the water column. At high latitudes, the water masses become increasingly isothermal which alters the position of the permanent thermocline.

Until 30 years ago, the oceans below the permanent thermocline were widely considered to be chemostatic, showing very little temporal or spatial variation (Menzies, 1965). This generalised view has however been modified by recent research into the deep-sea environment. In surface ocean waters, the temperature, salinity and density vary with latitudinal position. Such surface water variations have a consequence to the physical characteristics of deep-ocean water, as the bulk of the world's deep-water masses are formed at or near the surface. The surface waters of the ocean with time will sink at a level of neutral buoyancy and still carry the characteristics acquired during their formation. Slight changes in these characteristics may occur during or after sinking by processes such as mixing with neighbouring masses, respiration of organisms and hydrothermal vent activity (Stowe, 1996). The overall affects of such changes are however masked by the large volume of deep-sea waters.

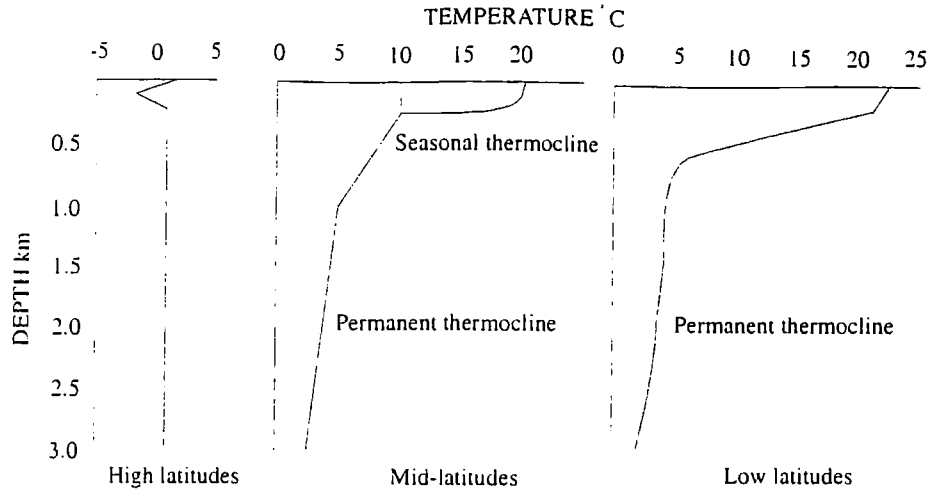

Text-Figure 1.4.2. The position of the permanent thermocline in relation to latitude, (drawn from Gage & Tyler, 1991)

Recent research into the deep-sea environment has revealed that a degree of heterogeneity does exist. Deep-sea storms, analogous to those on the land, profoundly affect temperature and bottom conditions over short distances. Differences in substrate consistency occur in deep-water environments and this environment is now considered to consist of small patches that vary with time (Gage & Tyler, 1991). These temporal variations include the seasonal arrival of surface-derived photodetritus at the deep-sea floor; a process observed to occur in many parts of the world's oceans (Tyler, 1988; 1995).

The temperature of the waters of the modern deep-sea varies from 4° C to -1° C (Gage & Tyler, 1991) although in modern oceans such as the Mediterranean and the Red Sea the temperatures can be considerably higher (13°C between 0.6 and 4km; 21.5°C at 2km respectively). The lowest temperatures (-1.9°C) are found in the deep waters of the Antarctic (Gage & Tyler, 1991). Salinity remains almost constant below 2km (Gage & Tyler, 1991) with values between 34.5‰ and 39‰ (Tyler, 1995; Stowe, 1996). Such a narrow range in salinity is though to have little effect on the deep-sea benthos (Tyler, 1995). Oxygen values are near saturation in most modern day deep-waters (e.g. deep North Pacific, oxygen concentration 3.6ml l^{-1}; Mantyla & Reid. 1983). In most of the open-sea areas, the bottom waters are oxygenated and the *in situ* oxygen value present at the time the block of water was at

the surface is subsequently reduced by the benthic fauna and microbiota (Tyler, 1995). As a result, deep waters of the North Atlantic and Antarctica have the highest oxygen concentration at the present day (6-7 ml l^{-1}). As deep-water masses move further from their source, these oxygen levels may be depleted by metabolic processes and therefore, the waters of greatest sub-surface age in the North Pacific have oxygen values of <3.6ml l^{-1} (Mantyla & Reid, 1983). Tyler (1995) inferred that despite these low oxygen values, no organisms at even abyssal plain depths will suffer anoxic conditions, except for occasional, highly localised effects. Totally anoxic conditions can also occur in areas of modern oceans but usually only at the intermediate exit area of hydrothermal vents and as this reduced water from the vents mixes with the surrounding water the oxygenation level will rapidly increase away from the vent itself (Tyler, 1995).

The pressure increase associated with depth in the water column represents the longest continuous environmental gradient on the Earth (Tyler, 1995). Hydrostatic pressure in the oceans increases at a rate of one atmosphere (1 bar or 10^5 Pascal) per ten metres increase in depth (Gage & Tyler, 1991). Pressure has been invoked as exerting a control on the distribution of deep-sea invertebrate embryos therefore, exerting a further control on the vertical distribution of individual species (Young & Tyler, 1993). Higher taxa such as crustaceans, anemones and echinoderms, do not occur below 6000m depth (Tyler, 1995) whereas polychaetes appear to be abundant below this level. This pressure level (~ $6x10^7$) has been invoked (Tyler, 1995) to explain the decrease in diversity seen in the higher taxa at increasing depths.

Greenhouse ocean models predict deep-sea anoxia and salinity stratification (Aldridge *et al.*, 1993b, Jeppsson, 1990, Armstrong, 1996). It is likely that the very deepest waters of the middle Ordovician oceans were anoxic because of the lack of circulating, cold deep-ocean currents. Ocean state models (Jeppsson, 1990) predict the existence of two end-members, S-State and P-State oceans. The former describes the poorly ventilated conditions of a greenhouse ocean with salinity stratification and anoxic deep-water conditions. P-state oceans are more characteristic of the modern conditions in the North Atlantic where dense cold oxygenated waters descend into the deep-oceans.

Distributions of ecozones in the middle Ordovician oceans must therefore have differed from those of modern oceans. Instead of a thermocline barrier in the water column models predict a well-developed pycnocline (a region where the density of the water varies quickly with depth). Although the distribution of ecozones would have been similar in continental slope and shelf areas, the anoxic deepest waters in the Ordovician oceans would have been uninhabited. Despite this, the water column of the middle Ordovician oceans would still be subject to the same constant increase in pressure, although salinity levels would increase with depth.

Therefore, deep-water, off-slope environments are subject to low and invariant temperature conditions, lack of tidal influences and high pressures. In the absence of environmental factors that control the growth of organisms in shallow water organisms, deep-water organisms should show fluctuations in growth controlled by factors such as variations in nutrient availability.

1.5 Nutrient fluxes to the deep-sea

The importance of the following section is to show that nutrient availability is potentially the primary control on the growth, reproduction and life strategies of deep-sea faunas (Gage & Tyler, 1991). The majority of modern deep-sea vertebrates show behaviour and growth synchronised with nutrient input into the deep-sea, which at mid-temperate and sub-tropical latitudes occurs during the spring and autumn blooms in phytoplankton productivity (Tyler, 1988; Gage & Tyler, 1991).

The main source of organic material for heterotrophy comes from production in the photic zone of the ocean. The environmental conditions of the deep-sea are affected as a result of this primary production in the surface layers and its subsequent downward vertical flux to the deep-sea bed. Research has shown the modern deep-sea to be a heterotropic system with autochthonous primary production being confined to areas of cold seep and hydrothermal activity (Tyler, 1995). Seasonal inputs of organic matter to deep-waters are mainly in the form of organic aggregates (Tyler, 1988) which fall to the deep seas as a 'rain' of small particles. The productivity in surface waters varies with latitudinal position. At tropical latitudes, surface productivity in central ocean regimes is low due to lack of available nutrients. At high latitudes although upwelling results in a high nutrient level,

sunlight is not sufficient to cause high productivity throughout the year. Temperate oceans show distinct seasonality in surface production. During March and April active upwelling promotes the rise of nutrients and sufficient sunlight is available to produce a peak in productivity, known as the spring bloom. As nutrient supplies are used there is a lull in productivity over the summer months despite high sunlight levels. As the surface waters cool in the autumn, a smaller upwelling again brings nutrients to the surface and a smaller autumn bloom is produced. This is short-lived compared to the earlier spring bloom. As days shorten in winter months, although there is a surplus of nutrients, energy levels are not sufficiently high to promote high productivity levels.

Sediment trap studies (Dueser, 1986) showed that only 1% of surface primary production reached the abyssal sea-bed. Other estimates state (Tyler, 1988) that between 1-3% of primary production from the surface reached the deep-sea floor where it was postulated to provide the main source of energy for deep-sea biota. Tyler (1995) later stated that the proportion lost decreased in shallower water so that bathyal depths (as shown in Text -figure 1.4.1) received a higher proportion of all the surface primary production.

Research has therefore confirmed the presence of 'pulses' of phytodetritus from the surface into the deep seas (Lampitt, 1985; Theil *et al.*, 1989 and Tyler, 1988). Although significant responses to these pulses are seen at bacterial, micro- and meiofaunal levels (Gooday, 1988; Jumars *et al.*, 1990), the benefits of this at macro- and megafaunal level are still largely under debate by marine biologists. Seasonal flux has also been observed in organic carbon, carbonate, lithogenic particles, sugars and amino acid levels in modern day deep-sea settings (see review in Tyler, 1988). These peaks were bimodal with maximum peaks in both June/July and February/March.

In addition to seasonal nutrient pulse to the deep-sea, marine biological studies have predicted that the seasonal variations in ocean currents at abyssal levels may also have an effect on the ecology (Dickson *et al.*, 1986). Although the full ecological implications of ocean current variations are largely unknown at present, it was predicted that an increase in kinetic energy may influence the spawning of deep-

sea species indirectly by a rapid transmission of spawn inducing substance (Gage & Tyler, 1984).

The primary control on an organism's life cycle, life-strategy and behaviour in deep-water environments at the present day and during the middle Ordovician would appear to be nutrient availability.

1.6 Growth of deep-sea organisms

Because of the presumption of vast constancy in the deep-oceans, growth banding in deep-water invertebrates had been largely ignored. Zezina (1975) was the first to document the presence of 6 growth bands in a deep-sea brachiopod (*Pelagodiscus atlanticus*) which she/he postulated may have reflected seasonality of growth. Subsequent studies on the skeletal plates of echinoderms have also revealed patterns of growth best explained by seasonal periodicity (Gage & Tyler, 1991).

It has also been postulated that due to the extreme conditions deep-sea organisms will possess a greatly reduced physiology and growth rate in comparison to those occupying shallower environments (Gage & Tyler, 1991). High pressure, low temperature environments have been shown (Somero *et al.*, 1983) to affect the rates of enzymatic catalysis in deep-sea organisms. Biochemical reactions in living organisms are temperature related and metabolic rates decrease by a factor of 2 to 3 for each 10°C drop in temperature (DeVries & Eastman, 1981).

Additionally, it has been proposed that due to reduced physiology there will be a shift towards smaller organism size in the deep sea. Theil (1975) described the deep sea as a small organism habitat and proposed that with increasing depth and decreasing food concentration, small animals gain importance in total community metabolism. For example, the deep-sea micro-nektic fish genus *Cyclothone* has species with body lengths between 20 and 70 millimetres and is ubiquitous in meso- and bathypelagic depths (200-2000m). Furthermore *Cyclothone* is claimed to be the Earth's most abundant vertebrate. Alternatively, Mosely (1880, Challenger expedition) was the first to observe that, whilst some deep-sea organisms appeared dwarfed by conditions, some attained gigantic proportions. This led to an early assumption that food limitation does not necessarily lead to a predominantly dwarfed

fauna. Such 'giantism' may be linked to the metabolic affects resulting from the high hydrostatic pressure or delayed sexual maturity (Gage & Tyler, 1991). In modern oceans, as a generalisation, giantism is seen more in opportunist megafaunal scavengers whereas dwarfism is more likely to be seen in the deposit feeding macrofauna (Gage & Tyler, 1991).

In light of the data and evidence provided for seasonal behaviour and growth in the modern deep-sea organisms it is important to assess whether similar environmental controls were operating in the mid-Ordovician. Furthermore, because seasonal growth is not seen across examples of all deep-sea organisms, this leads to questions about why this it is marked in only specific examples (Tyler, 1988). The implication therefore, is that different organisms must maintain and store their energy in different ways, maybe by exploiting widely different feeding strategies within the deep-biosphere.

The deep-sea environment is therefore not homogeneous as once assumed, and its inhabitants are subject to imposed conditions such as high pressure and to additional environmental fluctuations. Furthermore, the deep-sea is an area of high abundance and diversity despite the conditions it imposes on its inhabitants.

By way of comparison, it is important to note that growth in deep-sea fish has been attributed to various factors (Panella, 1971). Both scales and otoliths are widely used to determine the growth of fish although scales may not be an accurate means as scale growth can often cease during stressed conditions such as food deprivation (Campana & Neilson, 1985). Otoliths are calcified baro-receptors that occur in the inner ear of many organisms including most species of fish. Unlike scales they are not subject to frequent alteration or resorption once formed (Radtke & Kellermann, Wright *et al.*, 1997).

Otoliths show incremental structures believed to form over regular time scales ranging from sub-daily to annual (Wright *et al.*, 1997). It has been postulated that growth of otoliths may be related to environmental factors such as feeding and fluctuations in temperature (Campana & Neilson, 1985). However, similar growth increment patterns have been observed in both shallow and deep-water fish despite the lack of daily feeding and light rhythms acting on the latter. An alternative to explain this, is that growth in otoliths is fundamentally controlled by physiological

stimuli such as an endogenous circadian rhythm. In this case, if there were no additional entraining stimuli then secretion of the otolith would be expected to continue growing and displaying the same pattern. However, it is believed that prolonged absence of entraining stimuli would result in a change from the daily depositional rate (Wright *et al.*, 1997).

To test these hypotheses, a number of environmental manipulation studies on fish were conducted which showed a continued daily rate of increment deposition in the absence of entraining stimuli such as cyclical variations in light, temperature or feeding (Campana, 1984; Radtke & Dean, 1982; Wright *et al.*, 1991). However, these studies neither proved nor disproved the theory of endogenously related cycles in otolith formation, and other workers (Campana & Neilson, 1985) suggested that the endogenous circadian rhythm controlling accretion could be entrained by photoperiod activity but masked by sub-daily temperature or feeding cycles.

A comprehensive study using fish otoliths as growth rate indicators was conducted and described by Campana and Neilson (1985) who documented seasonal effects on the growth rates of deep-sea fish. They noted the presence of compressed increments in the region corresponding to the winter period and found some too closely spaced to identify discrete increments. This suggests that vertebrate growth can dramatically slow during the winter period and reinforces the inference of temporary growth cessation in deep-water conodont genera.

It is therefore important to note that the fundamental control on conodont growth may be related to a background circadian rhythm, which is ultimately hormone controlled. Furthermore, if 'background' conodont growth could also be adequately related to photoperiod activity then theoretically it would be possible to distinguish between conodonts with evolutionary origins in either shallow or deep-seas.

In the past, the majority of conodont growth studies have concentrated on the analysis of derived conodont taxa from the shallow-marine environment. This study represents the first analysis of the growth of deep-water (>200 metres) conodont taxa.

Part II – Chapter 2

2. Growth analysis of deep-water conodont genera

2.1 Introduction

Conodonts were primitive marine agnathan vertebrates ranging from the late Cambrian to the latest Triassic (Aldridge *et al.*, 1993, Gabbott *et al.*, 1995, Aldridge & Purnell, 1996, Donoghue *et al.*, 1998). They bore a complex feeding apparatus which functioned to grasp and process prey items (e.g. Briggs *et al.*, 1983, p.13). This apparatus was the first part of the vertebrate skeleton to be mineralised and was retained through life (Donoghue & Purnell, 1999).

Conodont elements are known to comprise two major parts, the crown and the basal body. The lamellar nature of the crown is well documented (e.g. Pander, 1856; Lindström, 1964; Barnes *et al.*, 1970) and conodont crowns are composed of enamel or a combination of enamel and white matter (e.g. Lindström, 1955, Müller, 1971, Sweet, 1988, Sansom *et al.*, 1992). White matter is currently best regarded as a tissue unique to conodonts (Donoghue, 1998) although it has been interpreted as various types of cellular bone (Sansom *et al.*, 1992), dentine (Donoghue, 1998) or a secondary demineralisation or resorption feature (Lindström, 1955, 1964).

Conodont basal body tissue can have either a lamellar (Donoghue, 1998, fig. 5 [fg], p. 644) or spherultic structure (Sansom, 1992, pl. 8, fig. 6, p.244) homologous to either lamellar dentine (Sansom *et al.*, 1994; Donoghue, 1998); or globular calcified cartilage (Sansom *et al.*, 1992). As with white matter, basal body tissue appears to be highly variable and no consensus has yet emerged as to which vertebrate tissue provides the best homologue.

Conodont animals with soft tissue preservation are known from several localities. These include the Carboniferous Granton Shrimp Bed (Briggs *et al.*, 1983, Aldridge *et al.*, 1986) the Upper Ordovician Soom Shale of South Africa (Aldridge *et al.*, 1993, Gabbott *et al.*, 1995) and the Silurian Brandon Bridge Dolomite in Winconsin (Mikulic *et al.*, 1985, Smith *et al.*, 1987).

These examples represent the three species *Clydagnathus*? cf. *cavusformis* (Globensky) (Text-figure 2.1.1), *Prommissum pulchrum* Kovács-Endrödy and *Panderodus unicostatus* (Branson & Mehl) respectively (Text-figure 2.1.2). Detailed

anatomical studies have shown these animals to have been active swimmers, possessing chevron musculature, asymmetrical fins, paired cephalic organs and a notochord (e.g. Briggs *et al.*, 1983; Aldridge *et al.*, 1986, Gabbott *et al.*, 1995).

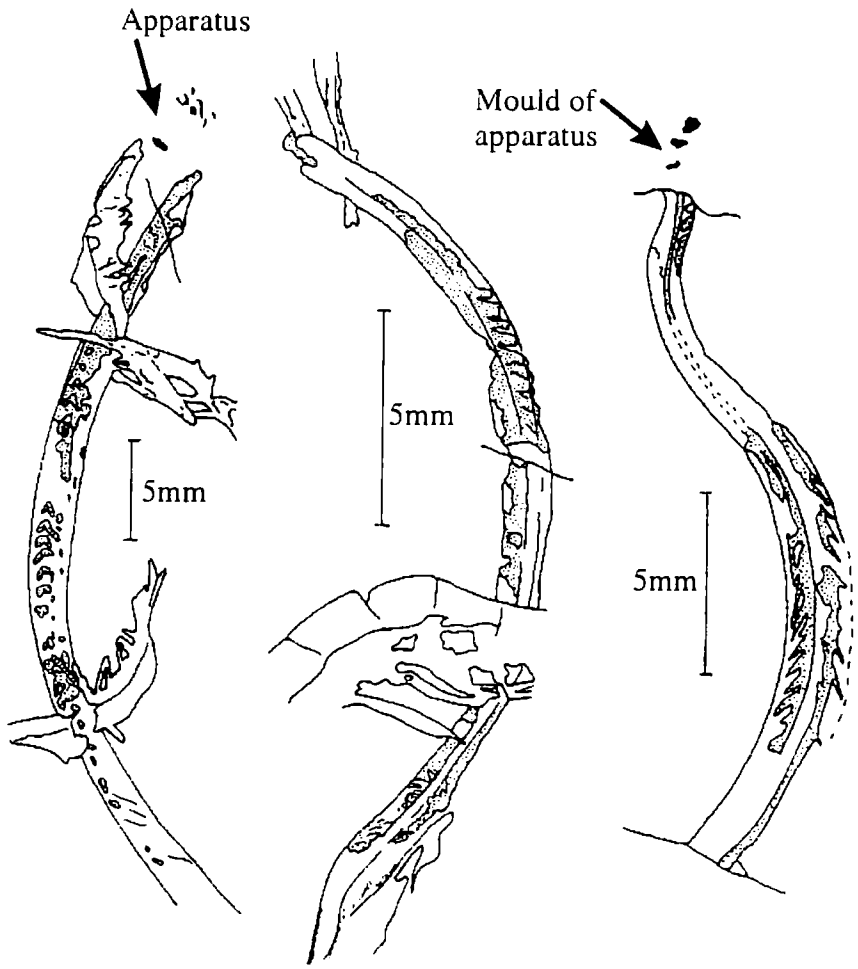

Text-Figure 2.1.1. Diagrams of three specimens of the conodont animal from the Granton Shrimp Bed, Edinburgh, Scotland. Adapted from Aldridge (1987).

The discovery of both coniform and non-coniform conodont animals may have important implications as to the life strategies of different conodont taxa. It is assumed that, because the overall body plan of the coniform conodont animal was dorso-ventrally (rather than laterally) compressed (Text-figure 2.1.2.), this could indicate that it had a pelagic mode of life. This is in contrast to the nektobenthic

mode of life as was postulated for ozarkodinid and prioniodontid conodont species (Smith *et al.*, 1987; Conway-Morris, 1989).

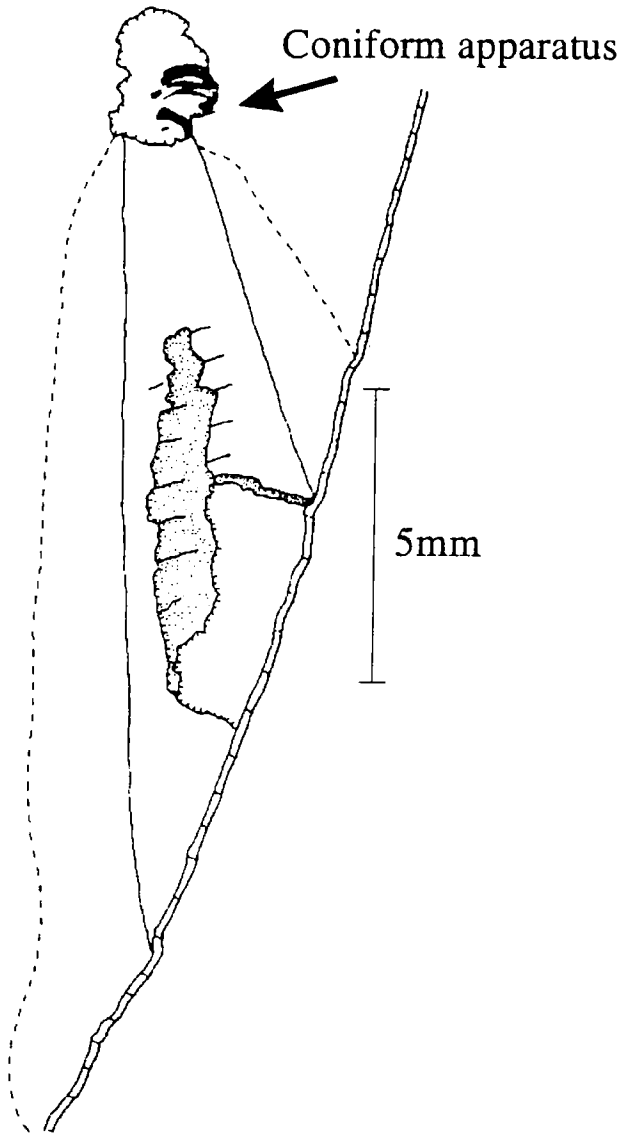

Text-Figure 2.1.2. Camera - lucida drawing of the *Panderodus* conodont animal showing the position of the apparatus and the segmentation in the trunk (drawn from Smith *et al.*, 1987).

2.2 Apparatuses and Function

Conodont elements are now known to be part of a complex multi-element and multi-functional apparatus. Based on his reconstruction for *Ozarkodina*, Jeppsson (1971) proposed a functional paradigm for the apparatus in which the M and S elements were in an anterior position acting as grasping elements, the Pa and Pb elements were in a more posterior position and performed cutting and crushing functions respectively. This has been largely substantiated by 3D modelling of a number of apparatuses (e.g. Aldridge *et al.*, 1987; Aldridge *et al.*, 1995; Purnell & Donoghue, 1997). The various apparatus reconstructions are outlined in the figures below (Text-figures, 2.2.1, 2.2.2 & 2.2.3).

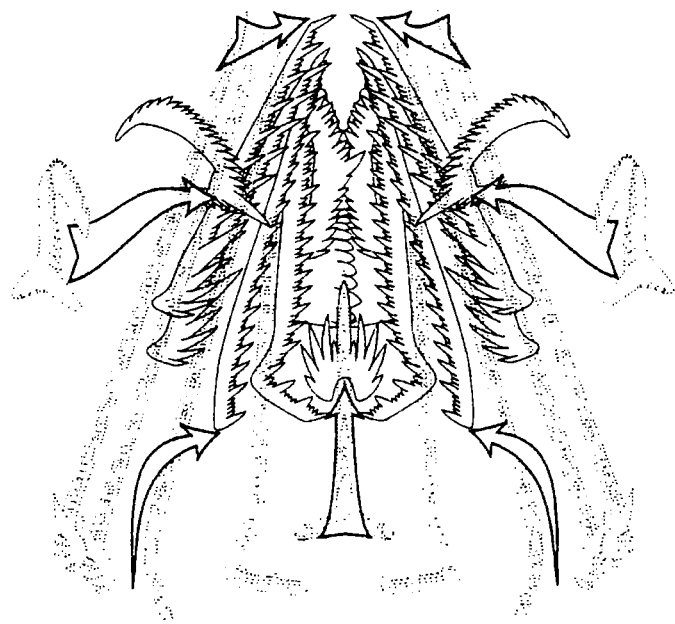

Text-Figure 2.2.1. Anterior view of the 3D apparatus architecture of *Idiognathus*. Elements with dotted lines indicate their proposed everted and functional positions and the arrows show the proposed movement of the S and M elements. Elements shown as solid lines are proposed to indicate the retracted closed position (drawn from Purnell & Donoghue, 1997)

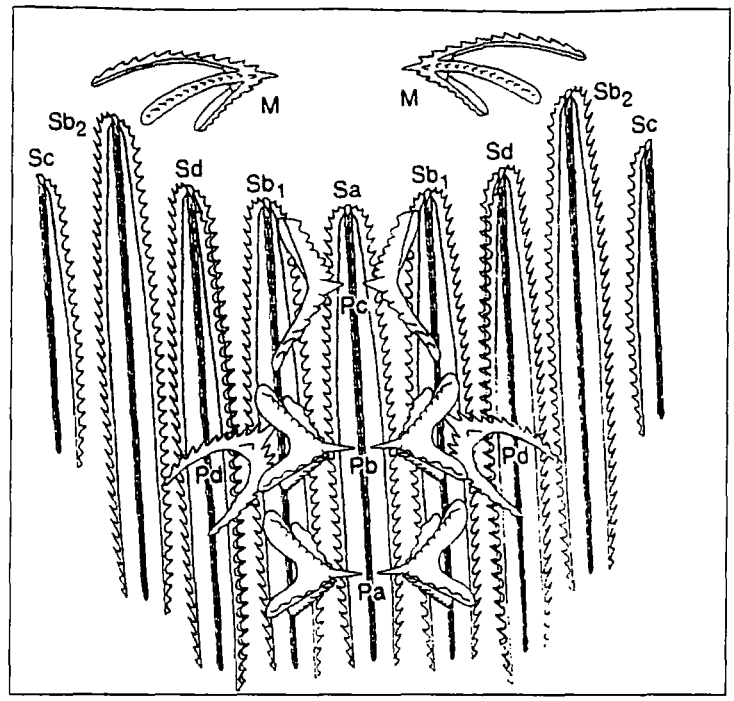

Text-Figure 2.2.2. Posterior view of the proposed apparatus plan of *Promissum pulchrum*. This shows the anterior array of M and S elements and the posterior sets of P elements. It is proposed (Aldridge *et al.*, 1995) that the S elements performed a grasping function and the P elements performed a processing function (drawn from Aldridge *et al.*, 1995).

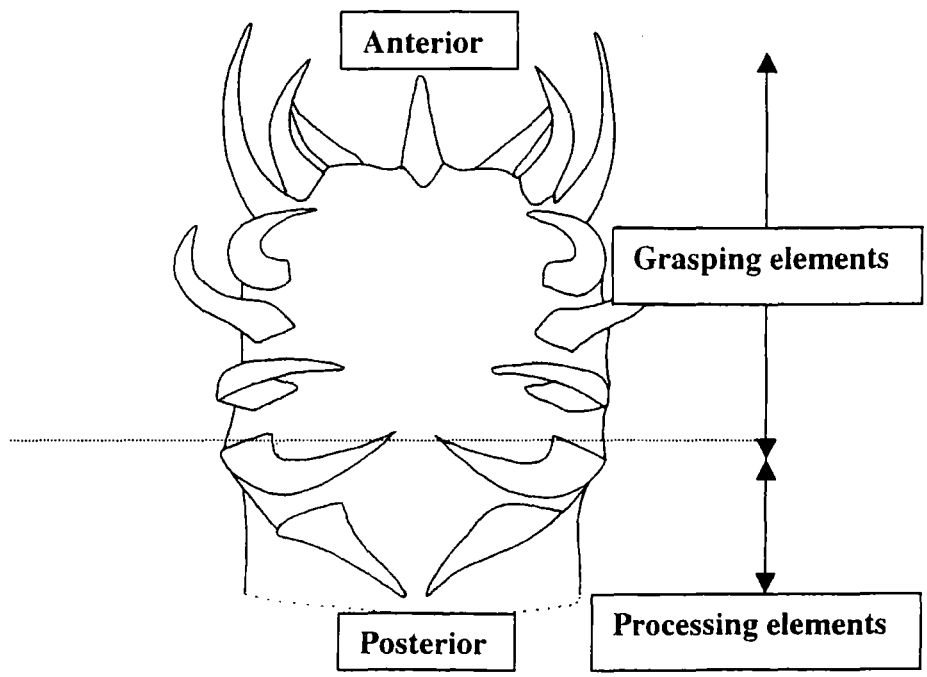

Text-Figure 2.2.3. Ventral view of the schematic representation of the 3D apparatus architecture (in a resting position) of a coniform conodont such as *Panderodus* (adapted from the observations of Sansom, 1992). The proposed functions of the pairs of elements are shown on the right.

The three-dimensional model of the *Ozarkodina* apparatus (Purnell & Donoghue, 1997) and the discovery of wear facets on some conodonts (Purnell, 1995) showed how different suites of element performed different food processing functions. In general, S elements are thought to grasp and process food whereas P elements are believed to perform a shearing function (cf. vertebrate incisors) or a crushing function (cf. vertebrate molars). This work indicated that conodonts were the first macrophagous vertebrates, an observation that refuted earlier hypotheses (e.g. Nicoll, 1985) that conodont elements operated as organs for a filter feeding life-strategy. Previously, Nicoll (1985) had assumed that the elements in the apparatus of *Polygnathus xylus xylus* and *Ozarkodina brevis* were located on the ventral surface in the oral cavity of the conodont animal. He postulated that each element was covered in a ciliated tissue serving both to secrete the hard tissues and move water (and therefore food particles) over the apparatus to assist feeding.

Therefore, in summary, conodont elements were mineralised grasping/food processing organs, functionally homologous with vertebrate teeth. Differences in apparatus architecture and wear facets have been ascribed to different modes of life or feeding strategies (e.g. Purnell, 1993, 1995; Aldridge *et al.*, 1995).

One of the outstanding questions in conodont palaeobiology remains the modes and controls of growth in individual elements.

2.3 Methodology and materials for morphometric analyses

The quantitative description of morphology of organisms is termed morphometrics. To distinguish and display possible related groups it is necessary to plot a bivariate scatter plot of morphological dimensions. For example, when studying conodont elements, the two values could be the linear dimension from the cusp to the basal margin, the length of platform elements or the widths of the basal cavity at specified positions.

On a bivariate scatter plot, measurements of the two dimensions taken from a single element type, will fall along some form of line - the relative line of growth. The confidence level can then be measured by linear regression statistics. A similar line can also be derived from scatter points in a plot of measurements taken from

many individuals in a single population, provided that a wide range of individual ages is represented in the sample. Because of slight differences in relative growth between organisms, a plot of growth derived from several specimens inevitably shows some spread of data points. To compensate for this scatter, it is necessary to fix a line to the plot.

A straight-line relationship between two dimensions, for example, in a conodont element would indicate that their growth was proportionate i.e. there was a constant ratio between the two rates of growth at all sizes. This pattern of growth is described as isometric and conforms to the equation: $y = bx + c$ (where b is the constant of proportionate growth (slope) for the variants x and y and c is the intersect at the y-axis). However, true isometric growth is exceptional in the fossil record (Skelton, 1993).

The differential relative growth between the two dimensions measured is called allometry and most lines of allometric growth conform to the equation: $y = bx^a$ (where x and y are the two measured variates under comparison and a and b are constants). However, the value of a, the allometric exponent, is important as significant changes of slope occur when a is not equal to one (i.e. the plotted line no longer goes through the origin). In this case, the line of relative growth will plot as a curve in exponential form. Positive allometry occurs when the value of a is greater than one and produces an upward steepening of the curve. Conversely, negative allometric growth plots as a line that decreases in slope upwards when the value of a is less than one. This shows that relative growth of the two variants is disproportionate. There are many reasons, both functional and biological why this may occur.

For example, as marine filter-feeding organisms grow their food requirements tend to increase in scale with the mass of their soft tissue, and its volume. However, if the filter-feeding organ grew isometrically, its capacity for the gathering of food would only increase in scale with its area alone. This would result in the organism obtaining less food per unit of body mass as it increased in size. It is usual, therefore, that the feeding apparatuses of marine filter feeders will grow disproportionately to increasing body mass i.e. they display allometric growth.

As noted by Skelton (1993) it is an important fact that age itself is not represented in these graphs as each pair of measurements only relates the size of one variant to another in a single specimen regardless of its age. However, if a large number of individuals are measured (generally > 25) then clusters along the relative line of growth may demark the "age" structure of the population or sample being measured.

Jeppsson (1976) documented the size distribution of the Silurian species *Ozarkodina confluens* and *Ozarkodina excavata* from Skåne in Sweden and Gogs in Götland, by measuring the length of elements between the process tips parallel with the aboral margin. The length of the process was measured parallel to the total length, from the aboral end of the white matter of the cusp or from the tip of the basal cavity. The results were displayed as scatter graphs plotting length of the anterior process against length of the posterior process (Text-figure 2.3.1.).

Jeppsson (1976) showed how in some samples conodont elements were found in three size groups or clusters and postulated that this indicated that the species had a limited spawning season and that the individual migrated regularly from one area to another during the year. He further postulated that it was most probable that individuals spent the same part of their life in the same area as their ancestors did at corresponding age, and generation after generation migrated in the same regular way. Furthermore, it appeared that, in some geographical areas, the individuals of *Ozarkodina excavata* appeared to regularly migrate during growth. In areas where they spent only part of their life, the collections contained only a partial size range of the species. However, *Ozarkodina confluens* was found to be an exception. In summary, the irregularities in life-size distribution were indicated by Jeppsson (1979) to not only be caused by brood or death of individuals, but also emigration and immigration.

The implications of data from Jeppsson's study can be divided into three distinct parts;

1. The clustering of data along the line as an indicator or a result of conodont size distribution, therefore suggesting the presence of three 'size cohorts' and,
2. The implications of the data as a result of population distribution.

3. The presence of distinct clusters indicative of post-mortem sorting processes.

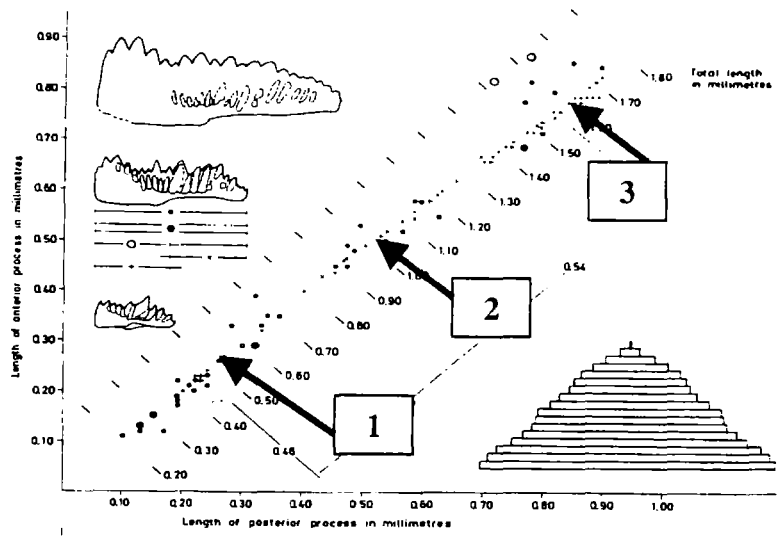

Text-Figure 2.3.1. The distribution of species (see text) from Jeppsson (1976) additionally showing the positions of the three data clusters. The element dimensions measured are indicated by the diagrams on the left of the plotted data.

Considering Pa elements of the ozarkodinid, *Idiognathus*, (Purnell, 1993, 1994) showed that the elements of the ozarkodinid conodonts exhibited slight positive allometry in terms of platform area and platform length. Using the positive allometry shown by the Pa element of *Idiognathus* relative to the platform length, Purnell (1993) also demonstrated how Pa element length could be used as a proxy for body size. As few whole conodont specimens are known it is important to have a figure upon which to test the apparatus for allometry. Therefore, additionally the surrogate body size presented a figure against which the S and M elements could also be tested. The S and M elements tested by Purnell did not display positive allometry as would have been predicted if they performed a filter feeding function. Instead, the S element showed isometric growth and M elements displayed significant negative allometry, suggesting to Purnell (1993) that they could not have performed a filter-feeding role. This study showed that growth was isometric and continued in the P, S and M elements of these conodont apparatuses (Text-figure 2.3.1.)

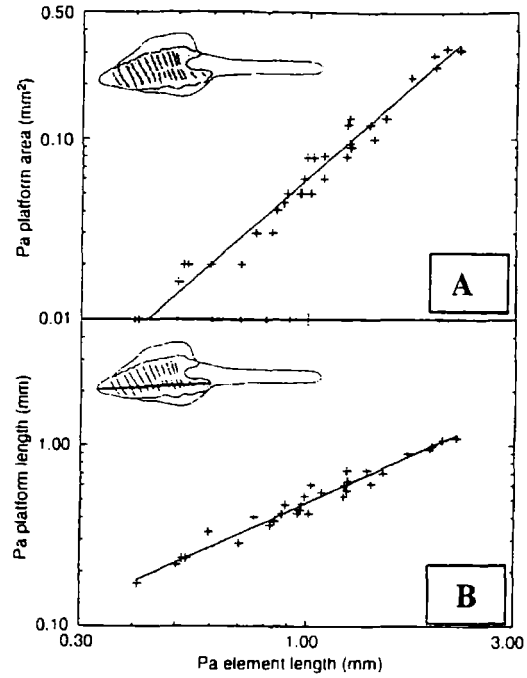

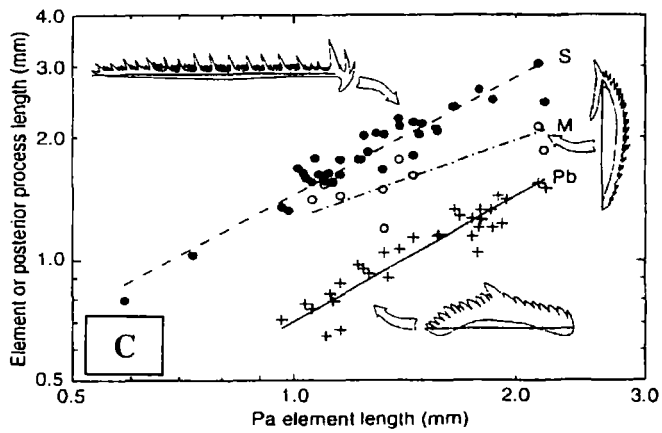

Text-Figure 2.3.2. Shows bivariate scatter plots of A. platform length vs. element length in the Pa of *Idiognathus* and B. Platform area against platform length and C. *Idiognathus* Pb, M and S element dimensions plotted against Pa element length (drawn from Purnell, 1993)

Donoghue & Purnell (1999) further showed that conodont growth was indefinite and that conodont elements were not shed. They documented the presence of wear discontinuities showing cyclic alternation of short growth episodes followed by longer periods of function. Therefore, it is concluded that conodont elements were retained through life and shedding hypotheses have been rejected.

2.4 Morphometric analysis of *Periodon aculeatus*

2.4.1 Methodology and materials

The middle Ordovician *Protopanderodus-Periodon* Biofacies was pandemic within the Iapetus Ocean and characterised deep-water settings (Sweet & Bergström, 1984; Rasmussen, 1997). The specimens analysed within Part II of this thesis were taken from sparry limestone clasts of conglomerates belong to the Lanark Group, Culzean Bay, Scotland. Samples were therefore derived from the outer parts of a mid-Ordovician carbonate platform within the sub-tropics (Armstrong & Owen, in press) and conodont specimens from these samples are characteristic of this deep-water biofacies.

In light of the size data provided from the work of both Jeppsson (1976) and Purnell (1993, 1994) a biometric analysis was conducted on Pa and M elements of the deep-water conodont species *Periodon aculeatus* (middle Ordovician).

In this study the linear dimensions measured are shown on Text-figure 2.4.1.

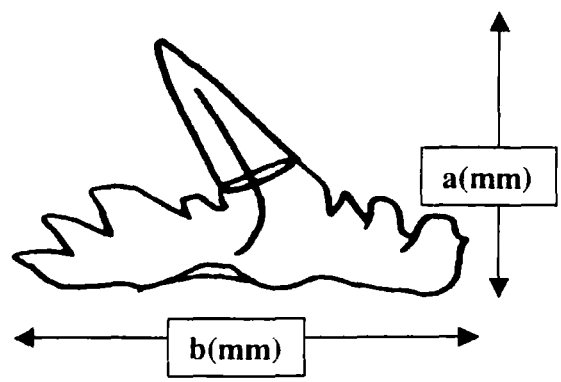

Text Figure 2.4.1. The dimensions measured for the biometric analysis of *Periodon aculeatus* Pa elements.

Dimension a (mm) indicates the height of the element from the basal margin to the tip of the element cusp while dimension b (mm) is the length of the process. Although Text-figure 2.4.1. shows a Pa element, similar measurements were also taken for M elements from the sample, although dimension b (mm) terminated at the edge of the outer edge cusp along the basal margin (Table 2.5). Dimensions were measured using standard light reflected microscopy and a calibrated graticule. The results obtained were plotted using Excel as scatter graphs and the confidence levels measured by linear regression statistics and the R^2 values are shown on Text-figures 2.5.2 & 2.5.3.).

2.5 Results of the *P.aculeatus* morphometric analysis

Table 2.5.

Element	Pa		M		Element	Pa		M	
Sample	a (mm)	b (mm)	a (mm)	b (mm)	Sample	a (mm)	b (mm)	a (mm)	b (mm)
1	0.5	0.35	0.84	0.2	11	0.71	0.59	0.6	0.15
2	0.7	0.7	0.65	0.18	12	0.59	0.35	0.65	0.2
3	0.8	0.9	0.66	0.2	13	0.4	0.3	0.75	0.15
4	0.55	0.32	0.6	0.16	14	0.76	0.81	0.66	0.17
5	0.37	0.28	0.58	0.2	15	0.39	0.28	0.65	0.18
6	0.51	0.44	0.63	0.15	16	0.45	0.24	0.7	0.15
7	0.35	0.28	0.65	0.18	17	0.5	0.43	0.65	0.17
8	0.47	0.37	0.64	0.14	18	0.51	0.36	0.5	0.16
9	0.37	0.26	0.8	0.25	19	0.34	0.26	0.6	0.18
10	0.36	0.24	0.66	0.16	20	0.49	0.41	0.71	0.15

Table 2.5. Dimension of Pa and M elements *of Periodon aculeatus* in millimetres.

Text-Figure 2.5.2. shows the presence of at least two cohorts or clusters. These correspond with the values along the x-axis (dimension Pa a mm) of approximately 0.4 mm-0.6 mm and 0.8 mm.

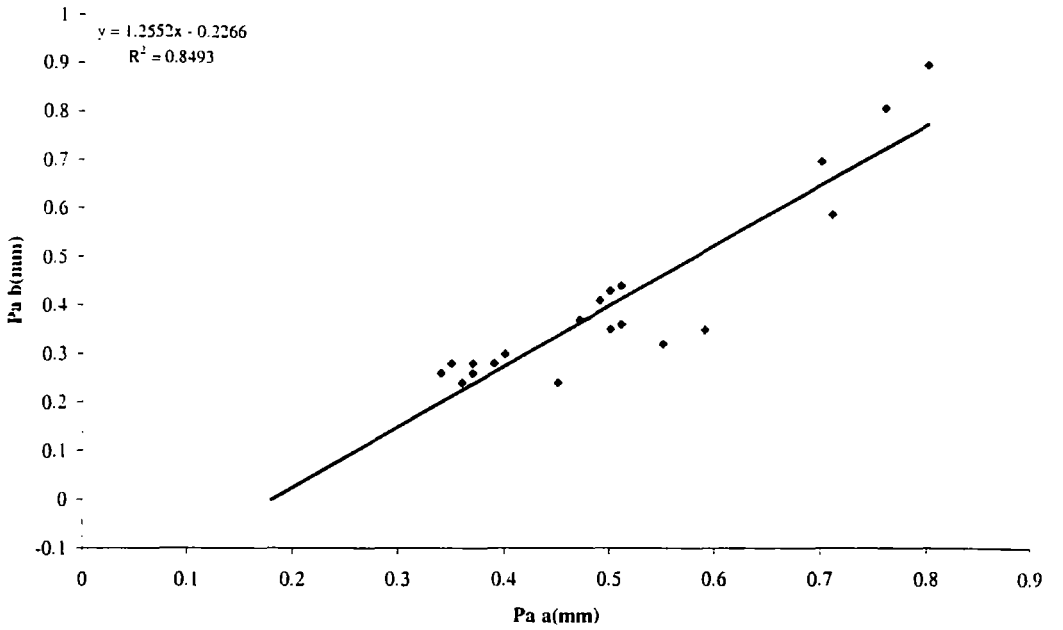

Text-Figure 2.5.2. Shows the biometric plot of dimension a (mm) against dimension b (mm) of the Pa elements of *Periodon aculeatus*. A line has been fitted to the data and the R^2 value is indicated top left.

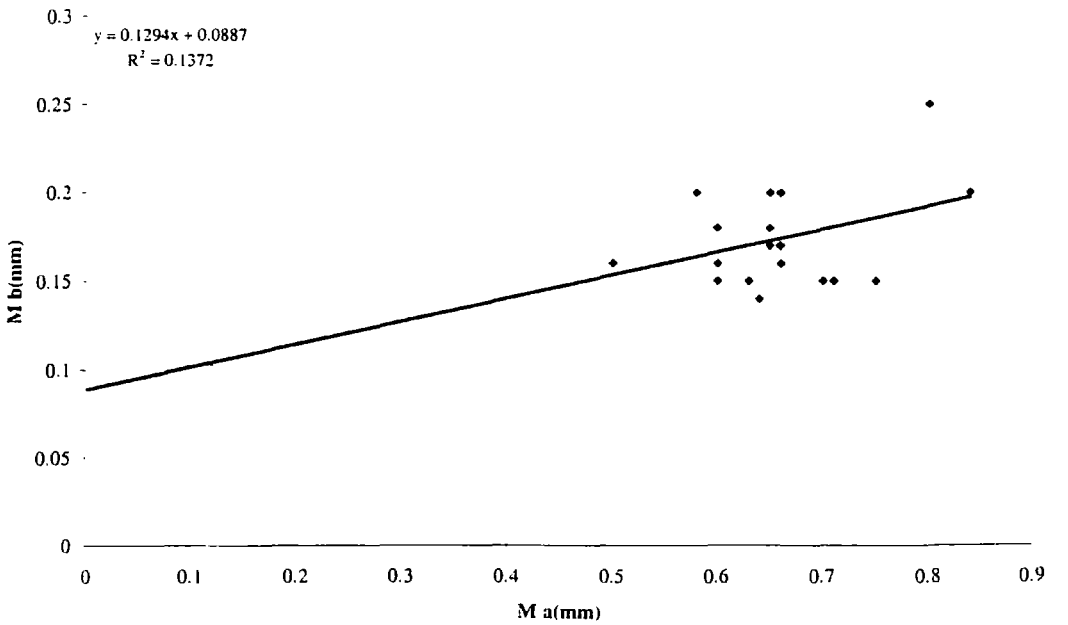

Text-Figure 2.5.3. The biometric plot of *Periodon aculeatus* M elements showing dimension a (mm) on the x-axis against b (mm) on the y-axis.

The majority of the data points in Text Figure 2.5.3. cluster around similar dimensions i.e. 0.5 – 0.8mm. There appears to be just one cluster of data.

2.5.1 Discussion and implications of the biometric data

With this small sample size interpretations are of a preliminary nature. The *Periodon aculeatus* Pa element data shows the presence of at least two distinct 'size cohorts' in the Pa element (as indicated on Text-figure 2.5.2.) whereas a single size cohort was obtained for the M element in the same sample (Text-figure 2.5.3.). This could imply;

1. Differential growth within the conodont element apparatus with the initiation of growth of Pa elements starting earlier in ontogeny or,
2. Taphonomic sorting of the elements.

In view of the fact that all elements were obtained from a single sample and there has been no apparent size sorting of Pa elements hypothesis 1 is favoured.

2.6 Introduction to microstructural growth analysis

Growth analysis of conodont elements can be conducted in a number of ways. As described above, analyses can be conducted on whole element dimension and growth. However, the lamellar nature of the enamel crown tissue facilitates the study of conodont elements at a different level. Donoghue (1998) has recently reviewed much of the work on growth in conodonts. Most of the literature supports the view that the conodont apparatus was retained throughout the life of the animal (Purnell, 1993; 1994, Donoghue & Purnell, 1999).

Dental enamel in vertebrates preserves fossilised tracks of growth. These include Retzius lines, perikymata, prism-cross striations, all of which reflect the incremental growth of enamel and represent an internal record of time and conditions under which the element or tooth grew (for a full review see Risnes, 1998; Fitzgerald, 1998).

One of the first interpretative studies on the growth of conodonts by detailed study of the lamellar enamel crown tissue was conducted by Zhang *et al.* (1997) who

inferred from their observations that conodont growth was periodic. Zhang *et al.* (1997) documented a characteristic lamellae pattern on the edge of the recessive basal margin of the Triassic shallow water conodont genus *Parapachycladina* describing a pattern in the enamel of 8-10 grouped sets of minor lamellae divided by broad inter-lamella spaces (Text-figure 2.6.1.). This pattern was interpreted as a growth periodicity, probably representing annual cycles.

None of the elements described by Zhang *et al.* (1997) exhibited more than four grouped sets or major increments.

Text Figure 2.6.1. Element of *Parapachycladina* showing the 3 major incremental breaks and minor incremental patters between, in the crown (from Zhang *et al.*, 1997)

Zhang *et al.* (1997) reviewed hypotheses that could explain the growth increments observed. They concluded that each lamella represented a period of growth, the element being periodically retracted into the epithelium and additional minor lamellae secreted and speculated that variations in minor increments may have represented internal biophysiological changes. Variations in major increments could therefore reflect physiological constraints imposed by the environment as originally proposed by Bengtson (1976, 1983). Furthermore, Zhang *et al.* (1997) discussed how variations in major lamella thickness may also reflect the seasonal variations in phosphate solubility whereby the larger gaps defining the major increments may have been due to winter pauses in secretion. The notion that major increments reflect an annular growth cyclicity was believed by Zhang *et al.* (1997) to support the work of Jeppsson (1975) who in a biometric study of Silurian conodonts (as previously

shown, Text-figure 2.3.1.) found three separate growth stages. They also found their data to be consistent with the work of Müller & Nogami (1971; 1972) who showed up to four apparent growth cycles in conodont elements.

In light of this data and the proposals of Zhang *et al.* (1997) it is important to address several fundamental questions;

1. Do the incremental lines observed in deep-water conodont element enamel crowns reveal any cycles or periodicity of growth?
2. On what time scale are these periodicities of growth in deep-sea conodonts and can we compare it with that seen in shallow water examples such as those seen in *Parapachycladina?* For example, do major incremental lines in deepwater genera also represent the proposed annual cycles of Zhang *et al.* (1997)?
3. If periodicity in growth is observed could this be used to (a) predict environmental conditions in the deep biosphere of the Ordovician and (b) to predict what causes the cyclicity seen? Furthermore, can patterns observed in conodont lamellae be attributed to environmental or physiological factors?
4. Additionally, can this data be used to make palaeobiological predictions about deep-water conodonts?

2.7 Methodology and materials for microstructural analyses

Analyses of element growth using crown enamel microstructure have been carried out on three middle Ordovician conodont species from the orders Panderodontaea and Prioniodontaea. The three deep-water conodont genera, *Protopanderodus*, *Drepanodus* and *Periodon* are from the sample described in section 2.4.1 and are characteristic of the *Protopanderodus – Periodon* deep-water biofacies.

Oriented, etched thin sections under immersion oils of various refractive indices did not provide images of sufficient quality to measure growth increments in some specimens. SEM images of oriented (tilted to flat) un-etched inner basal cavity

surfaces provided the best medium for analysis. The specimens chosen were thermally mature (CAI 5) and exhibited well-developed growth increments. Some degree of diagenetic etching may have occurred in this material.

The thickness of increments was measured directly from photomicrographs. Cumulative increment thickness (greater and less than the mean increment thickness) was calculated using Excel and plotted as Fischer plots (Fischer, 1964, Sadler *et al.*, 1993). Fischer plots are frequently used in sequence stratigraphy to show rates and cycles of sedimentary accumulation. Each cycle is given a number and plotted against the cumulative deviation from the average calculated cycle thickness, giving easily identifiable peaks and troughs of above average and below average sedimentation. This technique has therefore been used on the growth lamellae in the crowns of elements of *Protopanderodus*, *Drepanodus* and *Periodon*, in order to enhance potential patterns and cyclicity in conodont element growth rate. In the way that Fischer plots chart above and below average sedimentary accumulation, they can also be used to display periods of both above and below average element growth rate (i.e. the elements are grown as distinct additions or secretions of enamel tissue).

Fischer plots were constructed using the minor increment thickness. The widths of individual increments were measured (in microns) and then assigned a cycle number (where one is the first formed or oldest increment). After calculation of the average cycle thickness, the cumulative deviation from this average was plotted against each individual cycle number. Therefore, in the Fischer plots of element growth, each minor increment is represented as one cycle and plotted against the cumulative thickness, in microns, of the individual increments. Peaks and troughs on this plot therefore represent periods of above average and below average growth rates. Growth curves were constructed for all genera by plotting major increment thickness on the y-axis against the increment number on the x-axis.

2.8 Incremental patterns in the coniform taxa *Protopanderodus* and *Drepanodus*

The crowns of *Protopanderodus* and *Drepanodus* elements exhibit simple 'cone-in-cone' style of growth (Type I growth *sensu* Donoghue, 1998) indicating that the elements grew by outward accretion as a series of more or less complete increments around a central core (Text-figure 2.8.1.).

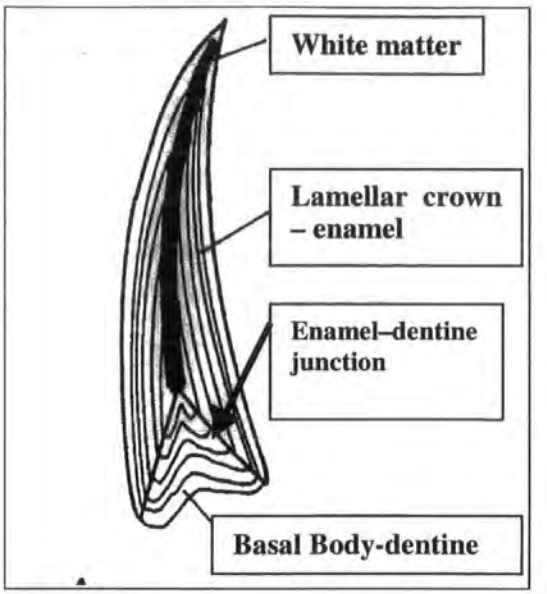

Text -Figure 2.8.1. Basic structure of a coniform conodont element showing the relationship of the crown, basal body and white matter and demonstrating the simple 'cone-in-cone' style structure of simple conodont elements (drawn from Sansom, 1992).

2.9 Microstructure of *Drepanodus* (specimen 692/14)

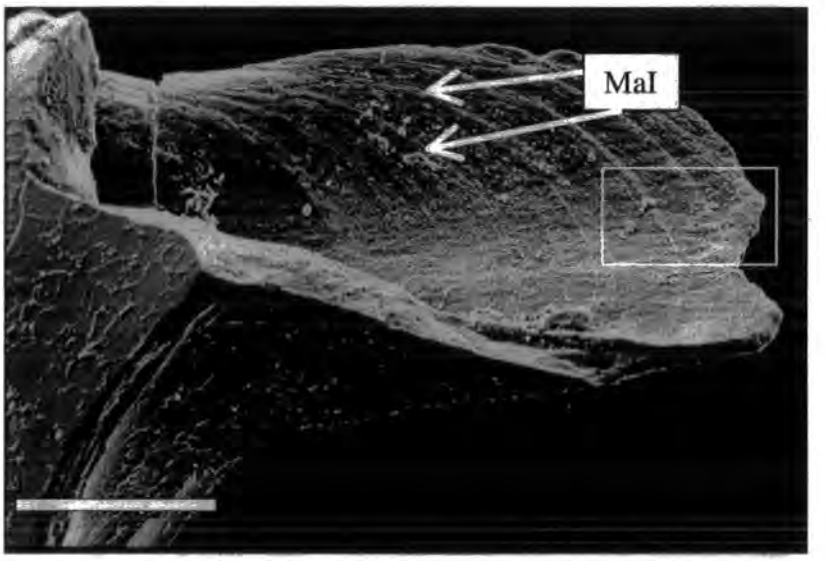

Text-figure 2.9.1. Shows a scanning electron microscope image of the basal cavity of *Drepanodus* (specimen 692/14) and the incremental lines in the crown. MaI shows the positions of some major incremental lines (scale bar botttom left = 100µm).

The crown tissue of *Drepanodus* displays a pattern of both major and minor increments in the crown tissue. In the specimen these can be seen particularly clearly across the basal cavity of the element (Text- figures 2.9.1. & 2.9.2.).

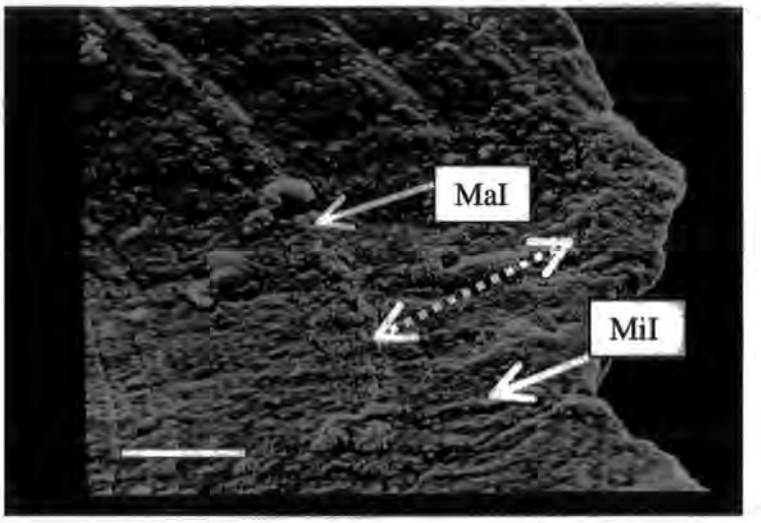

Text figure 2.9.2. High magnification SEM image of *Drepanodus* (specimen 692/14) shown by boxed area in Figure 2.9.1. MaI = major increment and MiI = minor increment (Scale bar = 20μm)

In *Drepanodus* (specimen 692/14), the 138 minor increments are between 1 and 3 μm thick and the majority are grouped in sets of 7-10 between major incremental breaks. The average major increment thickness is calculated to be approximately 22μm. Sixteen major increments are visible on this specimen of *Drepanodus* (Text-figure 2.9.1.), and these are given numbers in order of formation (1 = first formed &16=last formed, Table 2.9). Table 2.9. shows the data obtained for the thickness of minor increments and the position of major increments in the specimen of *Drepanodus*. The smallest, or basic, unit of secretion is 1.3μm and this is assumed to represent one single growth phase. Each minor increment fundamentally consists of this basic unit or is a multiple of this value. Based upon the assumption that thicker increments indicate periods of rapid or accelerated growth (i.e. time periods when more enamel was added to the crown), the sum of the individual minor increments was calculated to give the raw thickness, in microns, of each major increment. The cumulated totals (major increment thickness) are therefore also displayed in Table 2.9.

Table 2.9

Major Increment	Minor increment thickness (microns)	Major Increment	Minor increment thickness (microns)	Major Increment	Minor increment thickness (microns)	Major Increment	Minor increment thickness (microns)
1	4	5	4	9	4	13	1.3
	2.6		2.6		2.6		1.3
	2.6		2.6		2.6		1.3
	4		2.6		2.6		1.3
	2.6		2.6		2.6		1.3
	2.6		1.3		2.6		1.3
	2.6		1.3		2.6		1.3
	2.6		1.3		1.3		1.3
			1.3				1.3
			1.3				1.3
Total	23.6µm	total	20.9µm	total	20.9µm	Total	13µm
2	5.3	6	4	10	6.7	14	4
	4		2.6		4		2.6
	2.6		1.3		2		2.6
	2.6		1.3		2		2.6
	2.6		1.3				2.6
	2.6		1.3				4
	2.6		1.3				2.6
	2.6		1.3				2.6
	2.6		1.3				2.6
			1.3				2.6
Total	27.5µm	total	17µm	total	14.7µm	Total	28.8µm
3	4	7	4	11	2.6	15	2.6
	4		2.6		2.6		2.6
	4		1.3		2.6		2.6
	2.6		2.6		2.6		2.6
	4		1.3		2.6		4
	2.6		2.6		1.3		2.6
	4		1.3		1.3		2.6
	2.6				1.3		2.6
	2.6				1.3		1.3
Total	30.4µm	total	15.7µm	total	18.2µm	Total	23.5µm
4	2.6	8	4	12	9.3	16	2.6
	4		2.6		5.3		1.3
	5.3		2.6		4		1.3
	2.6		2.6		2.6		1.3
	1.3		2.6		2.6		1.3
	2.6		2.6		2.6		1.3
	2.6		2.6		1.3		1.3
	2.6		2.6		1.3		
	2.6		2.6		1.3		
			2.6				
Total	26.2µm	total	27.4µm	total	30.3µm	Total	10.4µm

Table 2.9. Minor increment thickness in microns for *Drepanodus* specimen (692/14) figured in Text Figure 2.9.1 Total major increment thickness displayed at the base of each section.

2.10 Minor increment growth pattern analysis for *Drepanodus* (specimen 692/14)

The Fischer plot for the minor increment thickness of *Drepanodus* (Text-figure 2.10.1) shows a series of peaks and troughs. Four peaks are observed and represent periods when the growth of the conodont element was higher (or faster) than the average (i.e. more crown tissue was added to the element than the calculated average amount). The Fischer plot indicates four periods of accelerated crown enamel addition during ontogeny.

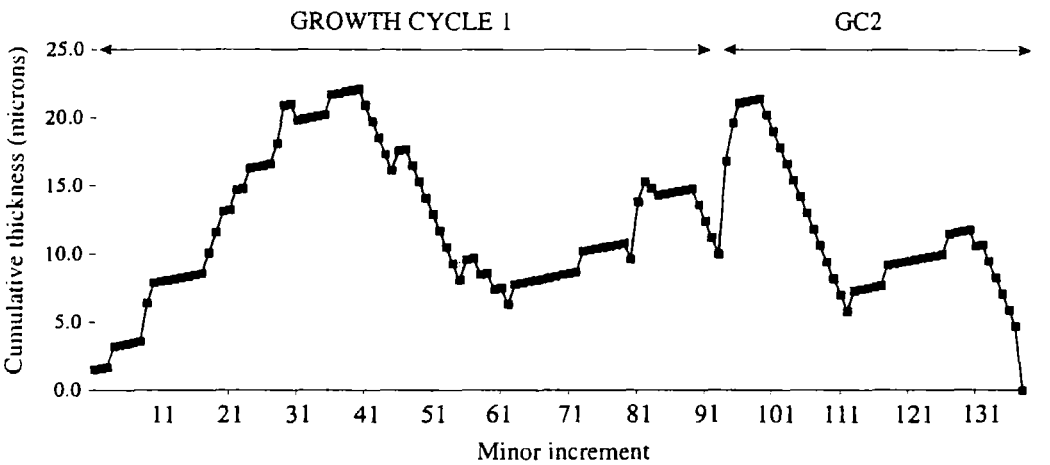

Text-Figure 2.10.1. Fischer plot constructed from the minor increment width as observed in *Drepanodus*. N.B. Cycle number 1 represent the first formed increment, successively higher numbers represent later additions. Cumulative thickness values (y-axis) are in microns. Vertical lines delimit major increments.

The pattern of cyclicity shown by the Fischer plot can be summarised as follows. An initial step-wise pattern of above average growth is followed by a small peak and trough at minor increments 26 to 33. This is followed by a peak in growth at minor increment number 35 to 39. At increment 39 there is a sharp decline to increment number 44 followed by a small peak at increment number 46. The line then declines to increment number 54. A small peak follows this decline which is again followed by a decrease (to increment number 61). There is three stage 'step-wise' increase leading to second large peak which occurs at increment 96-99. This is followed by a decrease to increment 112 and subsequent 3 stage step-wise increase to

a third, final peak at increment number 129. The final decline occurs from increment 129-138.

The observed overall similarity in pattern between in the first two and the last two peaks is considered here to indicate a repetition of growth cyclicity and therefore, the presence of two major growth cycles is interpreted for this *Drepanodus* element (represented by arrows on Text-figure 2.10.1). The first cycle appears to be expanded in comparison to the second i.e. it occurs over a greater number of increments. Cycle 1 contains increments 1-93 whereas Cycle 2 contains increments 94-138.

2.11 Major Increment thickness in *Drepanodus* (specimen 692/14)

In addition to the Fischer analyses of minor increment data, the data for the thickness of major increments in *Drepanodus* (specimen 692/14) has also been analysed in terms of simple growth patterns. In this case, the total widths of major increments in microns have been plotted against the increment number in order from the first, to the last formed increment. Measurements used for these analyses are shown on Table 2.9.

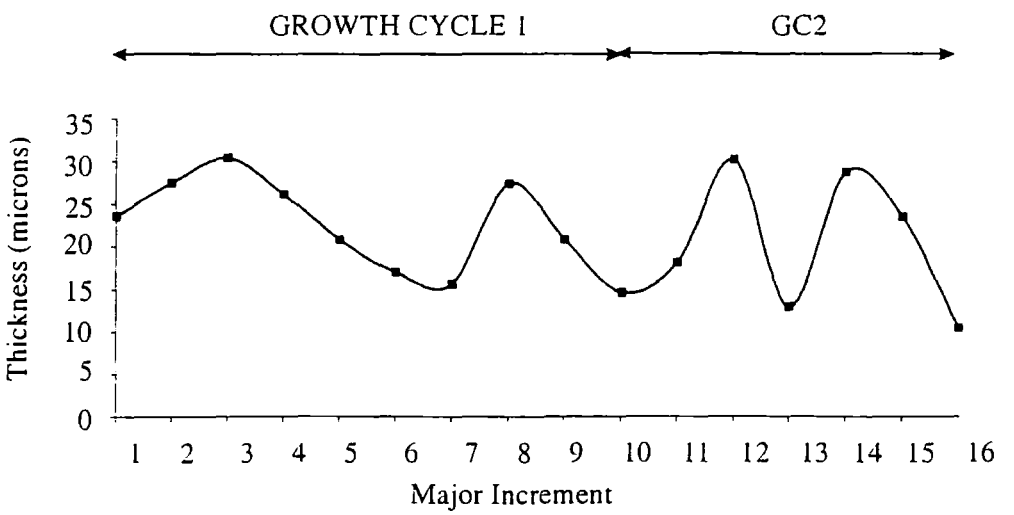

Text-Figure 2.11.1. Plot of raw thickness against major increment number in *Drepanodus* where 1 is the oldest increment and 16 is the youngest or last formed.

The growth curve for *Drepanodus* (692/14) major increment thickness shows 4 major peaks (Text-figure 2.11.1.). Between major increments 1 and 3 there is an increase in the thickness and therefore a peak on the growth plot. Between increments 3 and 7 there is a rapid decline in increment thickness. The transition of increment 6 to 7 represents the second peak of this graph. It can be observed to be slightly smaller than the first peak. This is followed by a decline in the values for major incremental line thickness between increment 8 and 10 producing the second trough observed on this growth plot. Between major increments 10 and 12 there is an increase in thickness producing the third peak on the plot. This peak is similar in amplitude to the first peak, both have a larger amplitude than peak 2. The third trough in the series, occurring at increment 13 follows this. The fourth peak represents the values of increments 13-15 and can be seen to have a smaller amplitude than that of the third peak. The incremental thickness then shows a final decrease in thickness and ceases at increment number 16. This growth plot again demonstrates that the first two-peak range (or growth cycle 1) is expanded in comparison to the second.

2.12 Microstructure of *Protopanderodus*

Protopanderodus is a panderodontid conodont (Sweet, 1988). A scanning electron microscope image of the *Protopanderodus* element (specimen 667/21) is shown in Text-figure 2.12.1. and clearly displays the growth increments in the basal cavity and across the recessive basal margin. At higher magnifications (Text-figure 2.12.2.) the minor increment divisions can be seen between the major incremental breaks. In *Protopanderodus*, the 72 minor increments are between 1 and 4 μm thick and are grouped in sets of 8-10 between major incremental breaks. The average major increment thickness is calculated to be approximately 12μm (approximately half that of *Drepanodus*). Nine major increments are visible on this specimen of *Protopanderodus*, and these are given numbers in order of formation (1 = first formed & 9= last formed, Table 2.12).

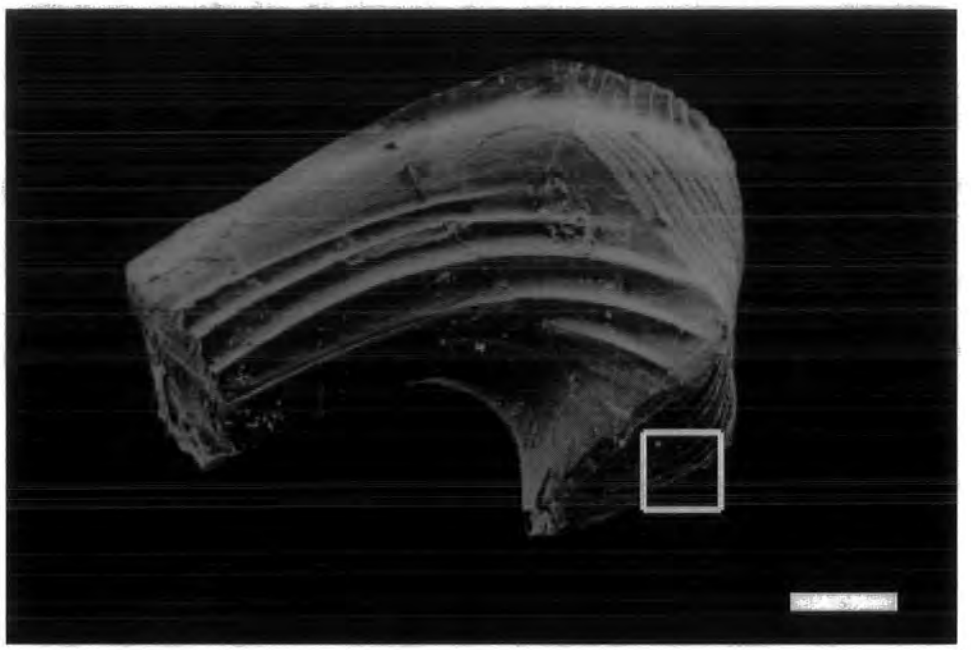

Text-Figure 2.12.1. SEM image of *Protopanderodus* pf element (specimen 667/21) showing growth increments at the basal cavity (scale bar = 200 µm). Boxed area represents the position of the image for Text Figure 2.12.2.

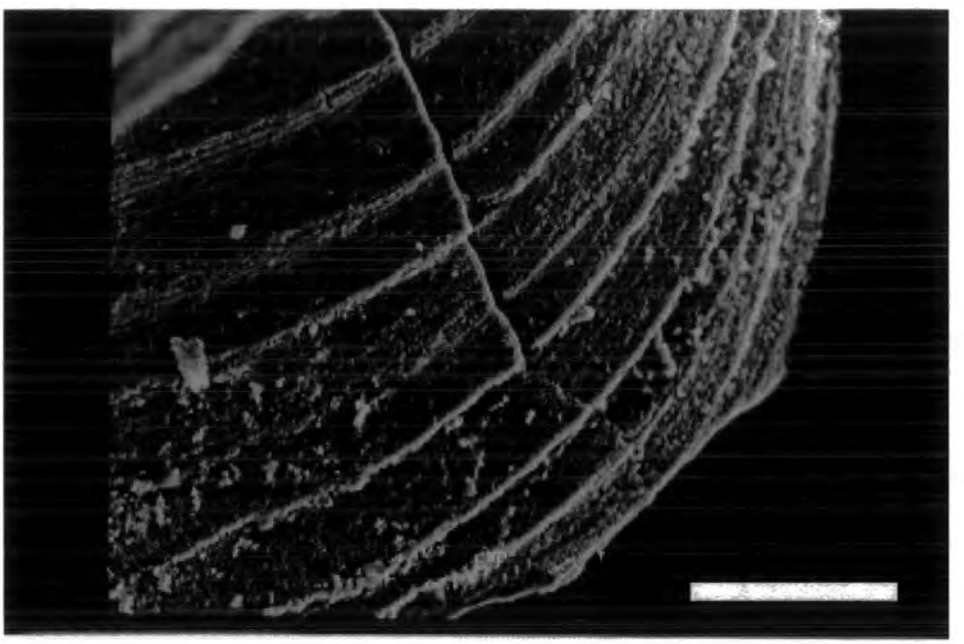

Text-Figure 2.12.2. High magnification SEM image of *Protopanderodus* element showing the nature of the major and minor lamellae sets (scale bar = 50µm)

Table 2.12

Major Increment	Minor increment thickness (microns)	Major Increment	Minor increment thickness (microns)	Major Increment	Minor increment thickness (microns)
1	3.3	4	1.7	7	3.3
	1.7		1.7		2.5
	0.8		1.7		1.7
	1.7		1.7		1.7
	0.8		0.8		1.7
	1.7		0.8		
	1.7		0.8		
	1.7		0.8		
	1.7		0.8		
	1.7		0.8		
total	16.8µm	Total	11.6µm	Total	10.9µm
2	1.7	5	0.8	8	1.7
	3.3		0.8		1.7
	1.7		0.8		0.8
	1.7		0.8		3.4
	1.7		0.8		1.7
	1.7		0.8		
	1.7		0.8		
	1.7		0.8		
	1.7		0.8		
total	16.9µm	Total	7.2µm	Total	9.3µm
3	0.8	6	1.7	9	1.7
	0.8		0.8		0.8
	0.8		0.8		3.3
	1.7		0.8		1.7
	1.7		0.8		1.7
	3..3		1.7		1.7
	2..5		1.7		
	1.7		1.7		
	1.7		0.8		
total	15µm	Total	10.8µm	Total	10.9µm

Table 2.12 Major and minor increment thickness in *Protopanderodus* (specimen number 667/21).

Table 2.12. shows the data obtained for the thickness of minor increments and the position of major increments in specimen 667/21. The smallest, or basic, unit of secretion is 0.8µm and this is assumed to represent one single growth phase. Each minor increment fundamentally consists of this basic unit or is a multiple of this value. Based upon the assumption that thicker increments indicate periods of

rapid or accelerated growth (i.e. time periods when more enamel was added to the crown), the sum of the individual minor increments was calculated to give the raw thickness, in microns, of each major increment. The cumulated totals (major increment thickness) are therefore also displayed in Table 2.12.

2.13 Minor increment growth pattern analysis for Protopanderodus (667/21)

Similar growth cyclicity to that in *Drepanodus* (692/14) is observed in Fischer plots constructed with the incremental width data set for *Protopanderodus* (667/21).

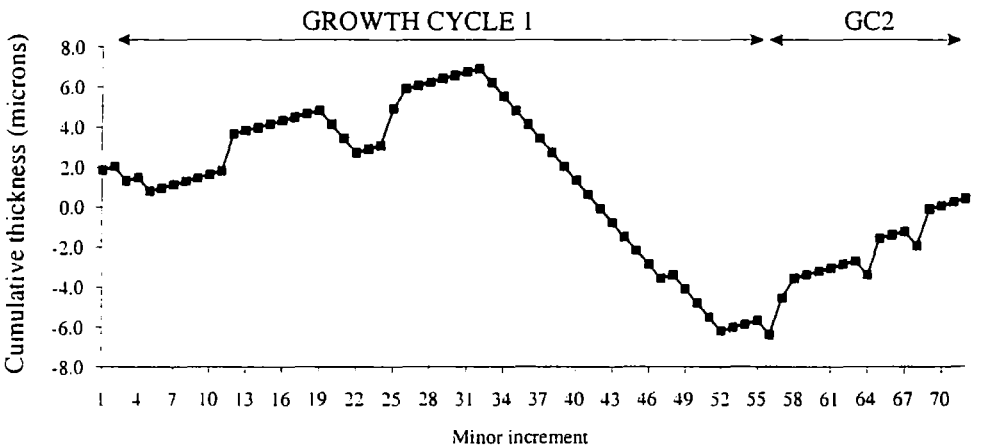

Text Figure 2.13.1. Fischer plot of the minor increment widths of *Protopanderodus* (667/21). Vertical lines show major incremental lines.

The Fischer plot (Text Figure 2.13.1.) shows a series of small peaks superimposed on the first largest peak. There is then a rapid decline in growth followed immediately by three similar step-wise peaks as growth rate increases. The Fischer plot pattern observed can be summarised as follows. Increments 1 to 6 show a slight negative slope. From increments 6 to 32 there is an overall positive slope. However, superimposed upon this are two step-wise troughs and declines. At increment 6 there is a positive slope which steepens at increment 12 but this increase ceases at increment 20. At this increment, the slope is negative until increment 24.

Here there is a resumption of the positive slope until increment 32. Increments 33 to 47 show a negative slope. Increment 48 represents a slight increase immediately followed by a decrease to increment 52. From increment 53 to increment 70 there is a general increase and a positive slope with superimposed small peaks and troughs.

Although the observed number of growth peaks for *Drepanodus* outnumbers those for *Protopanderodus*, there is an overall similarity in pattern. The data presented as Fischer plots for both *Drepanodus* (Text-figure 2.10.1.) and *Protopanderodus* (Text-figure 2.13.1.) shows clear cyclicity of conodont element growth. There are therefore, distinct and similar patterns in the Fischer plots for the panderodontids *Drepanodus* and *Protopanderodus*, which appear to show that growth in the crowns of these conodont elements is cyclical.

2.14 Major increment analysis in Protopanderodus (667/21)

The *Protopanderodus* growth plot (Text-figure 2.14.1) has a slightly less complex pattern than that of *Drepanodus*. The major incremental thickness values used to produce this plot are also shown in Table 2.12.

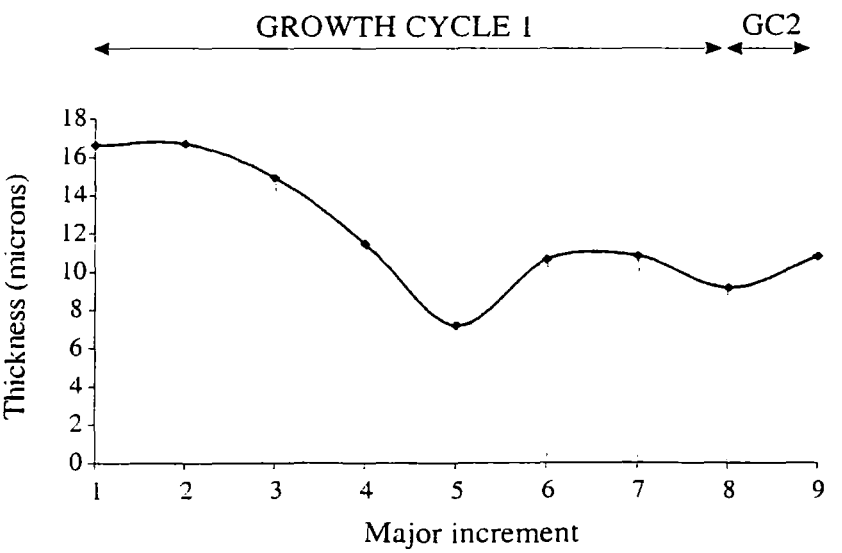

Text Figure 2.14.1. Growth curve for *Protopanderodus* (667/21) using raw thickness of major increments plotted against each individual increment.

In this data set the major increment thickness values plot as an initial peak followed by a decline in thickness from major increments 1 to 5. There is a small second peak occurring between increments 5 and 8. From increment 8 there appears to be a slight increase before the cessation of growth at increment number 9. This data therefore represents one growth cycle consisting of two peaks over major increments 1 to 8. Increment 9 appears to represent the start of a second growth cycle.

2.15 Microstructure of *Protopanderodus* (specimen 979912D)

In addition to observing growth increments across the basal cavity of *Protopanderodus* a further specimen has been analysed by use of an etched thin section. This technique produced a longitudinal cross section of the specimen, which could be etched and observed by use of SEM. A tracing of the photomicrograph produced is shown in Text-figure 2.15.1.

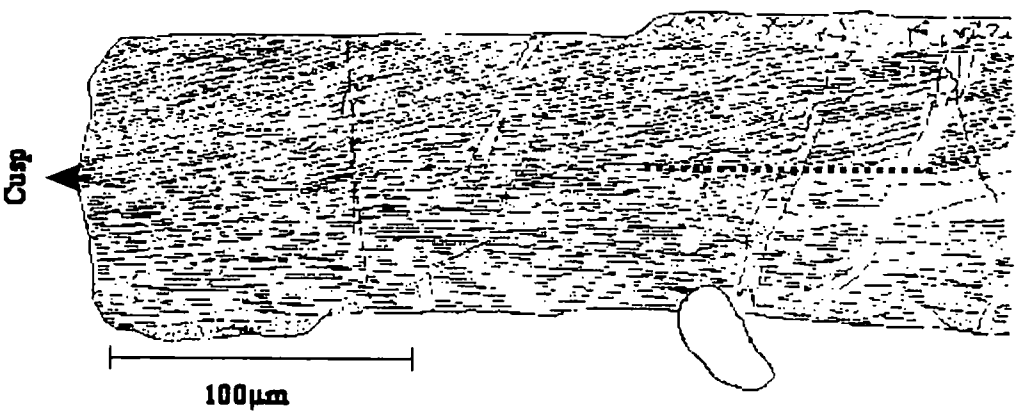

Text-Figure 2.15.1. Tracing of the enamel microstructure in *Protopanderodus* (specimen 979912D). The specimen is orientated with the inner edge down. Increment thickness measured for both the inner and outer sets from the midline (dashed line) of the element to the edge.

2.16 Minor increment growth pattern analysis for *Protopanderodus* (979912D)

Specimen 979912D has a total of 95 minor increments. The outer side of the specimen comprises a total of 65 minor increments. The thickness of these is shown in Table 2.16. The mean increment thickness is calculated to be 1.3μm.

Table 2.16

Minor Increment	Thickness (microns)	Minor Increment	Thickness (microns)	Minor Increment	Thickness (microns)
1	1.6	21	2.7	41	1.4
2	1.2	22	2.2	42	1.4
3	1.4	23	1.7	43	1.8
4	1.3	24	1.3	44	1.5
5	1.5	25	1	45	1.5
6	1.7	26	1.3	46	1.5
7	1.9	27	1.7	47	1.5
8	1.9	28	1.4	48	1.7
9	1.3	29	1.9	49	1.9
10	0.8	30	2.2	50	2.3
11	1.5	31	2.3	51	1.5
12	1.9	32	1.8	52	1.5
13	2.1	33	1.4	53	1.5
14	1.6	34	2.1	54	1.7
15	1.7	35	1.3	55	1.7
16	1.2	36	2.1	56	1.2
17	1.5	37	1.2	57	1.2
18	1.5	38	1.8	58	1.2
19	1.4	39	1.3	59	1.2
20	2.7	40	1.7	60	1.2
				61	1.8
				62	1.8
				63	2.2
				64	2.2

Table 2.16. Table of minor increment thickness for the outer side of *Protopanderodus* specimen (979912D)

Table 2.6A

Minor Increment	Thickness (microns)	Minor Increment	Thickness (microns)	Minor Increment	Thickness (microns)
1	1.4	11	1	21	1.7
2	2.7	12	1	22	1.7
3	2.1	13	1.5	23	1.1
4	2	14	1.3	24	1
5	1.7	15	1.3	25	1.5
6	0.8	16	1.3	26	1.4
7	1.5	17	1.3	27	1.2
8	1.6	18	2	28	2.1
9	1.6	19	2.6	29	1.8
10	1.4	20	1.7	30	1.5

Table 2.16A. Minor increment thickness in microns for the inner side of *Protopanderodus* specimen (979912D)

The inner side of the elements has fewer minor increments (Table 2.16A) comprising a total of 30 minor increments with a mean thickness of 0.6μm.

The thickness of these two sets of minor increments were used to construct Fischer plots (Text-figure 2.16.1).

Up to minor increment 15, the inner side of *Protopanderodus* (979912D) is characterised by above average growth. The plot for minor increments on the outer edge of the same element is characterised by average growth up to increment 15. At increment 15 there is a distinctive trough in both Fischer plots. After the small trough both elements show a short period of above average growth at increment 16. After this distinctive 'jog', both sides of the element show periods of below average growth and a general decline,

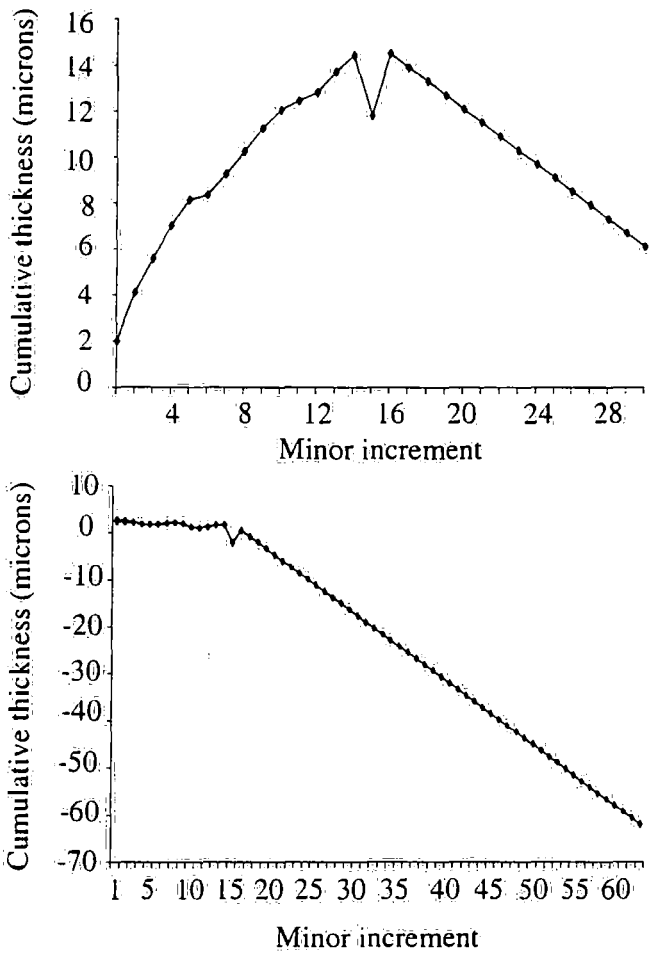

Text-Figure 2.16.1. Top. Fischer plot for the inner minor increments of specimen (979912D) Bottom. Fischer plot of outer minor increments in *Protopanderodus* specimen (979912D).

2.17 Major increment analysis in *Protopanderodus* (979912D)

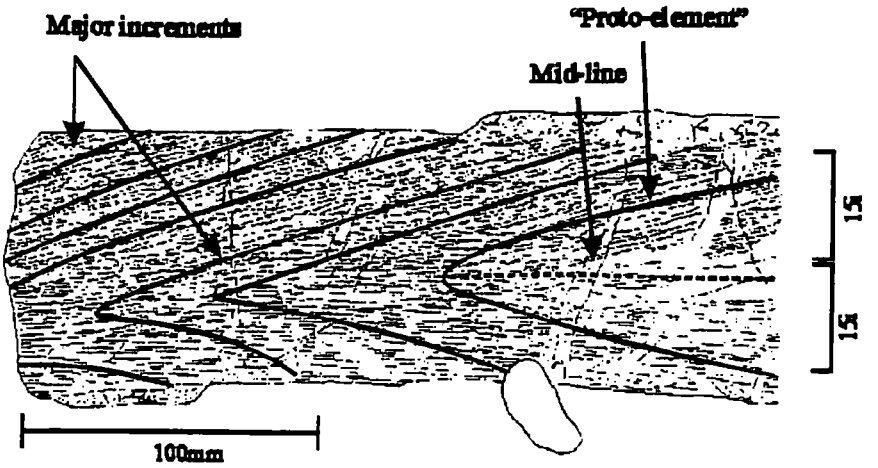

Text-Figure 2.17.1. Major increments in *Protopanderoudus* specimen 979912D (inner edge down). Major increment dicontinuities were interpreted from axially compressed images.

Text–figure 2.17.1. shows a tracing obtained from a photomicrograph of the etched longitudinal section of *Protopanderodus* specimen number 979912D. Major incremental boundaries are marked by low-angle discontinuities at bounding surfaces.

These major incremental thickness are plotted as growth curves (Text-figure 2.17.2.). The inner major increments show a general decline in rate between increments 1 and 5 (Text-figure 2.17.2. top). However, the growth curve for the outer major increments shows a distinct pattern (Text-figure 2.17.2 bottom). In the major increments at the outer side of this specimen there is an decline in increment thickness between the first and forth increments. This is followed by an increase in increment thickness to a peak at increment 6. This peak is succeeded by another decline in increment thickness at increments 7 and 8.

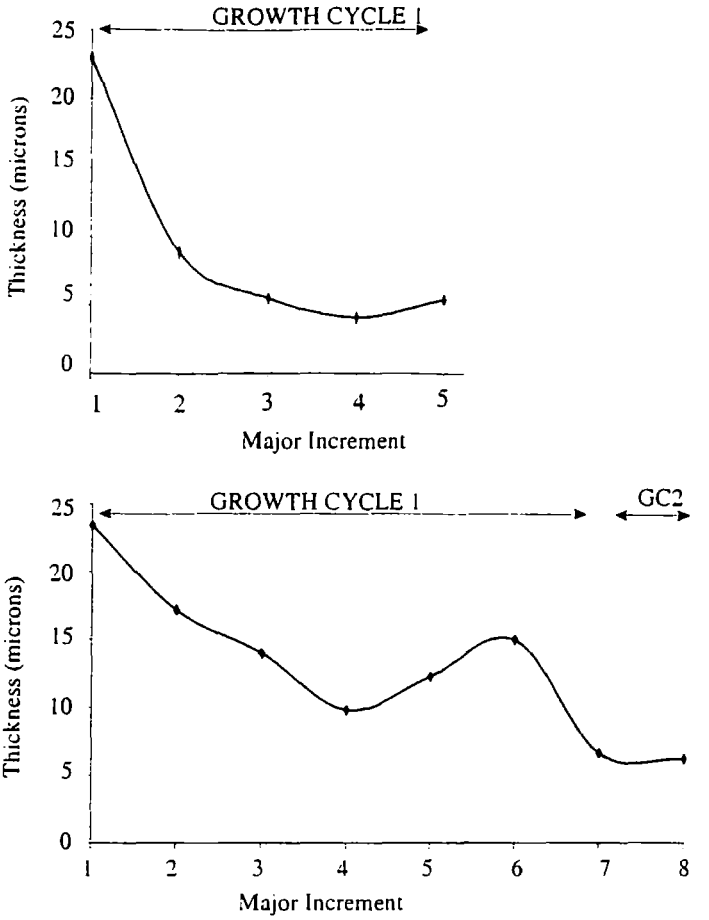

Text-Figure 2.17.2. The growth curves based upon the outer (btm) and inner (top) major increment thickness for specimen 979912D figured in Text-Figure 2.15.1.

2.18 Interpretation

Both the major and minor increment plots display a cyclicity in growth in the specimens of *Drepanodus* (692/14) and *Protopanderodus* (667/21 & 979912D). The growth pattern for *Protopanderodus* appears to lack the second growth cycle seen in *Drepanodus*. One complete growth cycle is inferred to consist of two distinct peaks of growth. Therefore, the crown enamel of the *Drepanodus* element (specimen 692/14) represents 2 complete growth cycles, whereas the enamel crown of both the *Protopanderodus* specimens represents one complete growth cycle.

2.19 Causes of growth periodicity in conodonts – calibrating the growth curves

The recognition of growth cycles in these data has important implications for the growth of conodont elements. As shown previously, Zhang *et al.* (1997) postulated that major increments in the shallow-water Triassic conodont *Parapachycladina* probably represented annual cycles.

Three hypotheses can be constructed for the time duration of each minor increment in *Drepanodus* and *Protopanderodus*. These are that they approximate to either one day, one month or one year.

Due to frictional slowing of the Earth's orbit day length has increased since the mid-Ordovician. Daily growth increments from various invertebrates (Scrutton, 1973) and theoretical approaches (Goldreich, 1982) have been used to calculate the mean day length increase throughout the Phanerozoic (Text-figure 2.19.1.). These data would indicate that the mean day length in the mid-Ordovician would be approximately 21.4 to 21.7 hours.

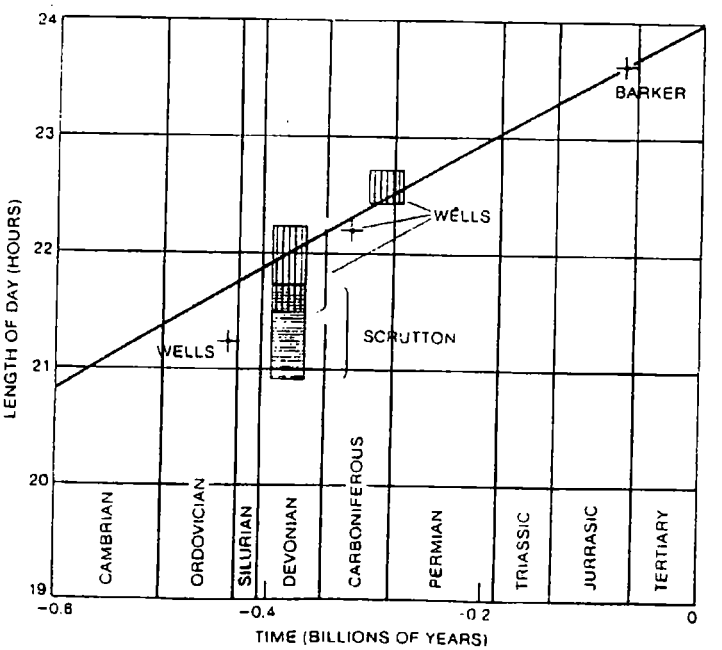

Text-Figure 2.19.1. Shows the various data sets (authors named) from the growth bands in corals and the extrapolated day length data based on the assumption that the present tidal lag has remained constant throughout the past half-billion years (drawn from Goldreich, 1982)

The thinnest minor increments found in *Drepanodus* and *Protopanderodus* are 1.3 and 0.8 μm respectively, and these are taken as the basic unit of secretion of a single lamella. The majority of minor increments in these taxa appear to be of this thickness or a multiple of this basic unit (Tables 2.9 & 2.12).

A major increment in *Drepanodus* comprises, on average 9 minor increments and an average of 16 basic units of growth. Taking a maximum number of 20 basic units for one major increment, then if one major increment represented a day (≡ 20 basic units) each basic unit would take 0.8 hours to secrete. If a major increment represented one month's growth (≡ 20 basic units) then a basic unit would be equivalent to 1.5 days (32 hours) secretion. If a major increment represented a year (410 days) then a basic unit would be equivalent to 15.7 days of secretion.

A major increment in *Protopanderodus* comprises an average of 8 minor increments and on average, 15 basic units of growth. Taking a maximum number of 23 basic units for one major increment, then if one major increment represented a day (≡ 23 basic units) each basic unit would take 0.9 hours to secrete. If a major increment represented a month's growth (≡ 23 basic units) then a basic unit would be equivalent to 1.3 days (~28 hours) secretion. If a major increment represented a year then a basic unit would be equivalent to 18 days of secretion (Table 2.19).

A growth period of between 1.3 and 1.5 days to secrete 1.3μm in *Drepanodus* and 0.8μm in *Protopanderodus* falls into the range documented for dental enamel in hominids (Beynon & Wood, 1987, Risnes, 1998) and other primates (Fukuhara, 1959, Table 2.19A).

Table 2.19

Major increment	21.5 hours (1 day)	30 days (month)	410 days (year)
Drepanodus (max. 20 BUGs) (unit 1.3 microns)	0.8	1.5	15.7
Protopanderodus (max. 23 BUGs) (unit 0.8 microns)	0.9	1.3	18

Table 2.19. Theoretical increment duration for *Protopanderodus* and *Drepanodus*. BUG's are basic units of growth as explained in the text.

Table 2.19A

Genera	BUG	Secretion time of basic unit	Rate
Drepanodus	1.3 microns	1.5	~0.87microns/day
Protopanderodus	0.8 microns	1.3	~0.62 microns/day
Hominid	5 microns	7-8 days	~0.66 microns/day

Table 2.19A. Comparison of Hominid enamel secretion rates and those proposed for *Drepanodus* and *Protopanderodus*.

2.20 Growth pattern analyses

It is concluded from this preliminary comparison that a major increment represented a months time duration in *Drepanodus* and *Protopanderodus*. If correct then these values can be used to calibrate the Fischer Plots and further suggest a growth cycle (consisting of two peaks of growth), approximates to one year.

For many years large-scale homogeneity in salinity, temperature and oxygen throughout large areas of the deep-sea led to the preconception of widespread constancy within this marine ecosystem (Menzies, 1965). Modern marine studies by Gage & Tyler (1988) and Tyler (1995), have argued for seasonality in the deep-sea based upon the amounts of organic matter reaching the ocean floor. Synchronisation of reproduction and spawning behaviour support this view and suggest that nutrient availability is a major controlling factor in the regulation of life-cycle events.

Seasonal inputs of organic matter that reaches the deep-waters, are mainly in the form of organic aggregates (Tyler, 1988) which fall to the deep seas as a 'rain' of small particles. As shown (Text Figure 2.20.1) the productivity in surface waters varies with latitudinal position. At tropical latitudes (Text Figure 2.20.1 top) surface productivity in central ocean regimes is low due to lack of available nutrients. At high latitudes (Figure 2.20.1 btm.), although upwelling results in a high nutrient level, sunlight is not sufficient to cause high productivity throughout the year.

Temperate oceans (Figure 2.20.1 middle) show distinct seasonality in surface production. During March and April active upwelling promotes the rise of nutrients and sufficient sunlight is available to produce a peak in productivity, known as the spring bloom. As nutrient supplies are used there is a lull in productivity over the summer months despite high sunlight levels. As the surface waters cool in the autumn, a smaller upwelling again brings nutrients to the surface and a smaller

autumn bloom is produced. This is short-lived compared to the earlier spring bloom. As days shorten in winter months, although there is a surplus of nutrients, energy levels are not sufficiently high to promote high productivity levels.

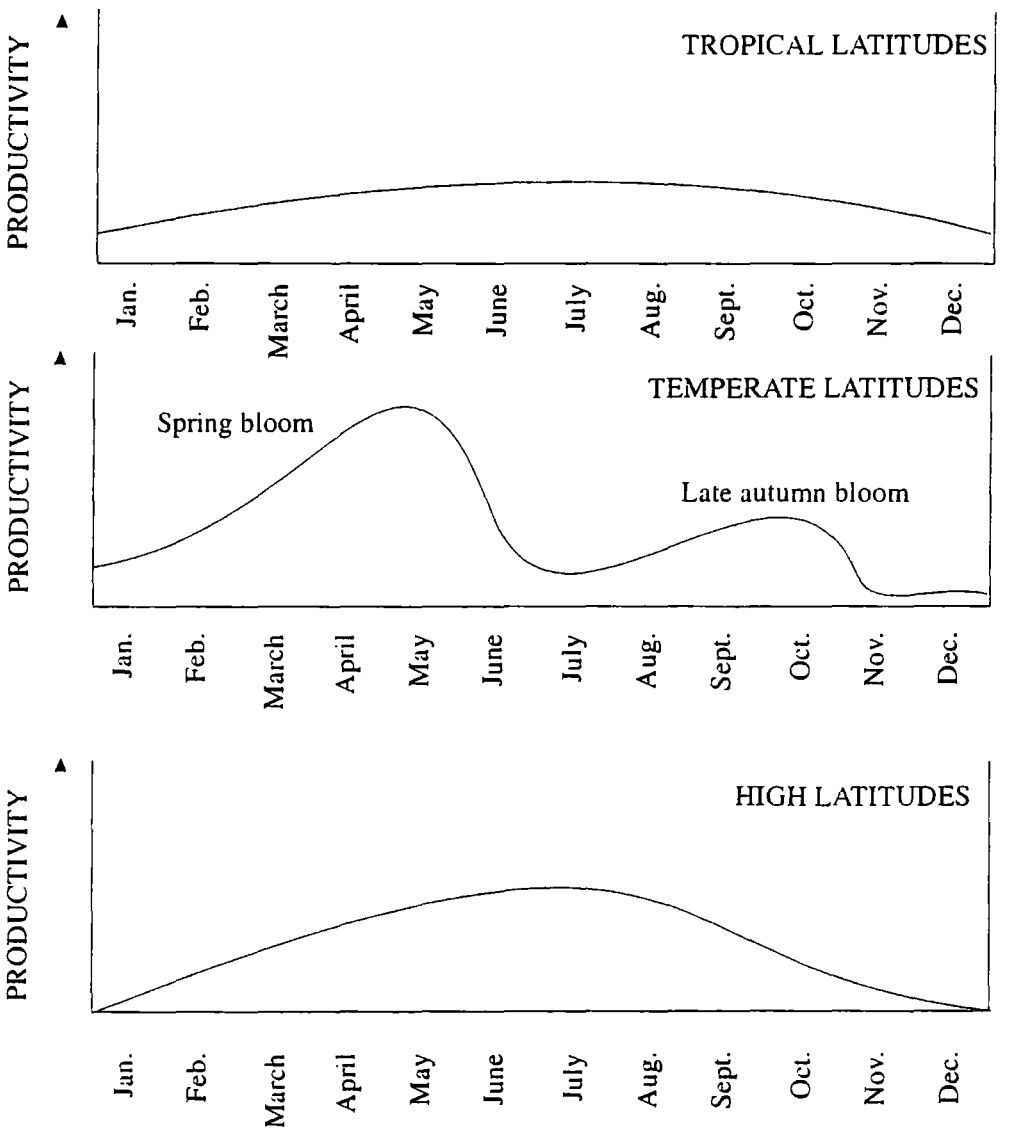

Text Figure 2.20.1 Variations in productivity occurring in the central oceans at different latitudinal positions (adapted from Stowe, 1986).

Using the assumption that one major increment is equivalent to one month of time then the growth plots for *Drepanodus* and both *Protopanderodus* elements can be calibrated.

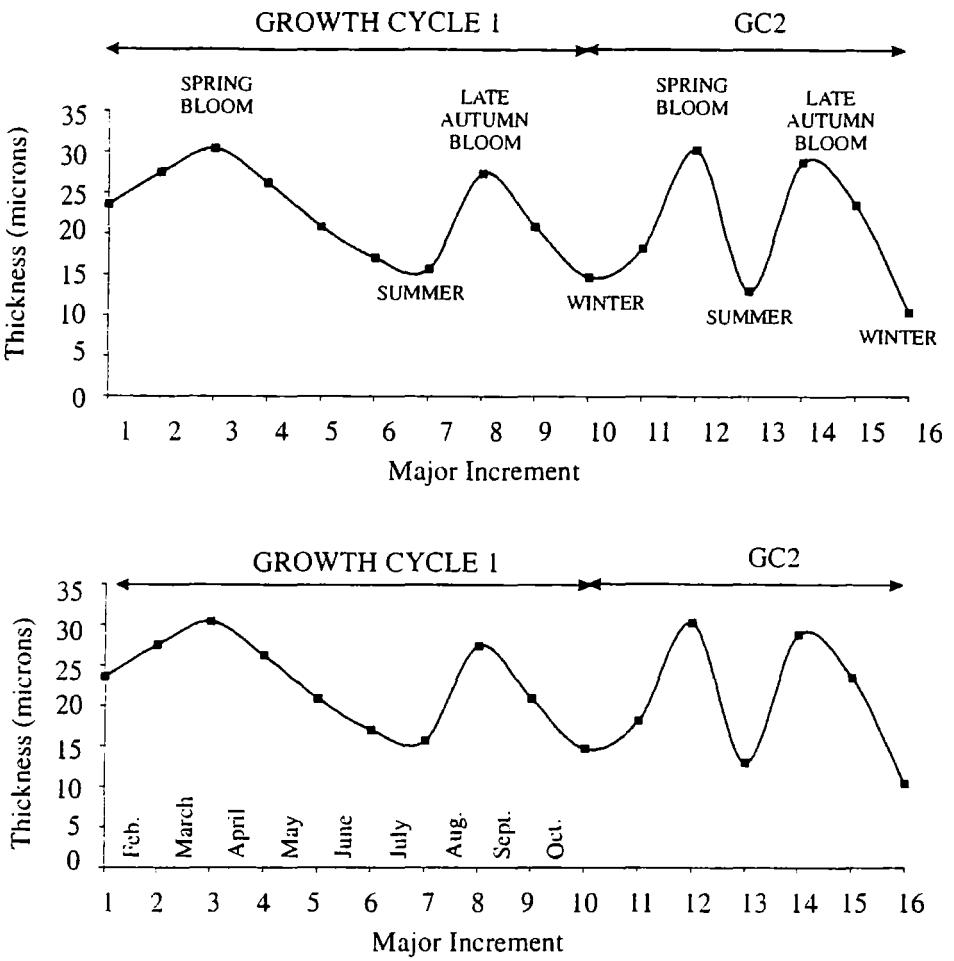

Text-Figure 2.20.2 Calibrated growth plots for *Drepanodus* (specimen 692/14). Dotted vertical lines mark the major increments. The upper diagram shows the proposed correlation between peaks of growth and the marine productivity blooms. The lower diagram shows the inferred positions of the months represented by each major incremental break.

It is proposed that the peaks in the growth plots for *Drepanodus* correspond to the spring and autumn blooms in productivity. This specimen therefore shows a total of two complete growth cycles the first of which is expanded relative to the second.

A similar interpretation can be made for the calibrated growth curves for *Protopanderodus* specimens 667/21 and 979912D, although both these elements show only one growth cycle consisting of two peaks (Text-figures 2.20.3 & 2.20.5).

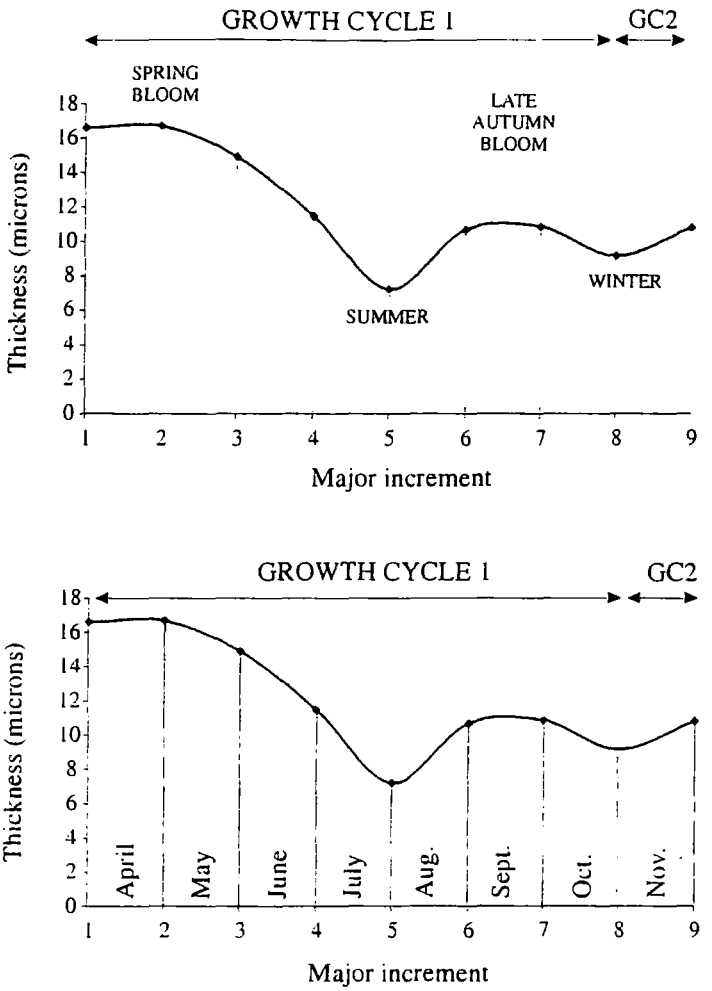

Text-Figure 2.20.3 Calibrated growth plots for *Protopanderodus* (specimen 668/21). The upper shows the inferred position of the spring and autumn bloom which correspond to the peaks of growth.

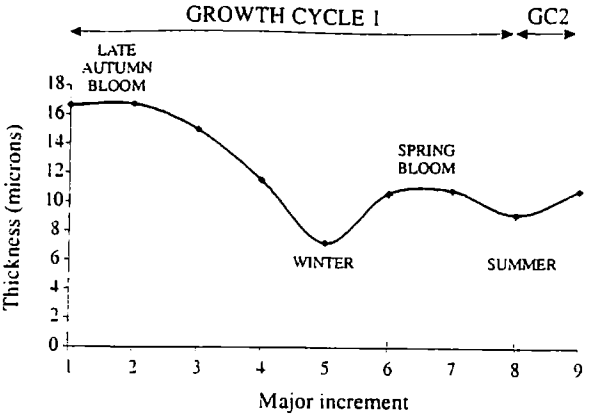

Text-Figure 2.20.4 Alternative interpretation of the *Protopanderodus* major increment plot.

Text-figure 2.20.5 shows an alternative interpretation (using the same basic assumptions) for specimen 668/21. This interpretation is necessary as it is as yet unclear when the elements initiated growth and whether this initiation was synchronous within populations, genera or species.

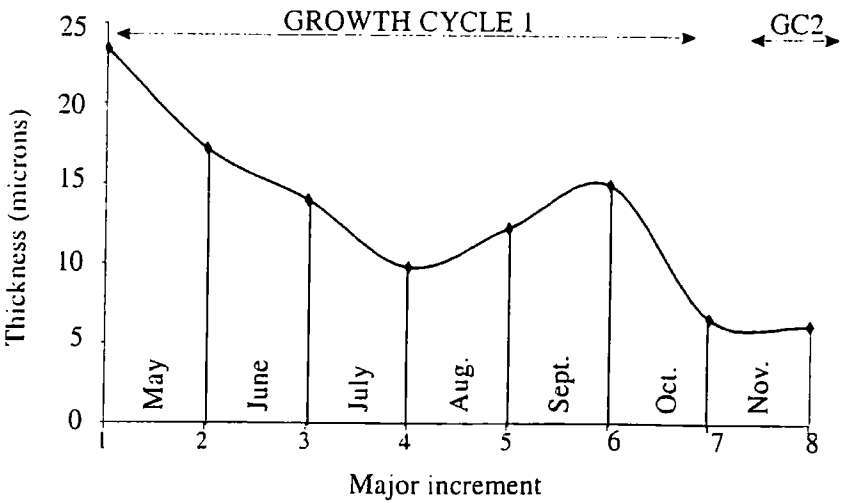

Text-Figure 2.20.5. Calibrated growth plot for *Protopanderodus* (specimen 979912D) outer major increments

2.21 Wider Implications

Tyler (1988) postulated that one of the most effective ways of determining if seasonality occurred in the physiology of deep-sea species would be to examine their reproductive biology. Seasonal stimulated reproduction has been documented in molluscs (Rokop, 1974), echinoderms (Tyler & Gage, 1979,1980), anemones (Van-Praet, 1983) and spider crabs (Hartnoll & Rice, 1985). There is, therefore, some evidence that reproduction is determined by seasonality in some deep-sea species, this being indicated by a larger number of juveniles during the summer compared to the winter (Schoener, 1968). The study of reproduction of deep-sea vertebrates is less well documented. In deep-sea fish, rhythmic activity and behaviour has been related to a number of factors. In many species of macrurids, spawning has been seen to occur in March, April-May, although sometimes this can be extended to October (Gordon, 1979).

If the growth cycles from the *Drepanodus* and *Protopanderodus* data are compared to the seasonal changes in productivity then this implies that larger scale growth peaks may relate to the spring and autumn blooms, or more likely, correspond to times at when the energy from such peaks reaches the deep-sea.

Two hypotheses prevail for the relative duration of growth – functional phases in conodonts.

1. Short growth periods followed by extended functional periods (Donoghue & Purnell, 1999) or,
2. Long growth phases followed by short functional phases.

The first hypothesis predicts that in the case of the coniform genera analysed, they grew over a period of 7-10 days and elements were functional for the remaining days of that month. This hypothesis is favoured. Therefore, it is inferred here that because the major increments have a periodicity approximating to one month, the growth function cycle is 7-10 days growth followed by 20-23 days of function. Major discontinuities in these coniform taxa therefore delimit functional periods. If the patterns described for *Parapachycladina* (Zhang *et al.*, 1997) were interpreted using the same basic assumptions, then this indicates that growth patterns in these two distinct conodont groups were remarkably similar.

2.22 Introduction to *Periodon* growth analyses

Periodon is a prioniodinid conodont and is the most abundant non-coniform species in the *Protopanderodus-Periodon* RSA or Biofacies. Although the morphology of *Periodon* elements is more complicated than that of *Drepanodus* and *Protopanderodus*, *Periodon* elements still appear to display simple 'cone-in-cone' growth (Type I *sensu* Donoghue, 1998) by outward accretion. *Periodon aculeatus* elements are consistently smaller than those of the coniform taxa in the same sample.

2.23 Microstructure of *Periodon* (specimen number 110996D)

Text-Figure 2.23.1. Photomicrograph illustrating the whole *Periodon* M (110996D) element showing growth increments in both the basal cavity and across the recessive basal margin. Scale bar = 50µm

This *Periodon* specimen (110996D, Text-figure 2.23.1.) only consists of 9 increments (Table 2.23.) observed either in the basal cavity or across the recessive basal margin. Close inspection of such increments in a number of specimens shows no apparent sub-division (Text-figure 2.23.2).

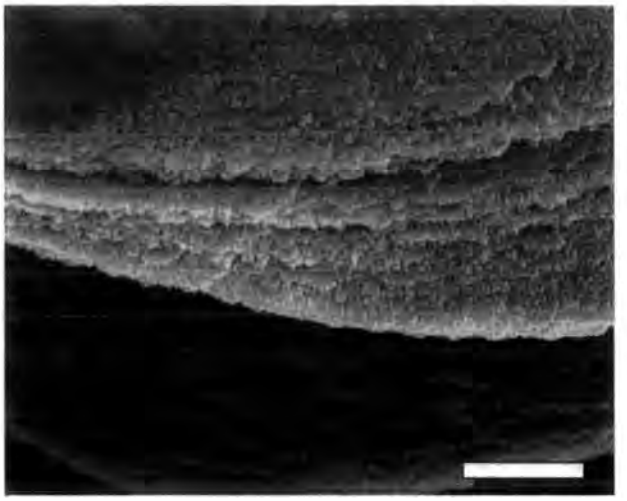

Text-Figure 2.23.2. Photomicrograph of increments in the basal cavity of the *Periodon* element (110996D) shown in Text-figure X. Scale bar = 10µm.

Table 2.23

Increment number (cycle)	Raw thickness of increment (microns)
1	1.8
2	4.4
3	4.4
4	5
5	6.3
6	3.1
7	2.5
8	2.5
9	1.8

Table 2.23. The raw increment thickness in a single M element of *Periodon aculaetus* (110996D)

Individual increments in this one specimen range in width from approximately 1.8 up to >8.5µm. The average width of increments was calculated to be approximately 3.5µm. In this specimen the basic unit of growth is considered 1.8µm. Following the methodology applied for *Drepanodus* and *Protopanderodus* then it is possible to calculate the duration of growth for a number of alternative scenarios.

2.24 Theoretical Increment Duration for *Periodon*

Table 2.24

Specimen	BUG (basic growth unit)	Total no. of Increments	Total number Of BUGs	Growth rate 1	Growth rate 2	Growth rate 3
110996D	1.8	9	35	35 days	35 months (2.9 year)	35 years

Table 2.24. Theoretical increment duration for Periodon. Growth rate 1 assumes 1BUG = 1 day, growth rate 2 assumes 1BUG = 1 month and growth rate 3 assumes 1BUG = 1 year.

It is therefore considered that each increment represents a one-month growth-functional cycle (as shown for *Drepanodus* and *Protopanderodus*). Fischer plots of growth increments in the *Periodon* element 110996D (Table 2.23) are based on a much smaller data set than was available from the *Protopanderodus* and *Drepanodus* elements. The Fischer plot shows a steady increase in growth rate from increments 1 to 3 and then a sudden shaper increase between increments 3 and 5. There is then a gradual decline ranging from increments 5 to 9 (Text-figure 2.24.1 top).

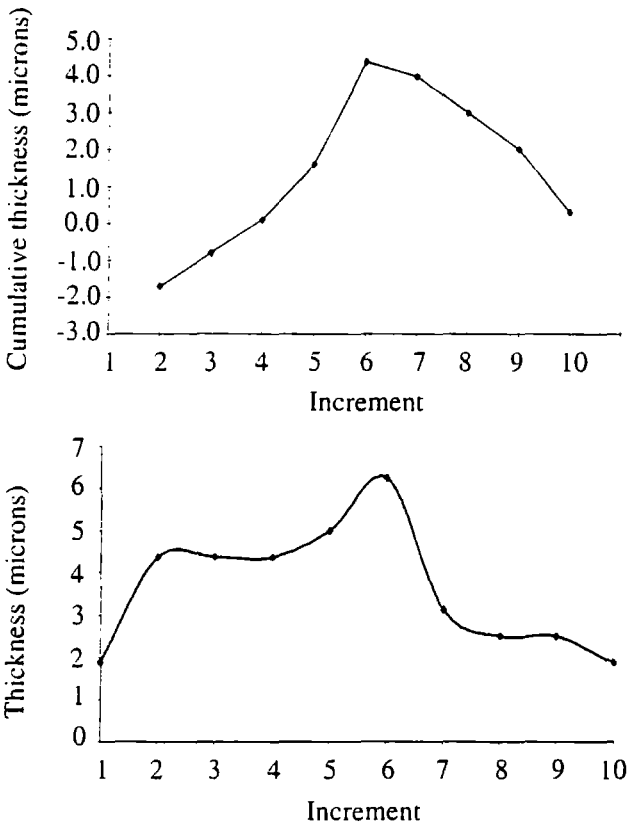

Text-Figure 2.24.1. Fischer plot of the increment thickness data for *Periodon* specimen 110996D (top). Simple growth curve for *Periodon* specimen 110996D. Increment number (first formed =1) on the x-axis plotted against the thickness of the increment on the y-axis (btm.)

The growth curve for *Periodon* 110996D (Text-figure 2.24.1 btm.) shows an increase in increment thickness between the first and second increments. The second peak occurs at increments 5 and 6 followed by a decline in thickness between increments 7 and 10.

2.25 Preliminary interpretation

It appears from the Fischer analysis that there is only one peak in this data. This is likely to be a result of the small number of data points used in this analysis. This data can therefore be considered in one of two ways, either;

1. the data represents 1 part of what has previously been inferred to be a complete growth cycle or,

2. cyclicity like that observed in *Drepanodus* and *Protopanderodus* is not apparent in *Periodon* elements.

To confirm which is the case, further analyses were conducted on a number of *Periodon* elements (Table 2.25). Therefore additional, growth data have been obtained for a number of *Periodon* elements in this sample. As demonstrated, all elements of *Periodon* studied have been found to possess far fewer incremental growth lines than the coniform taxa, usually between five and ten in each element. Within the sample studied, no elements have been found showing fewer than five major incremental growth lines and it is likely, therefore, that smaller elements than this are not represented or preserved.

The widths of individual major increments were measured in six *Periodon* M elements. The width of each increment was then plotted against the increment number starting with the first formed as previously described. This information (shown in Table 2.25), like that from the previous genera, was used to plot a series of simple growth curves (Text-figures 2.25.1. & 2.25.2.).

Table 2.25

Sample Increment No.	110992D (µm)	110993D (µm)	110995D (µm)	110996D (µm)	110998D (µm)	1109910D (µm)
1	7	2.9	1.5	4.5	5	5
2	6.7	4.3	3.1	4.5	5	8.6
3	4	2.9	4.6	4	3.5	6.4
4	2.7	4.3	1.5	4.5	2.5	4.3
5	3.3	2.9	0.8	5	1.5	2.1
6		2.9	2.3	3	1.5	
7		10	1.5	3	1	
8		5.7	3.9	2.5	0.5	
9		2.9	3.1	3		
10			3.8	1		

Table 2.25. Table of the data from *Periodon* element samples where 1 is the first formed increment and 10 is the last formed increment (youngest). Increment thickness values are in microns.

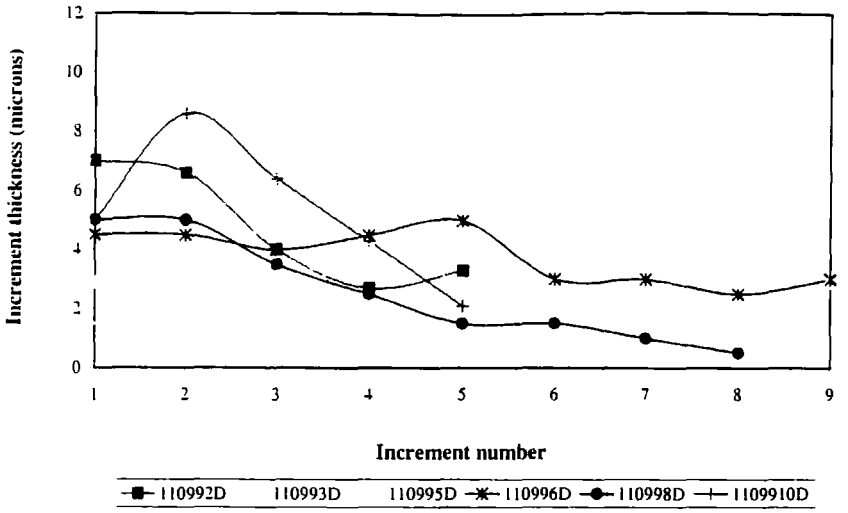

Text-Figure 2.25.1. Shows the complete data set for growth increment width of six *Periodon* samples (all M elements) plotted against the increment number (increment 1 is first formed, or youngest increment, increment 10 is the oldest or last formed increment). This figure assumes that growth was initiated at the same time in all elements.

Each of the data sets shown in Text-figure 2.25.1 (Table 2.25) has been plotted as a separate growth curve (Text-figure 2.25.2). The patterns of each of these are summarised below;

110992D shows an initially high growth rate followed by a rapid decline to a cessation of growth at increment five.

110993D shows three growth peaks in total across ten growth increments measured. The peaks correspond to increments 2, 4 and 7. Growth ceases at increment 9.

110995D shows three growth peaks across ten growth increments. The peaks correspond to increments 3, 6 and 8. Growth ceases at increment 10.

110996D shows three growth peaks across a series of ten growth increments. The peaks correspond to increments 5, 7 and 9. Growth ceases at increment 10.

110998D shows two growth peaks across a total of eight major increments. Peaks occur at increments 2 and 6. Growth ceases at increment 8.

1109910D shows initial rapid increases in growth at increments 2 and 3 followed by a rapid decline. Growth ceases at increment 5.

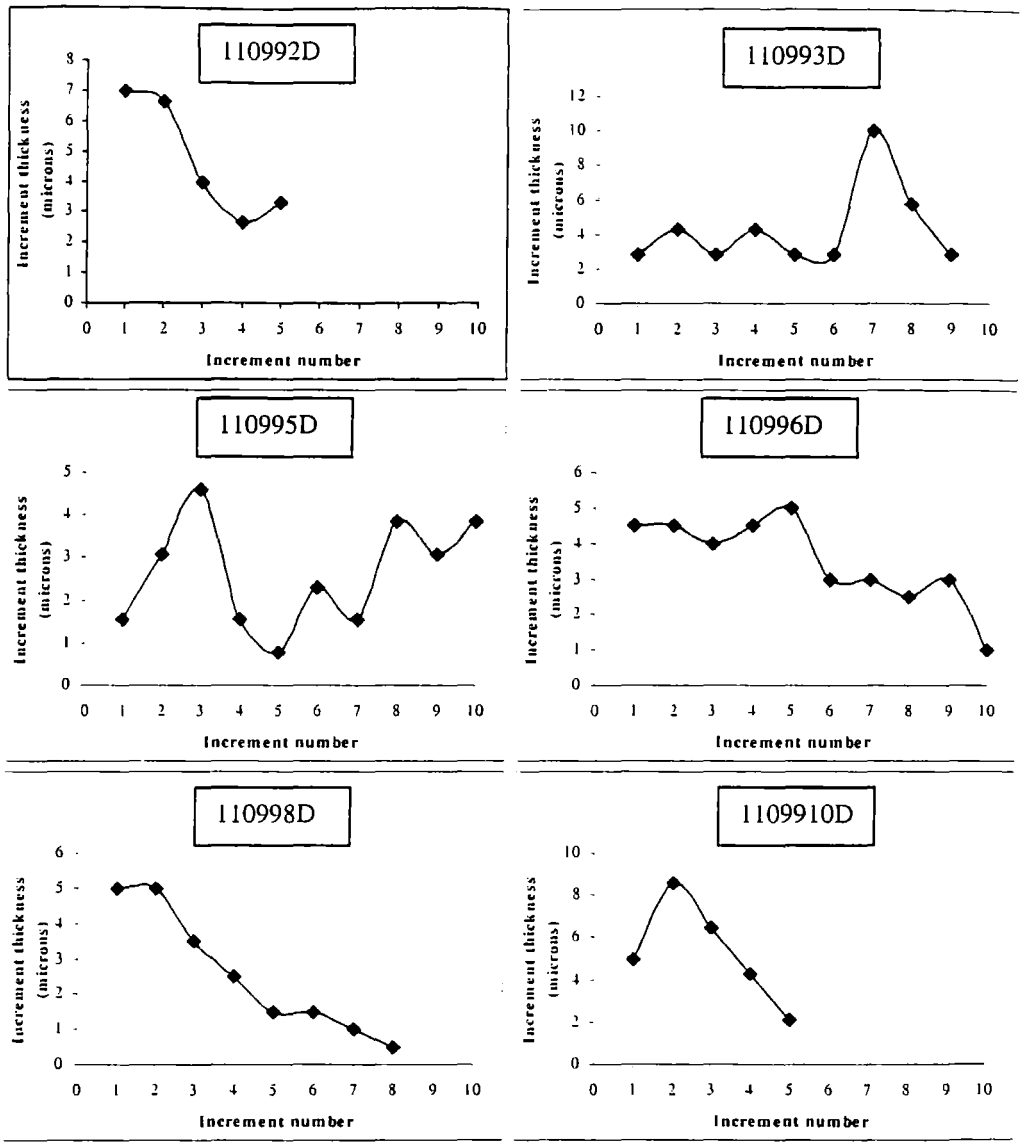

Text-Figure 2.25.2. Growth curves for the incremental thickness of specimens of the M element of *Periodon aculeatus* listed in Table 2.25. 1 is the first formed (youngest increment).

The general pattern of growth appears to be an initial peak followed by a decline. Several of the graphs show similar peaks and troughs, up to three in any one specimen. The growth pattern of *Periodon* is not simple but consists of one or multiple peaks.

The same hypotheses are presented for the relative duration of growth and functional phases in *Periodon* as were for the coniform taxa (Text-figure 2.25.3).

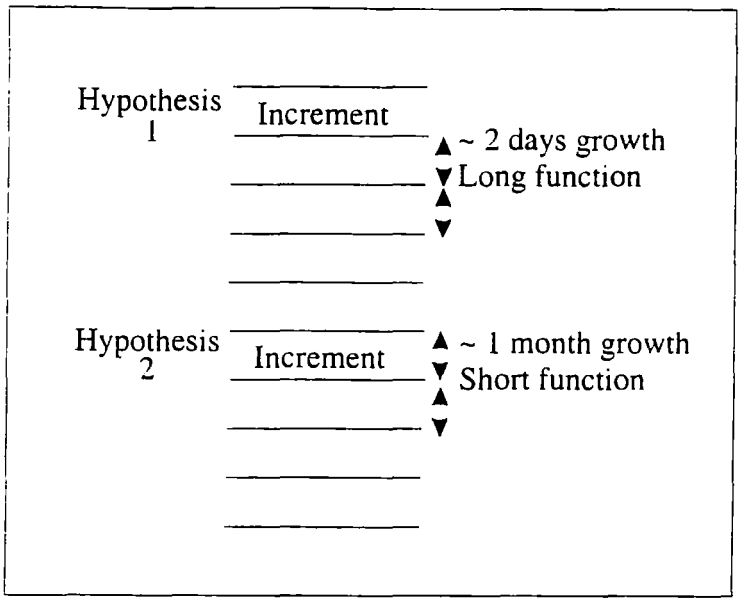

Text-Figure 2.25.3. The hypotheses for growth –functional cycles in *Periodon*.

1. Short growth over a period of approximately two days followed by a period of long function (up to 28 days i.e. increments represent 1 month growth and function in total)
2. Long growth over a period of a month followed by short functional episodes.

Most, if not all, vertebrates secrete enamel increment units in 1-2 days (Risnes, 1998). Therefore, by conservation of biochemistry, hypothesis one is favoured.

2.26 Interpretation of the *Periodon* growth analyses.

Polycyclic growth is less convincing in *Periodon* than the coniform taxa. Following the same basic assumptions of enamel secretion rate applied to specimens of *Drepanodus* and *Protopanderodus*, the increments in *Periodon* could approximate to daily growth within a monthly or other cycle. One interpretation of the *Periodon*

growth curve is provided in Text-figure 2.26.1. The growth curve and the positions of the month as interpreted using the assumption that each basic increment approximates to one day of crown enamel secretion and then the element spent the remainder of the month functional, each incremental discontinuity therefore delimits this functional period.

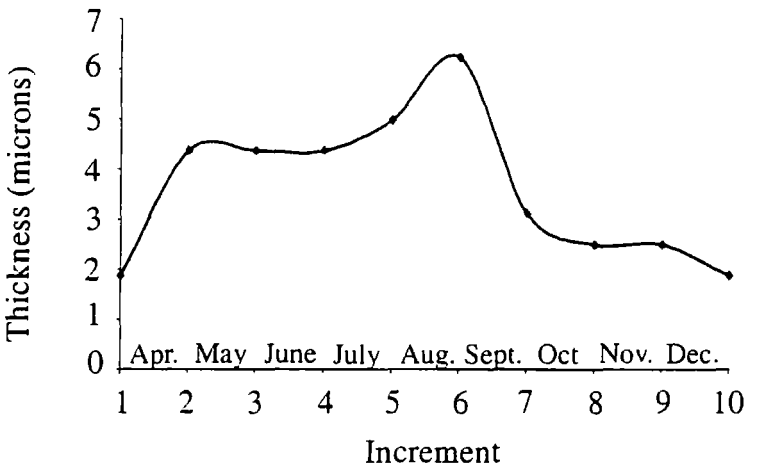

Text-Figure 2.26.1. Calibrated *Periodon aculeatus* (specimen 110996D) growth curve.

The small peak of growth (Text Figure 2.26.1. Increment 2) is observed to occur and this is inferred to correspond to the spring bloom in productivity. However, a second larger peak also occurs in the autumn before a decline during winter months.

2.27 Preliminary Implications

The preliminary implication these data sets provide is that growth in deep-water conodonts is related to feeding episodes and rate of growth is ultimately limited by the amount of food available. This further implies that, as a result of increases in surface productivity during spring and autumn, conodont element growth is accelerated.

However, the growth patterns observed can be fundamentally related to endogenous circadian rhythms with an overall hormonal control i. e. growth is controlled by physiological rather than environmental stimuli. Because organism

growth patterns are complex it must be assumed here that secretion of conodonts is largely controlled by endogenous circadian rhythms which can be entrained and accelerated by additional stimuli from feeding episodes.

The coniform taxa (specimens 667/21, 979912D & 692/14) comprise large numbers of minor increments which appear to have been secreted in approximately 1 day. Each major discontinuity (or increment) represents the functional phase and divides grouped minor increments in sets of 7-10. Therefore, coniform taxa appear to grow over a period of 7-10 days and are then functional for the remainder of the month. The *Periodon* element (specimen 110996D) however, comprises <10 increments with a mean increment thickness of 3.2μm per increment (min. 1.8μm, max. 6.3μm). There is no differentiation of these increments into minor and major increments. It is likely that these represent similar growth episodes of approximately 2-3 days with an apparent feeding period of approximately once per month.

Coniform taxa show continued addition of lamellae throughout a two-year growth cycle and growth patterns that appear to be correlated with seasonal fluctuation in nutrient influx. The growth of *Periodon* is best explained as short periods of secretion followed by long breaks.

In all taxa growth cycle 1 is typically expanded relative to later cycles. This observation implies that growth of some elements is faster in the first cycle relative to the second. High initial growth rates would increase survival rates in juveniles (Radtke & Kellerman, 1988) and increase the ability to utilise larger prey items earlier in ontogeny.

Smith & Baldwin (1984) and Smith (1986) showed how the *in situ* rates of oxygen consumption (and hence metabolism) in benthic communities were highest in the early summer and lowest in the winter. They related these variations to changes in food supply (i.e. the sinking of organic matter) inferring that total community metabolism showed seasonal variation in phase with surface-ocean productivity. It has also been recognised that an additional consequence of seasonal pulses to the deep-sea was that of stimulating reproduction and seasonal growth in deep-sea organisms (Gage & Tyler, 1991). Growth in mid-Ordovician deep-water conodonts appears to have been entrained by seasonally-controlled nutrient influx. This would

indicate a seasonal climate in "sub-tropical" latitudes, a feature at variance with the present day.

Nutrient supply and feeding events are the primary factors entraining growth and behaviour in deep-sea organisms. This preliminary study of growth in deep-water conodont species has indicated differential growth in two major conodont clades.

Deep-sea organisms are known to have reduced physiologies, growth rates and metabolic rates as a consequence of living in a lower temperature, high-pressure and low-energy environment (Gage & Tyler, 1991). Seasonal and relatively low nutrient input into the deep-sea places specific demands on deep-sea faunas. Organisms have therefore adopted contrasting life strategies and behaviour. For example, evidence of food hoarding and caching in the deep-sea was documented by Jumars *et al.* (1990). Although restriction of food input into the deep-sea environment should favour selection of long-lived organisms, Jumars *et al.* (1990) provided evidence of a contrasting life-strategy for deep-sea organisms where material would be assimilated rapidly and consequently population growth should also be rapid. This strategy would be best adopted and most effective for small organisms with rapid growth rates.

Constant grazing and active predatory lifestyles are typical deep-water feeding strategies. Macrurids dominate the benthic fish species and are found at or near the ocean floor. They feed with protrusible jaws on both swimming and motile prey adopting a tail-up nose-down posture for foraging the sediment surface (MacDonald, 1975). Active swimming predators or scavengers include the jawless hagfish, which rely on large nektonic food falls. In contrast, 'sit and wait' predators rely on the occurrence of occasional food falls, dominating modern high latitude waters.

Assuming feeding stimulated accelerated growth in conodonts then the two deep-sea conodont genera could have exhibited these different feeding strategies. These can be compared to those observed in modern deep-sea fish (e.g. MacDonald, 1975; Stowe, 1987). The abundance of morphological evidence described in the literature has suggested that conodonts were active swimming predators with either a pelagic or nektobenthic mode of life (e.g. Briggs *et al.*, 1993; Gabbott *et al.*, 1995;

Sansom, 1992). However, in light of the data presented in this thesis, this appears to be an over generalised approach to conodont palaeobiology.

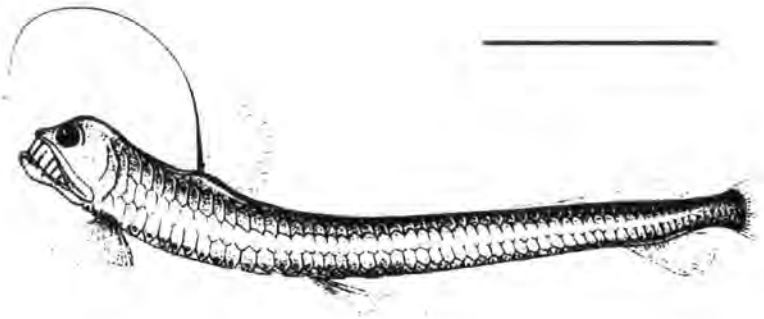

Text Figure 2.27.1. Shows the body plan of the benthopelagic Viperfish. Scale bar = ~10 cm (drawn from Stowe, 1987).

The Viperfish has a body plan typical of many benthopelagic active predatory fish. It has an elongated body form with large eyes. It has a reduced head in contrast to some 'sit and wait' predators, although it has large teeth in relation to the size of its body. The teeth of active benthopelagic deep-sea fish are often observed to be larger than those of benthic fish (Stowe, 1987). Evidence suggests that, in general, conodont animals may have had a similar body plan.

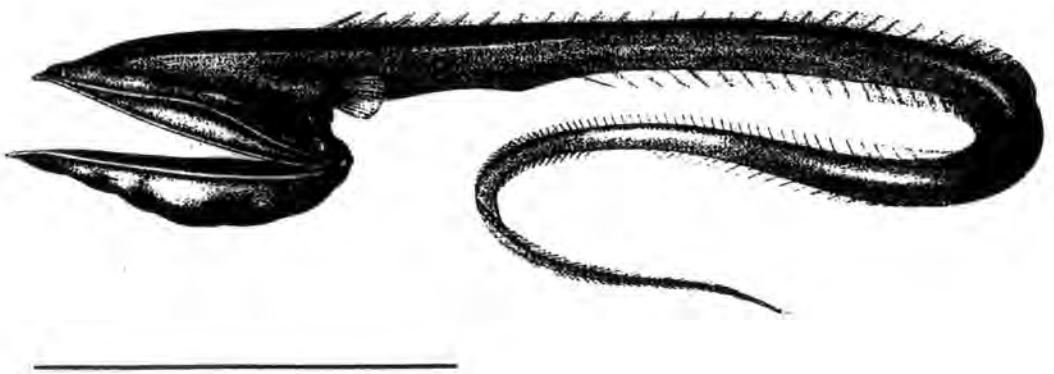

Text Figure 2.27.2. The body plan of the Gulper eel showing the reduced body size but enlarged jaws. Scale bar = ~10 cm (drawn from Stowe, 1986).

The Gulper eel is a deep-sea carnivorous fish. In contrast to the life-style of the Viperfish, the Gulper eel is a 'sit and wait' predator. It has several morphological adaptations to enable it to exploit the deep-sea environment in this way. Although the Gulper eel has an eel-like body much like that of the Viperfish, it can be seen to have a markedly enlarged head. This enables the Gulper eel to maximise the few food resources that become available to it. 'Sit and wait' predators rely on the occurrence of occasional food falls. Many deep-sea fish have adopted forms with enormous jaws and an ability to take in large prey. This is believed to counteract the fact that feeding is one of the main problems and limiting factors of dispersion in the deep-sea (MacDonald, 1975).

Therefore, rapid growth to exploit opportunist food falls, slow growth and low metabolic rates are all predicted adaptations for a deep-water nektobenthic mode of life (Gage & Tyler, 1991).

2.28 Conodont adaptations to a deep-sea mode of life – preliminary conclusions

Two of the adaptations found in living deep-water species, namely rapid initial growth and a variety of feeding strategies directed at utilising limited food resources, are found in deep-water conodonts of the North Atlantic Realm. Growth analysis thus suggests the differences in morphology and growth patterns in *Protopanderodus/Drepanodus* and *Periodon* reflect different metabolic rates and modes of life. Based on the assumption that minor increments approximate to 1 day of crown enamel secretion, and major increments or discontinuities to one-month time duration, then *Protopanderodus* and *Drepanodus* appear to have the same basic pattern of growth. That is, on average, 7-10 days of growth followed by eruption and function for 20-23 days. The presence of numerous major discontinuities (up to 16 in *Drepanodus* and 9 in *Protopanderodus*) indicates that the coniform taxa throughout underwent several distinct growth and functional stages. Using the same basic assumptions, it appears that *Periodon* went through only 2 days of growth followed by up to 28 days of function.

Therefore, the coniform taxa *Protopanderodus* and *Drepanodus* have an identical pattern of growth to *Parapachycladina* - a shallow water taxon of the early

Triassic (Zhang *et al.*, 1997). This may indicate that *Protopanderodus* and *Drepanodus* had their evolutionary origins in shallow waters or are living in shallow water depths i.e. they are pelagic. *Periodon* has a much slower growth rate (hence metabolism) than the coniform taxa suggesting this ramiform conodont was deep-water nektobenthic in habit. It is postulated that this data predicts all deep-water nektobenthic taxa should show reduced growth rates and therefore relatively small numbers of growth increments compared to coniform and shallow water conodont taxa. Growth rate reflects metabolic rate and clearly there are two groups of conodont animals present in the sample analysed in the *Protopanderodus-Periodon* biofacies. High growth rates and therefore high metabolism possibly reflects the planktonic/nektonic nature of the coniform taxa *Drepanodus* and *Protopanderodus*. It is further postulated that the lower growth rate (and therefore metabolic rate) of *Periodon* may reflect its deepwater nektobenthic mode of life.

Metabolic rate reflects habitat and mode of life. Therefore, the measuring of growth rates and patterns is potentially a powerful tool for differentiating mode of life in conodonts and separating those species that had their evolutionary origins in shallow or deep-water environments.

Part II – Chapter 3

3. Growth of conodont elements

3.1 Introduction

Conodonts are histologically similar to teeth and data from deep-water conodont genera (*Drepanodus* and *Protopanderodus*) indicates the addition of crown enamel minor increments on a daily rate. Longer-term growth cycles were entrained by abiotic factors, particularly feeding cycles. Current hypotheses to explain growth in shallow water conodont species indicate a cyclic alternation of short periods of growth followed by longer periods of function and wear (Donoghue & Purnell, 1999). The presence of wear discontinuities within some conodont elements clearly indicate that elements could be periodically withdrawn into an epithelial pocket and additional lamellae added and that elements were retained through the life of the animal.

Following this model, the growth patterns in *Drepanodus* and *Protopanderodus* suggest that retraction and growth was also occurring in these deep-water species. This observation has biological implications for conodont growth models and hence by implication, the origin of the earliest parts of the vertebrate skeleton.

3.2 Model systems of growth in Vertebrates

Conodont animals were the first vertebrates to mineralise their skeleton. The crown of conodont elements is composed of enamel and white matter and the basal tissue, although variable between clades, can be homologised with types of cellular bone or dentine (Sansom *et al.*, 1992, Donoghue, 1998). White matter is currently best viewed as being a dentine-related tissue unique to conodonts (Donoghue, 1998).

Tooth (or dental) tissues are part of the dermal skeleton as components, which differentiate within the dermis. Enamel is restricted to the teeth of all tetrapods but distributed in all dermal tooth-like structures (e.g. odontodes) and in the scales of fish. The origin of enamel is distinct from the other dermal hard tissues as 'true' enamel (as defined for mammals) is formed from the epidermis and involves

the use of specific proteins (e.g. enamelins and amelogens). Enamel has no collagen in its extracellular matrix. In contrast, dentine is a mesodermal, mineralised connective tissue with an organic matrix of collagenous proteins. Dentine is characterised by centripetal deposition around the pulp cavity close to the epidermis but below the enamel (for a full review see Ten Cate, 1989; Carlson, 1992)

Conodont elements functioned as teeth (e.g. Purnell, 1995) so the hypothesis that teeth evolved from dermal denticles linked with the origin of jaws may therefore no longer be valid, as conodont 'teeth' appear first in the fossil record. An alternative is that teeth and scales may both be alternative manifestations of a common morphogenetic system (Smith & Coates, 1998).

Biochemical systems and ontogenetic development sequences are extremely complex processes and once evolved are retained through evolution. It should therefore be possible to apply aspects of known vertebrate growth models to conodonts. A common constraint on skeletal growth is that it is non-intussusceptional (Francillon-Vieillot *et al.*, 1992). This means that skeletal growth will not occur by expansion of hard tissues within and growth must occur by the deposition of the new hard tissues on 'free' surfaces. This is termed appositional or accretional growth. Growth patterns are therefore recorded in the mineralised tissues of vertebrates. Such growth patterns must be accounted for when developing a model for conodont element growth.

Patterns of vertebrate growth can be characterised into two types; continuous or cyclical. In the former, growth curves will progressively change but always with positive rates and without cyclical influences. The latter, cyclical growth, is characterised by regularly changing growth rates according to one or several cycles (daily, yearly, lunar, seasonal) with the growth rate possibly reaching zero once in every cycle. Conodonts clearly display cyclical growth patterns.

Growth can also be characterised in terms of whether it is definite or indefinite. In definite growth, growth only occurs at an early phase of the animal's life so once the animal attains adult size, the growth rate drops to zero. Indefinite growth describes the situation when some growth can occur as long as the animal is alive. With the onset of sexual maturity, this growth rate may drop dramatically but will not totally cease.

As present it is unclear whether growth of conodont elements was terminated by death or the onset of sexual maturity. Until a clear link is established between conodont element and somatic growth conodont element growth should be characterised as "retractional" cyclic growth. The growth of mammalian dental enamel provides the best studied and homologous (?) model system for conodont enamel growth.

Vertebrates exhibit two modes or styles of growth when producing parts of the dermal skeleton (with dental tissues) such as teeth, odontodes and scales. Complete formation of the 'tooth' within the (dental) papilla followed by eruption and function ("definite growth") and continual growth of the structure throughout life ("indefinite growth"). The latter is often facilitated, in the case of scales, by retraction of structures into the epidermis post-function.

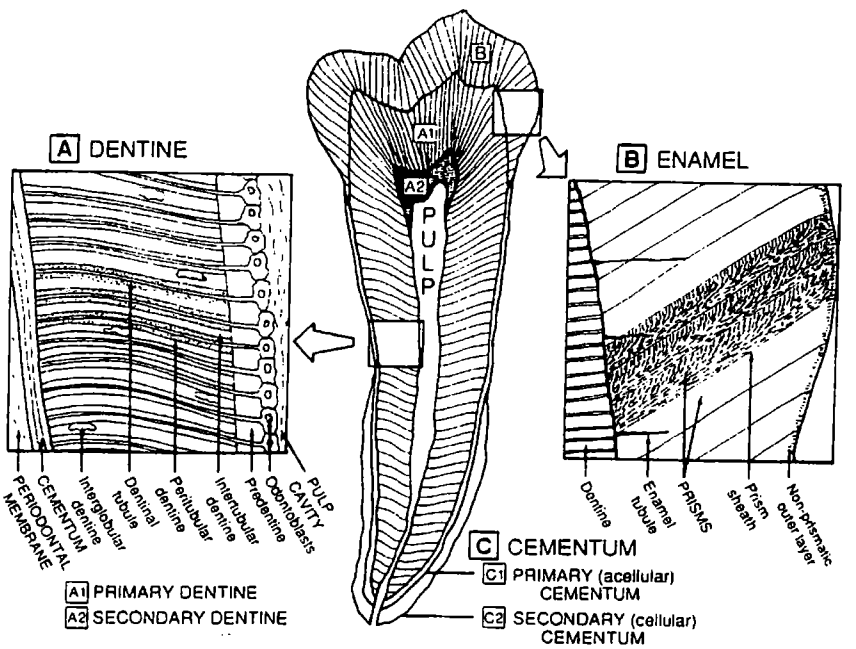

Text-Figure 3.2.1 The components and structure of vertebrate teeth (drawn from Carlson, 1992). A. Shows the lamella structure of the dentine and its relationship to the cementum (left) and the pulp (right). B. Shows the lamella micro-and ultrastructure of the crown enamel and its relationship to dentine.

An example of 'definite', cyclical growth in the vertebrate record is the formation of permanent teeth in humans and other vertebrates. Mammalian teeth are composed of three tissues, enamel, dentine and pulp. Enamel forms a hard, brittle tooth crown, which surrounds the inner layer of dentine and central pulp cavity (Text-figure 3.2.1.).

The development of a mammalian tooth can be divided into a series of events as illustrated in Text-figure 3.2.2. and the general principles of tooth development are synthesised from Carlson (1992).

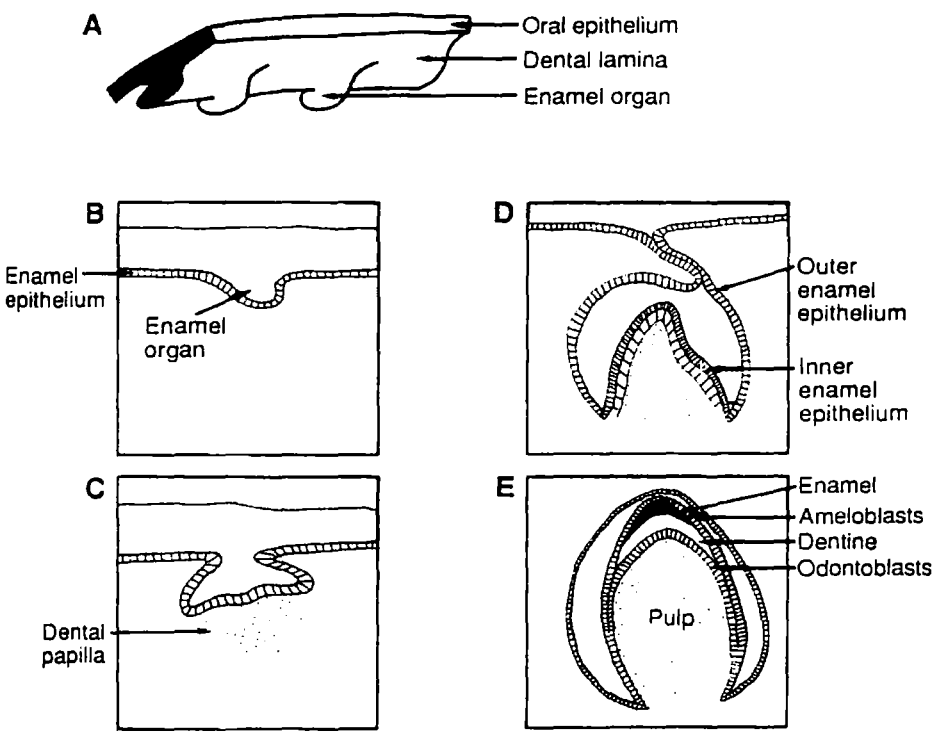

Text-Figure 3.2.2. The developmental stages of a mammalian tooth (drawn from Carlson, 1992)

The oral epithelium differentiates (Text-figure 3.2.2, A). Tooth development in mammals begins with the proliferation of the epidermal cells of the

oral epithelium. This forms a tooth bud. The tooth bud is connected to the oral epithelium by a band of cells that make up the dental laminae. In amphibians and reptiles this structure is persistent and successive tooth germs are budded off from the dental laminae. In contrast, mammals produce only one tooth germ from the dental laminae per tooth locus and permanent teeth are budded off from the corresponding deciduous (milk) teeth. A fold develops called the dental lamina and this develops an oral epithelium and the enamel organs appear along the dental lamina (Text-figure 3.2.2. B). Ectodermal tissues of the enamel organ (from which the enamel will develop) are now located adjacent to the mesodermal tissue (which proliferates to form the dental papilla (Text-figure 3.2.2.C). Cellular processes result in the formation of a dental papilla and the developing dental follicle gives rise to the supporting tissues of the tooth. The enamel organs differentiate and dentine and enamel begin to mineralise soon afterwards (Text-figure 3.2.2. D&E).

The dental organ, papilla and follicle constitute the tooth germ. Continued growth of the tooth germ leads to histo- and morpho-differentiation. Histo-differentiation involves the transformation of epithelial cells into morphologically and functionally distinct components. The cells bordering the dental papilla divide into two histologically distinct components; the internal dental epithelium and the stratum intermedium and ultimately these are both responsible for the formation of the enamel forming the outer cap of the tooth (Ten Cate, 1989).

Odontoblasts are dentine-producing cells and their activity results in the formation of dentine at the sites of future cusp tips of the tooth. Odontoblasts elaborate the organic matrix of dentine, collagen and ground substance and these eventually mineralise. After formation of the first dentine, the cells of the internal epithelium differentiate. This enables them to perform a secretory role producing an organic matrix against the newly formed dental surface. This surface is later mineralised and forms the enamel of the tooth crown. The ameloblasts (enamel producing cells) move away from the dentine leaving behind an increasing thickness of enamel. Therefore dentine forms from the enamel dentine junction (EDJ) towards the centre of the tooth and enamel forms from this junction towards the outside of the crown (Ten Cate, 1989).

The mechanism of initial mineralisation in enamel is thought to be an extension from the apatite crystals of dentine. In newly formed enamel, hydroxyapatite crystals are randomly produced and interdigitate with crystals of dentine to produce a structureless layer of enamel. The ameloblasts now move away from the EDJ. Secretion of enamel subsequently becomes staggered and produces two differing enamel types, interrod and rod enamel. The structured layers continue to form until the final few enamel layers are deposited. The final layers, like the initial ones, are frequently structureless. The production and mineralisation of the organic matrix of any hard tissues, including dentine and enamel are phasic and result in the production of incremental lines (Carlson, 1992). During the alternating periods of activity and rest the nature of the organic matrix varies and results in variations in the degrees of mineralisation observed.

After the enamel forms it continues to change structurally and chemically, a process known as maturation. However, dentine formation can continue throughout the life of the tooth because extensions of the odontoblasts are contained within the dentinal tubules (although it is not remodelled). Conversely, when enamel is mature, it is no longer in contact with the cellular elements and formation ceases.

The two hard tissues of vertebrate teeth, enamel and dentine, do not remodel (Carlson, 1992). The incremental lines in the crown of the tooth therefore record a fixed pattern of the individual's metabolic history. Minor physiological changes are, however, recorded in the enamel and dentine as accentuated incremental lines. True growth bands at several spatial scales have been recognised in mammalian dentine and can provide evidence of growth cycles that relate to physiological or environmental changes occurring during growth (Carlson, 1992, Risnes, 1998, Fitzgerald, 1998). Dentine mineralisation may also respond to external stimuli (e.g. light, temperature and food availability) that can also vary on daily, monthly, seasonal or yearly cycles (Carlson, 1992).

Teeth grow *in vivo* and then become functional. In the mammalian tooth model, once eruption has occurred and the element becomes functional the destruction of the enamel organ occurs and the tooth cannot re-grow. If elements were subsequently damaged there would be no capability of repair in the crown enamel. However, abundant microstructual evidence exists to imply that conodonts

were capable of periodic growth and non-function or function and non-growth (e.g. Müller & Nogami, 1971; 1972, Jeppsson, 1976, Purnell, 1995; Donoghue, 1998; Donoghue & Purnell, 1999). Clearly in conodonts, eruption and function either does not destroy the enamel organ or the enamel organ re-forms.

Therefore, evidence suggests that the definite cyclical formative mechanisms of vertebrate dental enamel are not directly applicable to the growth mechanism of at least some conodont elements. However, the formative biochemical processes of enamel and dentine are clearly relevant.

Because of the difficulty of directly applying the mammalian tooth growth model to conodont elements, it is necessary to assess other vertebrate systems that produce dental hard tissues (i.e. dentine and enamel). Recent literature has proposed that conodont elements and their growth mechanisms offer closer comparison to vertebrate odontodes (Sansom, 1992; Smith *et al.*, 1996, Donoghue, 1998) and dermal scales (Donoghue, 1998) rather than vertebrate teeth.

Francillon-Vieillot *et al.* (1992) noted how odontodes have been recognised as the earliest constituents of the dermal skeleton. Elements of the dermal skeleton include odontodes, teeth, branchial denticles, dermal bone, scales, fin rays and fine spines, odontocomplexes and odontoderivatives (Huysseune & Sire, 1998; Appendix A for further definitions). As noted by Huysseune & Sire (1998, p. 444) even though odontodes (placoid scales) show differences in shape and size, and despite separate evolution for hundreds of millions of years, all odontodes are characterised by a dentine crown, surrounding a pulp cavity, all covered by a hypermineralised tissue.

3.3 Odontode structure, composition and formation

Odontodes are tooth-like structures and were first described by Ørvig (1976) as hard tissue units of the skin, which correspond to simple teeth and are difficult to distinguish from teeth by any rational criterion. Odontodes are well known in the placoid scales of selachians, in the placoderms and many primitive osteichthyans (Francillon-Vieillot, 1992).

Odontodes develop as independent tooth units on the surface of the dermal skeleton. Each odontode generally consists of a core of dentine (or dentinous tissue)

surrounding a pulpar cavity. A superficial layer of enamel or enameloid surrounds the dentine and the basal attachment is usually cellular or acellular bone. There is a wide variety of dentine found in both the teeth of vertebrates and the scales of fish, and enameloid, although superficially resembling enamel, is a specialised form of dentine (Francillion-Vieillot *et al.*, 1992). Enameloid is therefore a particularly hard dense hypermineralised dentine and appears to have both a mesodermal and ectodermal origin (Reif, 1979, Francillion-Vieillot *et al.*, 1992).

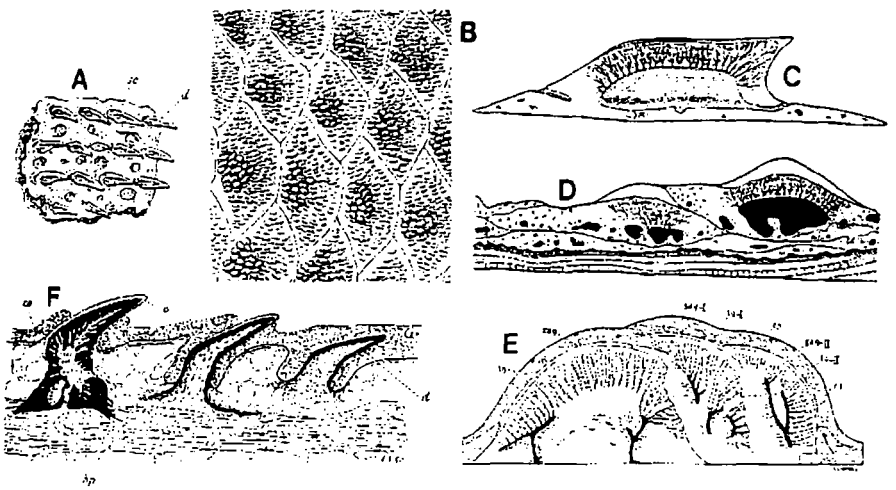

Text-Figure 3.3.1. Shows the elements of the dermo-skeleton, both odontodes and the odontocomplex. A. Odontodes from *Plecostomus commersonii*, B. Scales from *Latimeria chalumnae* with odontodes, C. Isolated odontode of a *Latimeria* scale. Shows an osseous basal plate, a pulpar cavity lined by dentine and its thin covering of enamel (or enameloid), D. Vertical section of a scale from *Latimeria* with two successive odontodes, E. Odontocomplex, with three odontodes and F. Three successive stages of development of a dogfish placoid scale (from right to left). Redrawn from Francillion-Vieillot *et al.* (1992).

The formation of odontodes takes place in an undifferentiated dental papilla of mesochymal tissue (Text-figure 3.3.1.F). This is bounded at its outer surface by an epithelial dental organ, which lacks the complicated structure of tooth germs and consists of a single layer of turgid columnar cells in the basal epidermis (Francillon-Vieillot *et al.*, 1992). Mesodermal tissue comprises the single dental papilla located in the upper part of the vascularised connective tissue (Carlson, 1992).

Odontodes are erupted after formation and are periodically shed and replaced throughout life. This is in contrast to odontocomplexes. Odontocomplexes have been defined as, 'an agglomeration or cluster of odontodes forming directly upon one another or beside each other during consecutive stages of growth' (Ørvig, 1977) and this situation occurs in many fossil groups such as acanthodisans, polypterids and lepisoteids. Odontocomplexes are large flat structures and do not erupt.

In terms of general morphology and the potential variability of tissue types, conodonts are closer to odontodes than teeth. Donoghue (1998) noted that odontodes are flexible enough to allow any of their component enamel, dentine and bone to be evolved before the others. Furthermore, it is possible that each of the hard tissues of odontodes could be present independently of the others by regulation of the cellular activities producing each hard tissue (Smith & Hall, 1993). Bone is not always present in odontodes and is absent from the odontodes of jawless fish such as thelodonts and the scales and teeth of most chondrichthyans (Donoghue, 1998). This indicates that simple odontodes show a wide variety of compositional forms in terms of their hard tissues.

However, unlike conodonts, odontodes, being non-dental parts of the dermal skeleton, do not fulfil similar functions to teeth (Francillon-Vieillot *et al.*, 1992). Furthermore, odontode units show definite growth patterns, which is not an acceptable comparison with the proposed periodic growth of conodont elements (as suggested by data herein and various literature). Therefore, the fundamental question arises as to whether periodic growth of dental tissues (enamel, dentine etc) occurs in the vertebrate record.

3.4 Scales and Scale Growth

Scales are composed of both enamel and dentine. The growth of scales may therefore provide a mechanism for re-growth of structures containing vertebrate dental tissues. In contrast to both vertebrate teeth and dermal odontode units, evidence suggests that elasmoid scales and the skeletal elements bearing odontodal tissues are never replaced but can grow indefinitely by the addition of successive layers (Huysseune & Sire, 1998). Scales can therefore grow continuously and can show similar ornamentation to odontode-like elements. Scales in some advanced

teleosts resemble the placoid scales (odontodes) of chondrichthyans, but do not have the structure of teeth. These similarities do not imply that these organs are homologous but, more likely, reflect adaptive convergencies (homoplasies) probably by epigenetic factors during growth (Huysseune & Sire, 1998). The function of scales is mainly protective but many have ornamentation believed to play a useful hydrodynamic role (Huysseune & Sire, 1998).

Donoghue (1998) noted the process of growing and periodic re-growing of scales is more common than growing teeth in the vertebrate record stating that scales have a facility for post-eruptive repair. This has been observed to occur in some acanthodian and actinopterygian scales (Donoghue, 1998) where after time, the scale sinks within the dermis and is enlarged by another odontode unit around, above or to one side of the pre-existing structure. Scales can therefore be enlarged and repaired by the periodic addition of layers of gangoine (an enamel homologue). Growth in scales can therefore be cyclic and occur by a 'retraction' of the scale back into the formative tissues.

The characteristics of conodont elements, vertebrate teeth, odontodes and scales are outlined in Table 3.4.

Table 3.4.

Skeletal element Feature	Vertebrate teeth	Odontodes	Scales	Conodont elements
Tissues	Enamel, various dentine types including enameloid, cementum and pulp	Dentine, pulp and enameloid with cellular or acellular bone in various combinations.	Pulp, dentine and bone at the base. Often composed of cosmine (a form of dentine)	Homologues of enamel, dentine types, cellular bone and globular calcified cartilage
Function	Food processing by cutting, slicing etc	Hard tissue unit of the skin	Units of the epidermis, hydrodynamics, protective.	Food processing by crushing, slicing etc.
Growth pattern	Definite Shedding and replacement	Definite Shedding and replacement	Growth by periodic additions	Growth by periodic additions or continuous growth (*Panderodus*) No evidence of shedding and replacement

Table 3.4. A comparison between the tissue and functions of vertebrate teeth, odontodes, scales and conodont elements.

It is clear that none of the growth models described above are adequate mechanisms by which to grow a conodont element, as the majority of evidence predicts that addition of crown lamellae to many conodont elements occurs periodically as part of growth-functional cycles. In the deep-water coniform conodonts analysed in (Part II) Chapter 2, this is inferred to occur over a period of several days prior to the longer functional episodes.

Tooth and odontode and formation mechanisms do not serve to explain the mechanisms by which conodont elements could function and then retract still maintaining all the necessary cellular connections for the continuing production of the enamel crown. The facility of scales to sink back into the epidermis to enable repair and enlargement by the addition of enamel may however provide a useful analogue for conodont crown growth (Donoghue, 1998).

3.5 Paraconodont growth model

Continual growth processes are well displayed by the Paraconodonts. Although they resemble coniform conodonts in form, they are distinctly different in both histology and mode of growth (Sansom, 1992).

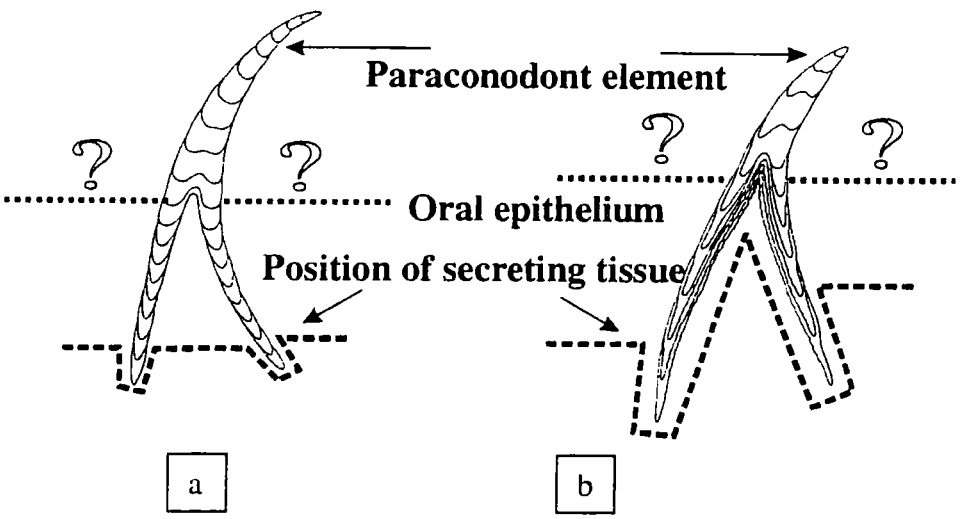

Text-Figure 3.5.1. The Paraconodont elements a. *Prooneotodus gallatini* with short lamellae progressively added to the base of the element and, b. *Problematoconites* sp. where lamellae are interrupted on the outer side but continuous on the inner side. The proposed position is shown of the secreting tissue (dashed line) required to build a paraconodont element (adapted from Szaniawski & Bengtson , 1993).

Paraconodonts have been postulated to grow by addition of lamellae to the base of the element (Müller & Nogami, 1971) either along the basal area (Text-figure 3.5.1. a) or along both the interior and exterior surfaces (Text-figure 3.5.1. b).

Paraconodonts are not true conodonts (Szaniawski, 1982) and are composed of very fine phosphatic crystallites (Müller, 1981; Szaniawski & Bengston, 1993). This mechanism of continually additive growth for paraconodonts requires a simple model that needs only to mineralise one component tissue. The tissue is either added to the base of the element or to the base and external margins as shown on Text-figure 3.5.1.

The cellular processes required to mineralise paraconodont elements are therefore much less complex than those of tooth, odontode and scale growth and may reflect a more simple odontode condition without the differentiation of oral tissues into distinct ecto- and mesodermal components. In terms of comparisons to euconodont element growth the nearest analogous mechanism may be that inferred for the growth of *Panderodus* elements which, in the latter stages of growth, appear also to grow (and be erupted?) by additions to the basal sections of the element (Sansom, 1992).

3.6 Euconodont growth models

3.7 Retractional

Bengtson (1976) first proposed the theory of periodic function and retractional growth episodes to explain conodont element growth. This model is, however, oversimplified in terms of explaining the suites of hard tissues in conodont elements. The model is supported, in principle alone, by a range of ultrastructural studies (Furnish, 1938; Hass, 1941, Donoghue, 1998), by the presence of internal discontinuities in elements (Müller & Nogami, 1971,1972; Jeppsson, 1976), by the observation of wear facets on juvenile conodont elements (Purnell, 1995) and by the analysis of growth of elements from bedding-plane assemblages (Purnell, 1993, 1994). Bengtson's (1976) model for conodont element growth was based on the assumption that elements were secreted by the epithelium (Text-figure 3.7.1.).

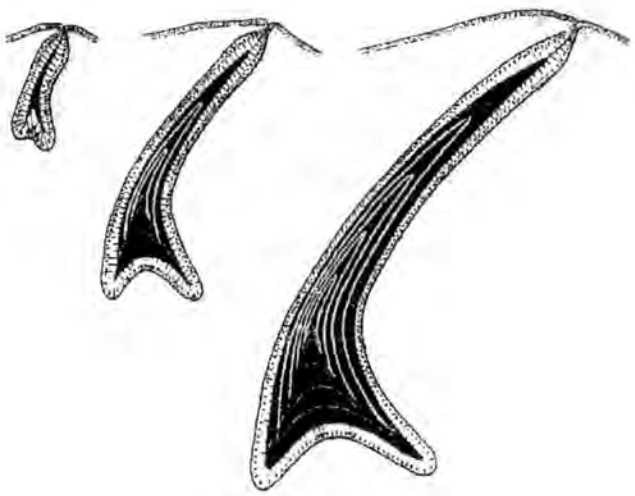

Text-Figure 3.7.1. The proposed relationship (after Bengtson, 1976) of the conodont element and the secreting tissue.

The implication of this model was that element tissue was derived from an ectodermal epithelium. Bengtson (1976) further postulated that conodonts were completely engulfed in epithelial pockets enabling them to grow holoperipherally

and assume more complex shapes that could be maintained during ontogeny, therefore, implying that conodont elements erupted to function externally after the growth phase. This led to the further implication that they alternated between a retracted non-functional growth stage and a protracted functional non- growth stage.

Bengtson (1976) advanced this model stating that the secreting epithelium adhered only to the basal body of the (eu) conodont, the crown being exposed to the aquatic medium when the apparatus was in use.

This was later disputed by Sansom (1992) who noted that although the model did adequately explain centrifugal growth of conodonts, enamel was formed within the dental papilla usually without periodic eruptions of the odontode. Sansom (1992) however based this work largely on observation of *Panderodus* elements which may have grown by different mechanisms from most other conodont genera.

In contrast to the eruption of higher vertebrate teeth, and the formation of *Panderodus* (and odontode units), the enamel producing facility of other conodont genera must not be destroyed when they reach a functional stage in their ontogeny. Among conodont elements proposed to exhibit retractional growth there appears to be,

a. a wide range of tissue types

b. a wide range of tissue-type combinations

c. a wide range of simple to complex morphologies

d. potentially different mechanisms of growth between Orders

Because in teeth and odontodes the enamel producing organ is formed from epidermal tissue and the dentine from the mesoderm, Bengtson's primarily one-layer model can not be applied to conodont elements, as the model is highly oversimplified and does not account for the variables as listed above. It is not an adequate explanation for the occurrence of enamel, cartilage and dentine homologues in conodont elements.

Nicoll (1985, 1987) who suggested that there would be problems accommodating the secretory tissue around elements with complex morphologies

also disputed Bengtson's (1976) model. However, recent models of single element morphogenesis (Donoghue, 1998) serve to refute arguments of lack of accommodation space.

3.8 Odontocomplex growth model

Before a growth mechanism can be proposed it is necessary to adhere to several lines of evidence, which have been used to determine the order of mineralisation of each conodont element hard tissue. The histological study of conodont elements has helped considerably in both confirming the affinity of the conodont animal (Dzik, 1976, Sansom *et al.*, 1992) and proposing mechanisms for individual element growth (e.g. Donoghue, 1998). To enter fully into the historical aspects of conodont histology is beyond the scope of this thesis (for a full review see Donoghue, 1998).

The microscopical study of conodonts can be considered at three scales; macrostructure, microstructure and ultrastructure. Macrostructure relates to the component tissues of the conodont element; the crown, basal body and white matter. Microstructures describes the morphologies exhibited by the tissue types (e.g. the lamellar nature of the crown) and ultrastructure which describes the nature and orientation of crystallites within the microstructure. These relationships are demonstrated in the figures below.

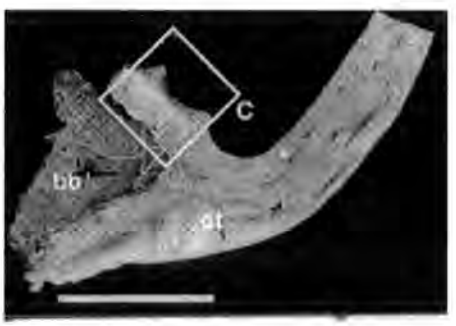

Text-Figure 3.8.1. Macrostructure of *Cordylodus* showing the relationship between the basal tissue and the crown. Scale bar = 200µm (from Sansom *et al.*, 1992)

Text-Figure 3.8.2. ***Microstructure*** **– SEM image of the lamellar structure of the crown in** ***Cordylodus*** **Pander also showing the** ***ultrastructure*** **in the form of prismatic crystallites orthogonal to the growth lamellae which run right to left across the picture as shown by the arrow (from Sansom, 1992). Scale bar = 5µm**

Text-Figure 3.8.3. ***Microstructure*** **- Globular structure of the basal tissues in** ***Cordylodus*** **Pander (from Sansom, 1992). Scale bar = 20 µm**

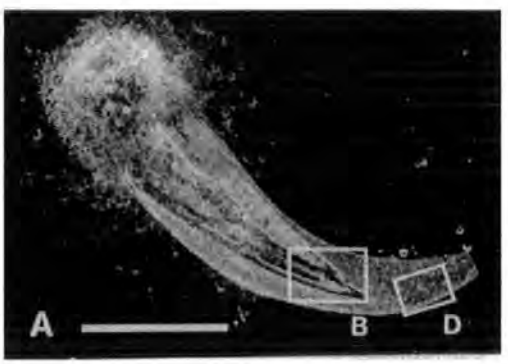

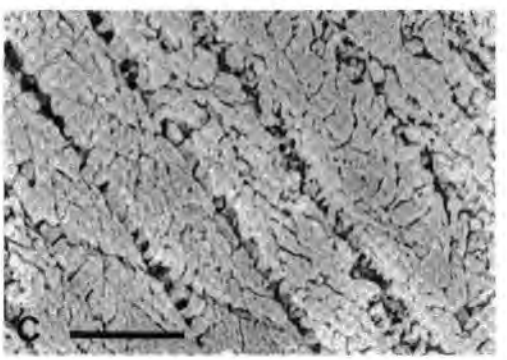

Text-Figure 3.8.4. A. ***Macrostructure*** **of** ***Panderodus*** **element showing the relationship between the lamellar tissue, white matter and basal cavity. Scale bar = 200µm. B.** ***Micro- and ultrastructure*** **'Fish-tail' alignment of crystallites in the crown lamellae. Lamellae are shown by the dark lines running diagonally top left to bottom right of the image as shown by the arrow (from Sansom, 1992). Scale bar = 2µm**

To produce an accurate growth model the proposed inter-relationship of the tissues on each of the scales indicated above is vital.

Donoghue (1998) considered conodont growth in terms of the pattern of formation and documented four distinct patterns that he believed to have derived from a primitive condition (Text-figure 3.8.5.). In this work, he outlined the morphogenetic pattern of inter-growth between the two structural units and three component tissues of mostly ozarkodinid conodonts (for a full discussion see Donoghue, 1998, pp. 647-651) based on macro-, micro- and ultrastructural inter-relationships.

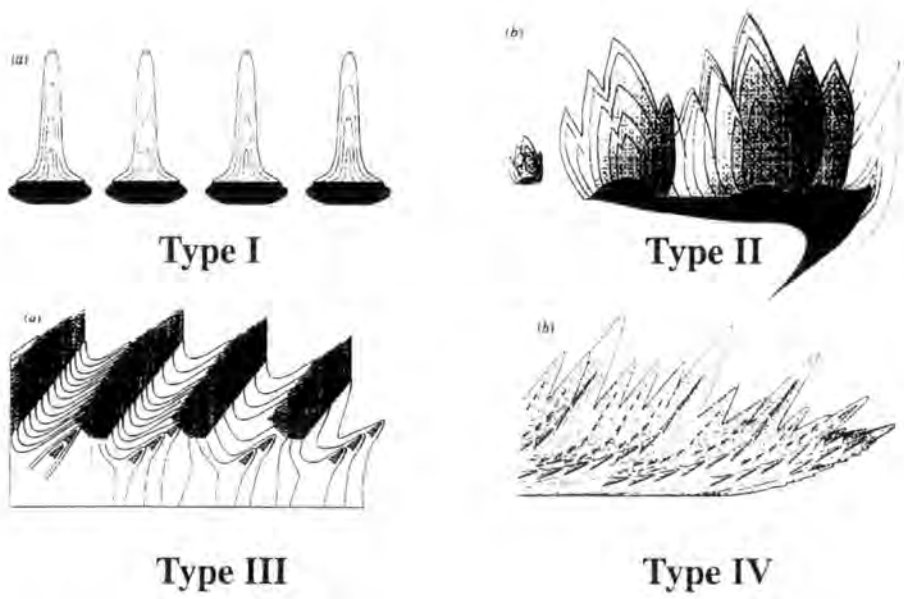

Text-Figure 3.8.5. The four 'types' of conodont formational patterns *sensu* Donoghue (1998). Drawn from Donoghue (1998)

From his detailed histological studies Donoghue (1998) concluded that the basic structural component of a conodont element is a denticle consisting of an enamel crown cap and a dentine base, an 'odontode' unit. Type I conodonts were therefore proposed to be composed of many of these basic units united by a supporting structure lying underneath. Type II elements were postulated to be made up of 'histologically distinct basic units with a lack of structural identity' (Donoghue,

1998, p. 659). For this reason, Donoghue inferred that the resultant type II element was an odontocomplex (*sensu* Reif, 1992) and therefore able to grow by the addition of 'basic units' above, to the side of or below the existing structure. Type III and IV elements were also compared to odontodocomplexes exhibiting circumferential addition of successive units. Elements of this type therefore grow by the establishment of a new dental papilla for each basic unit or odontode at the boundary between the pre-existing crown and basal body (Donoghue, 1998). Donoghue further arranged these growth 'types' into an evolutionary sequence; II-(I)-III-IV where Type I, the most primitive was an evolutionary offset occurring only in genera such as *Promissum* and *Icriodus*. Additionally, Donoghue (1998) provided evidence of periodic repair, evident particularly in Types III and IV, where the elements were grown by marginal secretion and enlarged by accretion surrounding the existing structure. Many type I and II elements show independent marginal growth interpreted by Donoghue (1998) to indicate that at least some elements were partly enclosed within soft tissue throughout life.

3.9 Panderodus

Panderodus elements have a number of distinct component tissues (see Sansom, 1992 for a full discussion).

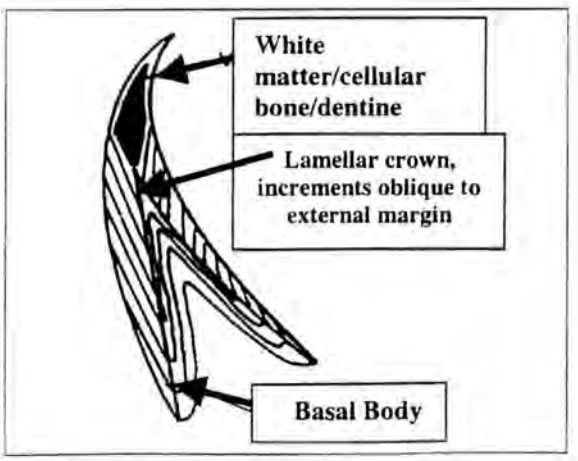

Text -Figure 3.9.1. Diagram of *Panderodus* element showing the relationship between the crown white matter and basal body and the oblique growth lamellae in the crown tissue.

Furthermore, the pattern of lamellar crown growth in *Panderodus* is distinct from all other conodont genera studied to date. The most comprehensive study of *Panderodus* was conducted by Sansom (1992) who observed that minor growth increments in the crown were oblique to the external margin of the element as shown in Text-figure 3.9.1. Sansom (1992) also observed that the individual crystallites of each lamella were sub-parallel to the external margin of the element. This is in contrast to the 'cone-in-cone' style lamellar crown of elements of *Protopanderodus* and *Drepanodus* as outlined in the previous chapter. The control of orientation of hydroxyapatite crystals in enamel is unknown and a number of possible mechanisms have been proposed (see Risnes, 1998)

Table 3.9. shows the proposed distribution of hard tissues across four conodont genera after Sansom (1992).

Table 3.9

	Panderodus	*Parapanderodus*	*Pseudooneotodus*	*Ozarkodina*
Perpendicular enamel			Lamellar crown	Lamellar crown
Parallel enamel	Lamellar crown	Lamellar crown		
Dentine			Basal filling	
Cellular bone	White matter	White matter		White matter
Globular Cartilage	Basal filling	Basal filling		?

Table 3.9. Proposed distribution (after Sansom, 1992) of hard tissues across three conodont genera showing that up to five different hard tissues can be found in conodont elements (enamel, parallel enamel, dentine, cellular bone & globular cartilage).

As shown, the white matter in *Panderodus* was interpreted as cellular bone and observed to occur in the tip of all *Panderodus* elements, covered by a thin layer of enamel (Sansom, 1992). In contrast to other genera however, the growth lamellae have an asymptotic relationship to the external margin (Text-figure 3.9.1.). These relationships were clearly demonstrated in histological analyses conducted by Sansom (1992, pls. 6,7&8, pp. 242-244).

The suites of hard tissues occurring in *Panderodus*, *Parapanderodus*, *Cordylodus* and *Ozarkodina* (Table 3.9.) led Sansom (1992) to postulate that conodont elements must form in a homologous way to vertebrate odontodes. He

further noted that in order to produce a growth model for *Panderodus* he would have to make the inference that the white matter was the first hard tissue to form within the element. In this growth model for *Panderodus*, Sansom (1992) postulated that the white matter (or cellular bone) formed as a single event and because the growth lamellae were discontinuous around the tip of the cusp this indicated that the element was gradually erupted during formation. In order to explain the sequence of hard tissue formation Sansom (1992 unpublished thesis) constructed a four-stage model for *Panderodus* element genesis. Regarding elements of *Panderodus* Sansom suggested that the cellular bone and cartilage appeared to have an ectomesenchymal or mesodermal origin, with development of the enamel from the epidermis. As the element erupted Sansom (1992) stated that the enamel producing cells must have maintained contact with the basal portion of the element in order to produce the incremental pattern observed. *Panderodus* elements therefore grow in an analogous way to paraconodont elements i.e. by successive additions of crown tissue to the base of the element. Continuous mechanisms of growth in *Panderodus* are reinforced by further observations (Sansom, 1992, figure 5.19, p 117) of the presence of a 'stringer' of white matter running along the core of each element. However, given the 'cone-in-cone' style of growth observed in *Drepanodus* and *Protopanderodus* it is unlikely that this 'continual' growth mechanism can be applied to most other conodont genera. *Panderodus* growth would therefore appear to be distinct from *Drepanodus*, *Protopanderodus* and *Periodon*. *Panderodus* appears to have gone through a period of growth in the odontode after which basal lamellae were added to facilitate eruption and function. Other panderodontids (e.g. *Protopanderodus*) appear to show distinct growth-function cycles by retraction into the enamel forming tissues.

3.10 *Protopanderodus* crown growth and element function

It is postulated here that *Panderodus* elements are formed by a period of growth in the odontode and subsequent addition of basal lamellae facilitated eruption and function. However, evidence suggests the panderodontid conodont *Protopanderodus*, shows a distinct pattern of growth from that of *Panderodus*. In this case the element appears to have also undergone a period of growth in the

odontode but this was followed not by gradual eruption but by periodic growth, eruption and function. An anchorage may facilitate this eruption either by the basal body structure or retraction of the epidermis. The thin section of *Protopanderodus* (979912D, Part II, Chapter 2, Text-figure 2.17.1) shows differences in orientation of minor lamellae. These are low angle wear discontinuities and did not form during growth episodes. Moreover, the pattern of increments in *Protopanderodus* enables us to make more detailed interpretation about the way in which the element grew

As shown in (Part II) Chapter 2 (Text-figures 2.17.1, 2.17.2.), *Protopanderodus* appears to show differential growth. The first phase of enamel growth produces a "Proto-element" which is symmetrical about a midline (Text-figure 3.10.1.). The first major discontinuity appears at increment 15. Until this point it is inferred that the element is still situated in the epithelium or ectodermal tissue. The "Proto-element" is then erupted and may function. It is inferred here that this period of eruption and function is longer (up to 3 times) than the growth period.

After eruption and function the "Proto-element" is again surrounded by ectodermal tissue and the second growth phase can begin. The second growth phase is distinct from that of the first. During the second growth phase increments are added at different rates to the inner and outer sides of the element. The outer side therefore adds an increased thickness of enamel to facilitate growth of the curved twisted morphology of the adult element. This second phase therefore produces the asymmetry in element shape.

It is proposed here that major discontinuities in the second phase of growth mark the prolonged periods of function as minor increments form low-angle disconformities at these major breaks (Text-figure 3.10.1.). The cause of growth cessation is unknown; therefore, it is assumed the element alternates between these growth and functional phases until either the animal dies or reaches sexual maturity.

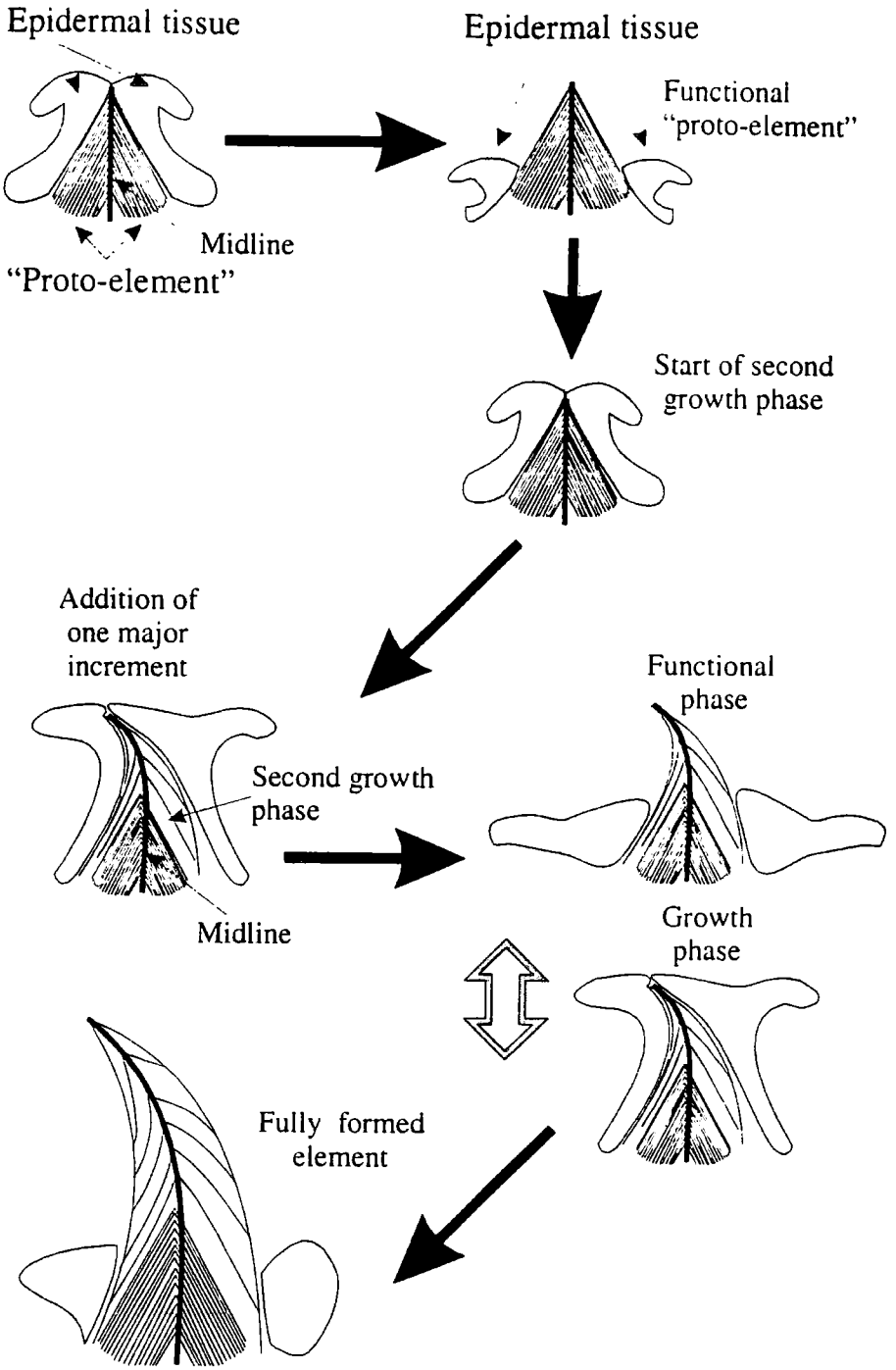

Text-Figure 3.10.1. The proposed growth stages in an element of *Protopanderodus* showing the initial phase of growth producing the "Proto-element" and the subsequent alternation of growth and functional phases producing the adult element. Shaded grey areas indicate the epithelium or enamel secreting tissue.

3.11 An additional conodont growth model – a definite cyclic growth model for some conodonts.

Evidence suggests that the definite cyclical formative mechanisms of vertebrate dental enamel are not directly applicable to the growth mechanism of at least some conodont elements. However, the formative biochemical processes of enamel and dentine are clearly relevant. None of the growth models can adequately explain the simple 'cone-in-cone' structure and the presence of minor increments and daily growth of enamel. It must be assumed from the growth analysis study in (Part II) Chapter 2 that the enamel organ is not destroyed or must reform over a time scale of ~23 or ~28 days in *Protopanderodus* and *Periodon* respectively following a growth and eversion phase.

To produce an integrated growth model *a priori* decisions have to be made regarding the tissues comprising the element.

Conodont crown tissue is an enamel homologue (Sansom *et al.*, 1992) and therefore ectodermal/epidermal in origin. It has a lamellar structure (Pander, 1856; Hass, 1941; Gröss, 1954; Lindström, 1964) and grows by addition of lamellae to the external margins of the elements (centrifugal or appositional growth).

White matter (*sensu* Lindström, 1954) only occurs in albid conodonts (Barnes *et al.*, 1970) although not all albid areas in conodonts are true white matter (Donoghue, 1998). Insufficient microstructural analyses of white matter have been conducted to for a consensus view to emerge as the range of variations in this tissue type makes interpretation difficult. Three main hypotheses prevail;

- White matter as a resorption product

Lindström (1954; 1964) suggested that white matter represented a zone of resorption or demineralisation where phosphatic material had been removed to supply other areas of the conodont with more rapid growth. Barnes *et al.* (1973) also considered white matter as a secondary replacement of crown tissue. Sansom (1992), who found no evidence for relict crystallites within the white matter he examined, disputed these observations.

- White matter as cellular bone (Sansom, 1992)

The lacunate spaces observed in many examples of white matter were compared to the osteocyte lacunae (spaces for the cell body) and canaliculi (spaces for the cell processes) from both fossil and recent bone

- White matter as dentine or a dentine related tissue (Donoghue, 1998)

Donoghue (1998) characterised white matter on the basis of its finer crystalline composition, lack of growth increments and found that the tubules he had observed in white matter were comparable to the sites of mineral secreting cells such as the odontoblasts of living vertebrates. Donoghue (1998) postulated that these features indicated a homology with mesodentine.

The basal body is only rarely found preserved inserted into the basal cavity of conodont elements. Donoghue (1998) suggested that the reason for lack of preservation of the basal body in unknown, although he speculated it could be due to incomplete mineralisation. Conodont basal body tissue has been described by workers such as Lindström (1955), Schwab (1965), Gross (1957; 1960), Müller & Nogami (1971; 1972), Barskov *et al.* (1982). This work showed that basal body tissues displayed a number of different textures; sphericular e.g. *Panderodus* (Sansom, 1992) or globular (Lindström, 1954), lamellar e.g. *Coryssognathus dubius* (Donoghue, 1998) or both lamellar and sphericular (Lindström, 1955, e.g. *Cordylodus* Sansom *et al.*, 1992)

As with white matter, basal body tissue appears to be highly variable and no consensus has yet emerged as to which vertebrate tissue provides the best homologue. Current views include basal body tissue as bone (Barskov *et al.*, 1982), globular calcified cartilage (Schwab, 1965) and atubular dentine (Sansom, 1992, Sansom *et al*, 1992; 1994; Sansom, 1996, Donoghue, 1998). All these homologies indicate that basal body tissue is most likely to have a mesodermal origin.

3.12 Relationship between tissues

The suggested inter-gradation between crown and white matter (Barnes *et al.*, 1973) was refuted by Sansom (1992) and Donoghue (1998, p.641) who found sharp boundaries between crown tissue and white matter. Although white matter is often planar there is sometimes a stepped margin between crown and white matter

(Donoghue, 1998). Sansom (1992) noted that variation in the distribution and extent of white matter and enamel indicated the timing of formation of each hard tissue varied from genus to genus.

Gross (1960) suggested that the basal body grew by outward apposition of lamellae at the same time as growth of the crown enamel and proposed the idea that the surface between the crown and basal body was a resorption feature. This was disputed (Müller & Nogami, 1971; 1972) who showed specimens with continuous lamellae between the two tissues, though these were not always continuous around the base of the element. However, Lindström *et al.* (1972) suggested that lamellae of the crown and basal body may not have been produced at the same time. Donoghue (1998) extended the study of the basal body tissues and found that successive increments in the basal body extended over the lower surface thereby encapsulating all previous increments, indicating a totally different growth in the basal body and the crown. Additionally, he described various styles of basal tissue across many generic examples finding that some of the concentric increments in the basal body were equivalent to the growth striae in the crown. He discussed how the innermost layer represented the earliest growth stage and the outermost the latest so the two basic units of the conodont element grew in opposing directions relative to the crown and basal body junction.

Because the order of tissue formation is fundamental to producing an integrated growth model the main points of this review are summarised below;

1. The enamel crown grows by outward accretion and crown growth is punctuated (stepped boundary of Donoghue, 1998)
2. Crown and basal body grow by outward apposition.
3. Basal tissue grows from the crown –basal body junction inwards towards the centre of the structure
4. Basal body shows different growth to crown
5. Crown and white matter grow synchronously
6. Core of white matter controlled at margin by secretion of crown
7. White matter shows continuous growth.

It has to be assumed for modelling purposes that conodont white matter and basal body tissue are most likely to be dentine – related tissues and therefore it is inferred here that they are likely to be mesodermal in origin. However, white matter and basal body tissue are clearly different in appearance and texture (refer to previous references) so therefore probably originate from a different organic template i.e. from different mesodermal tissue components.

3.13 Retractional cyclic growth

The basic unit of growth for a conodont element is a simple 'denticle –like' structure composed of a lamellar crown and a dentinous base (Donoghue, 1998). Hence, this simple unit can be adapted, by processes similar to that seen during the formation of odontocomplexes, to produce the more complex morphologies of many conodont elements.

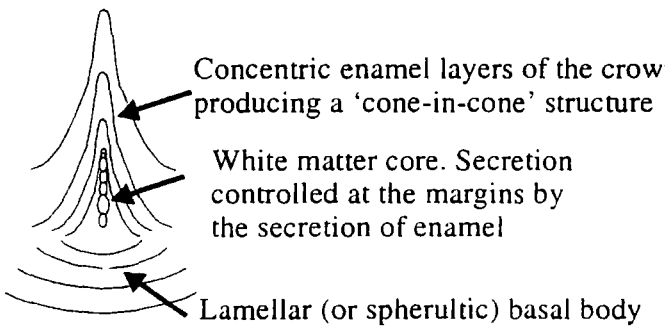

Text-Figure 3.13.1. The general relationship between the hard tissues of a coniform conodont element.

In order to form an individual coniform conodont with a simple 'cone-in-cone' lamellar crown structure, a core of white matter and a lamellar (or spherultic) basal body (Text-figure 3.13.1.) it is proposed here that it is necessary to have a three-layer model.

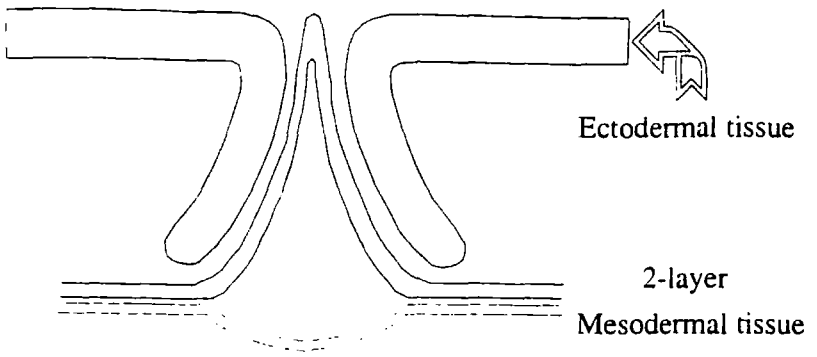

Text-Figure 3.13.2. The proposed tissue association necessary to produce a conodont element with 'cone-in-cone' lamellar crown tissue, a core of white matter and lamellar/spherultic basal tissue.

In this model, the white matter and basal body tissues are produced from a differentiated mesoderm in the relationship shown in Text-figure 3.13.2. This shows the three-layer tissue model required for constructing a simple basic "denticle unit". The lower layer of mesodermal tissue is necessary to produce the basal body tissue whereas the upper layer would be responsible for secretion of white matter. The upper layer of epidermal tissue is required to secrete the enamel crown of the conodont element.

It has been assumed that all three component tissues in a conodont element are produced from the activity and migration of different cells. Because of the widely different structures seen in the white matter and basal body tissues it seems likely that a different organic template would be required to mineralise each although both are mesodermal in origin. Differentiation of cells within the dental papilla would be necessary to produce two odontoblast layers that later mineralise the two types of dentine crystals. Mineralisation therefore begins nearest the boundary between the enamel organ and the mesodermal tissue (EDJ).

Basal body tissue and white matter start to mineralise synchronously with the initial layers of crown enamel. Dentine formation in vertebrates is documented to occur (Ten Cate, 1989) faster than that of enamel, 4μm per day. The enamel formation for conodonts is approximately 1-2 μm per day. Therefore, it is inferred that white matter and basal body formation proceeds at a faster rate than that of the

enamel and advances in the direction indicated on Text-figure 3.13.3. Enamel is therefore deposited on the newly mineralised dentine substrate. As the first layer of enamel is maturing the white matter and basal body are well formed. It is important to note that whereas basal body tissue may not be completely mineralised (Donoghue, 1998) the white matter more likely is.

It is inferred here that the initial stage of conodont element formation occurs over a period of several days prior to eruption. When the enamel is sufficiently mature and the element is biomechanically strengthened, eruption and function can occur. By this time the white matter and basal body are in more advanced stages of formation. Both white matter and basal body formation may cease due to eruption. However, it is likely that cellular contacts could have been maintained if eruption occurs in the way proposed in Text-figure 3.13.3.

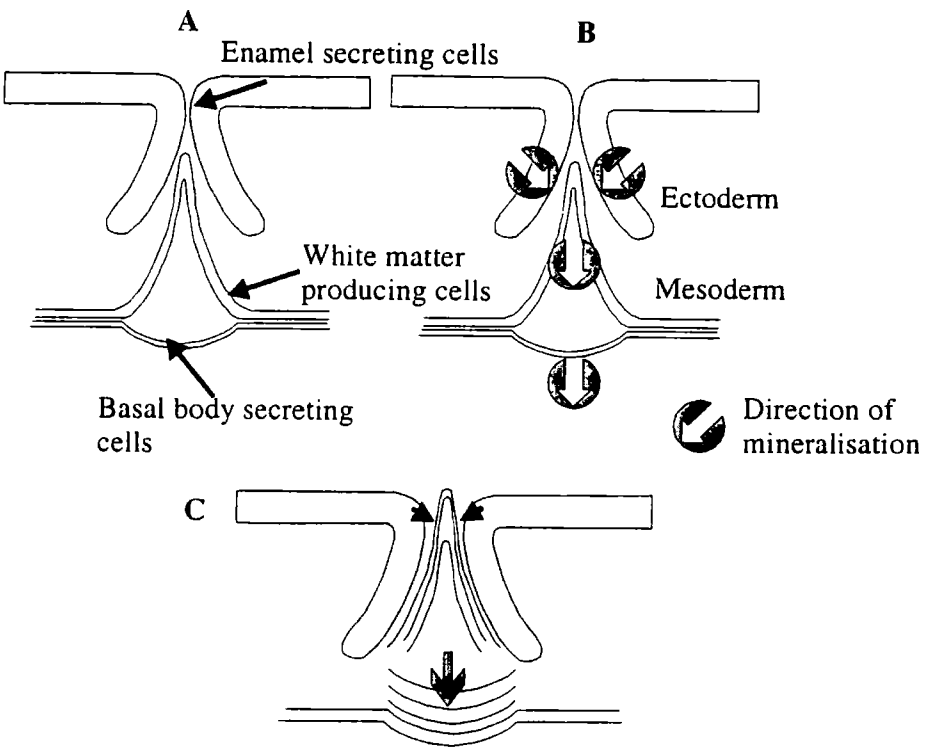

Text-Figure 3.13.3. Formation of conodont elements in a differentiated mesodermal dental papilla. The cells producing the conodont element components (grey = epidermal tissue, upper and lower mesodermal \components are indicated). Arrows show direction of mineralisation of all three component tissues. The initial formation of the lamellar hard tissues of the conodont element occurs so the crown builds by outward accretion and the white matter forms a continuous core. The basal body grows in an opposing direction to the crown.

In order to erupt a conodont element for functional purposes, bearing in mind that it has to be retracted periodically, it may be necessary to retract or 'sink' the epidermal tissue rather than actively push the element from the epithelium.

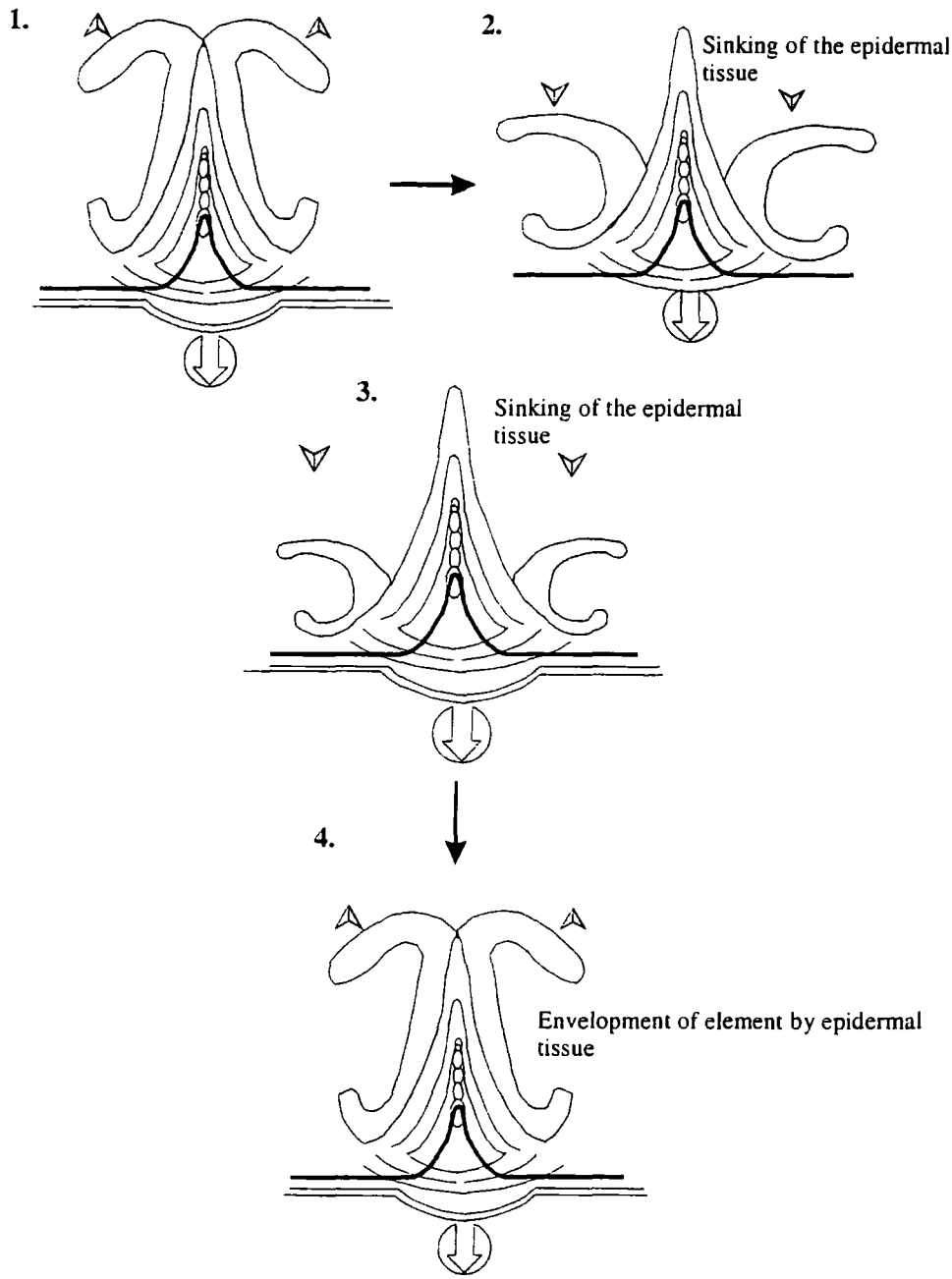

Text-Figure 3.13.4. Function, non-growth and growth non- function in conodont elements. 1. The element is surrounded and enveloped by epidermal tissue as formation continues 2. The epidermal tissue starts to sink and the element is functional. The cellular contacts are maintained with the mesodermal tissue. 3. Element is fully functional. 4. Envelopment by epidermal tissues and subsequent periodic enamel secretion.

In this way the element would more likely stay in contact with the mesodermal tissue and this would act as an 'anchor' for the element within the oral cavity. Additionally, white matter core secretion and basal body secretion could continue post-eruptive episodes.

Once the element protrudes from the epidermal tissue it can be used for feeding prior to a time when retraction must occur. Retraction would be achieved by the envelopment of the element by the epidermal tissue. Periodic secretion of enamel can therefore occur without the conodont element losing contact with the cellular processes necessary to produce all three composite tissues.

3.14 Conclusions

Through utilising the same biochemistry the Conodonta appear to include more than one model system for element formation. Of the observed taxa, shallow and deep-water conodont genera show a predominance of 'retractional cyclic growth'. In contrast, *Panderodus* appears to show growth, which is indefinite and starts enclosed within the odontode with later growth stages characterised by addition of lamellae to the basal portion of the element alone.

The retractional cyclical growth model predicts that conodont elements took between 12 and 18 months to fully develop and data predict that elements were grown over short periods of time (2-3 days in *Periodon* and 7-10 days in *Protopanderodus* and *Drepanodus*). In addition, this growth period was followed by longer periods of function (up to ~ 23 days in the case of the case of the coniform taxa and ~ 28 days in *Periodon*). Although the two orders exhibit the same style of growth, this is occurring at a slower rate in *Periodon* elements.

The growth of *Protopanderodus* (specimen 979912D) appears to be characterised by two distinct phases. The first is the production of the symmetrical "Proto-element" followed by differential addition of lamellae to the outer and inner sections of the element crown. The change in growth rates between the inner and outer side of the *Protopanderodus* element facilitated final shape production. Initiation of the second growth phase therefore facilitated the curving and possibly tortion/twisting of the adult element and implies strong genetic control on the

addition and thickness of minor increments in coniform genera. It is therefore concluded that minor increments in coniform conodont crown enamel are homologous to cross-striations in vertebrate enamel and the bounding surfaces at major increments mark periods of function.

This has further implications for the mode of life between adult and juvenile coniform elements and the function of the "Proto-element". The absence of curvature in the triangular, symmetrical "Proto-element" suggests it cannot have functioned efficiently as a grasping element, as curvature is a ubiquitous feature of grasping spines in all Chaetognaths, all coniform p elements and a number of groups with grasping mouthparts. If this first major discontinuity in the *Protopanderodus* element corresponds to the first functional phase of the conodont animal then the "Proto-element" may have formed pre-hatching, or juvenile animals fed in a different way to the adults. If the former is the case then the first discontinuity is homologous to the neonatal line in hominoid teeth. If juveniles fed a different way (or on different prey items) from adults then this trophic partitioning could indicate another adaptation to survival in a nutrient restricted, deep-water environment.

Conodont element ontogeny, comprising short periods of growth followed by longer periods of function is the same in the Ozarkodinida, Prioniodinida and Panderodontida and in a number of ecologically distinct clades.

Part II – Chapter 4

4. Conclusions

Although the physio-chemical conditions of the deep-sea are relatively stable, the environment is an unfavourable habitat for organisms due to instability in nutrient supply. The high pressures, low temperatures and reduced nutrient influxes in the deep-sea results in inhabitants with slow growth patterns, reduced metabolic rates and highly specialised behaviour.

The crown tissue of *Drepanodus* (692/14) has a pattern of both major and minor increments. Minor increments are between 1 and 3μm thick and the majority are grouped in sets of 7-10 between major increments. The average major increment thickness is calculated to be ~ 22μm. Minor increments were secreted at a daily rate. The crown tissue of *Protopanderodus* (667/21) also has both major and minor increments. The 72 minor increments are between 1 and 4μm and are grouped into sets of 8-10 between major incremental breaks. The average major increment thickness is 12μm and minor increments were also secreted on a daily basis. *Periodon aculeatus* elements have between 5 and 10 increments with no subdivisions. Individual increments have widths from ~ 1.8 to 8.5μm. The average increment thickness of *Periodon aculeatus* (110996D) is ~ 3.5μm. Although these three genera were taken from the same sample, the coniform taxa *Protopanderodus* and *Drepanodus* have much larger elements than those of *Periodon aculeatus*.

Fischer plots of enamel increment thickness indicate two peaks in growth in the early and late part of the growth cycle. This is assumed to be due to the increased flux of DOM in the spring and autumn indicating seasonal entrainment of growth. Based on this assumption growth episodes in *Periodon* were 2 to 3 days whereas in *Drepanodus* and *Protopanderodus* they were between 7 and 10 days.

Skelton (1993) summarised the life strategies organisms adopt under different environmental conditions. *K*-strategists are organisms adapted to stable environments such as those of the deep sea, where species specialise in gathering resources, have narrow niches and diversity is high, whereas r-strategists are associated with unstable conditions where species show more rapid development and smaller body sizes.

Growth analysis of *Periodon* suggests it had slow, intermittent growth and a small adult body size compared with *Drepanodus* and *Protopanderodus*. Samples containing *Periodon* are also commonly dominated by this genus, indicating populations containing a large number of individuals. These are features of an r-strategy mode of life. If *Periodon aculeatus* had an r-strategy mode of life then the general model also predicts it should have had early first reproduction, rapid onset of sexual maturity, a short life span and short generation time. This strategy is ideal where explosive reproduction enables the exploitation of scarce and ephemeral nutrient supply (Text-figure 4.1).

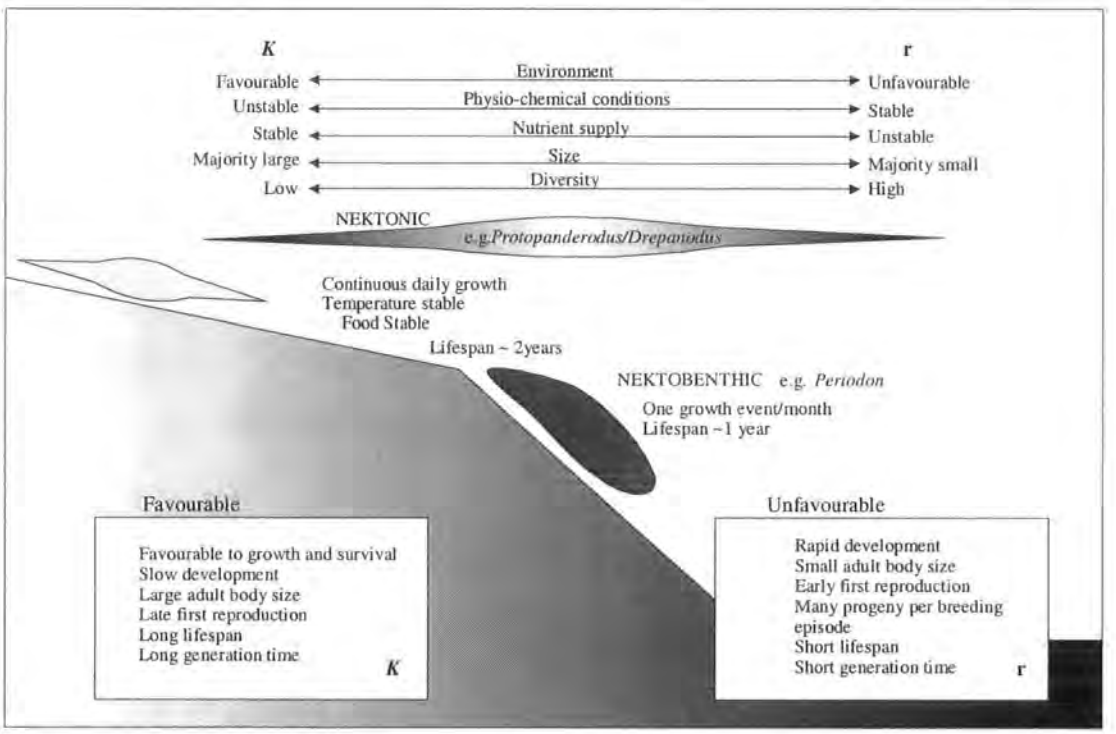

Text-Figure 4.1. The conceptual model for conodont life strategies.

In contrast, *Drepanodus* and *Protopanderodus* show more continued growth, much larger element sizes and have similar growth patterns to shallow shelf species such as *Parapachycladina*. This growth pattern is characteristic of a *K*-strategy mode of life where emphasis is placed on slow development, long life span and late reproduction. The *K*-strategy is typically found in environments which are favourable to growth and survival.

Deep-water nektobenthic conodonts of the North Atlantic Realm were characterised by low diversity and high abundance of small sized individuals when compared to the faunas of coeval shelf settings. This is exactly the pattern exhibited by the deep-water crustacean dominated meiofauna in modern oceans.

References

Aldridge, R.J., 1987. Conodont palaeobiology: a historical review. In, Palaeobiology of Conodonts, Aldridge, R.J.(ed). Ellis Horwood Limited. 13-68

Aldridge, R.J. & Smith, M.P., 1993. Conodonta, *The Fossil Record 2*, (Benton, M.J. ed.), Chapman and Hall, London 563-572

Aldridge, R.J., 1976. Comparison of macrofossil communities and conodont distribution in the British Silurian, *Geological Association of Canada Special Paper,* **15**, 91-104

Aldridge, R.J., Briggs, D.E.G, Clarkson, E.N.K. & Smith, M.P., 1986. The affinities of conodonts – new evidence from the Carboniferous of Edinburgh, Scotland. *Lethaia,* **19**, 279-291

Aldridge, R.J., Jeppsson, L., & Dorning, K.J., 1993. Early Silurian oceanic episodes and events. *Journal of the Geological Society of London,* **150**, 501-513

Aldridge, R.J., Purnell, M.A., Gabbott, S.E. & Theron, J.N. 1995, The apparatus architecture and function of *Promissum pulchrum* Kovács-Endrödy (Conodonta, upper Ordovician) and the Prioniodontid plan. *Philosophical Transactions of the Royal Society of London,* **347,** 275-291

Aldridge, R.J., Smith, M.P., Briggs, D.E.G., Clarkson, E.N.K. & Clark, N.D.L., 1993a. The anatomy of conodonts, *Philosophical Transactions of the Royal Society of London,* **B 340**, 405-421

Aldridge, R.J., Smith, M.P., Norby, R.D. & Briggs, D.E.G., 1987. The architecture and function of Carboniferous polygnathacean conodont apparatuses. In, *Palaeobiology of conodonts*, (Aldridge, R.J. ed). *British Micropalaeontology Society Series*, Ellis Horwood, Chichester, 63-75

Armstrong H.A. & Owen, A.W., 1998. Age and provenance of limestone clasts in Lower Old Red Sandstone conglomerates; implications for the geological history of the Midland Valley Terrane. *In press* .

Armstrong, H..A., 1995. High resolution biostratigraphy (conodonts and graptolites) of the Upper Ordovician and Lower Silurian - evaluation of the late Ordovician mass extinction. *Modern Geology,* **20**, 41-69

Armstrong, H.A., 1996. Biotic recovery after mass extinction - the role of climate and ocean state in the post glacial recovery of conodonts. In, *Biotic Recovery from Mass extinction Events.* (Hart, M.B. ed). *Geological Society Special Publication* No. **102**, 105- 118.

Armstrong, H.A., 1997. Conodonts from the Shinnel Formation, Tweeddale Member (middle Ordovician), Southern Uplands, Scotland. *Palaeontology,* **40**, 763-799.

Armstrong, H.A. & Coe, A.L., 1997. Deep sea sediments record the geophysiology of the late Ordovician glaciation, *Journal of the Geological Society of London*, **154:6**, 929-934

Armstrong, H.A., 1990. Conodonts from the Upper Ordovician- Lower Silurian carbonate platform of North Greenland, *Grønlands Geologiske Undersøgelse,* **159,** 151pp

Armstrong, H.A., Johnson, E.W. & Scott, R.W., 1996. Conodont biostratigraphy of the attenuated Dent Group (Upper Ordovician) at Hartley Ground, Broughton in Furness, Cumbria. *Proceedings of the Yorkshire Geological Society,* **51(1)**, 9-21

Arntz, W.E., Tarazona, J., Gallardo, V.A., Flores, L.A. & Salwedel, H., 1991. Benthos communities in oxygen deficient shelf and upper slope areas of the Pervian and Chilean coast, and changes caused by El Niño. In, *Modern and ancient continental shelf anoxia*, (Tyson, R., and Pearson, T.H. eds.), *London Geological Society Special Publication* **58** 131-154.

Barnes *et al.*, 1978. Ordovician and Silurian conodont biostratigraphy, Manitoulin Island and Bruce Peninsula, Ontario. *Michigan Basin Geological Society Special Paper*, **3**, 63-71

Barnes, C. R. & Fåhraeus, L. E., 1975. Provinces and communities and the proposed nektobenthic habit of Ordovician Conodontophorids, *Letheia*, **8**, 133-149

Barnes, C. R. 1992. The uppermost series of the Ordovician System. In *Global perspectives on Ordovician Geology*. (Webby, B. D. and Laurie, J. R. eds.) Balkema 185-192

Barnes, C.R & Slack, D.J., 1975. Conodont ultrastructure: the Subfamily Acanthodontinae. *Life Sciences Contributions Royal Ontario Museum*, **106**, 1-21

Barnes, C.R., Ferretti, A. & Serpagli, E., 1999. Late Ordovician conodonts from Europe, (d) Wales. *Ordovician News,* **16**, 21-22

Barnes, C.R., Kennedy, D.J., McCracken, A.D., Nowlan, G.S. and Tarrant, G.A., 1979. The structure and evolution of Ordovician conodont apparatuses, *Lethaia,* **12**, 125-151

Barnes, C.R., Sass, D.B. & Monroe, E.A., 1970. Preliminary studies of the ultrastructure of selected Ordovician conodonts. *Life Sciences Contributions Royal Ontario Museum*, **76**, 1-24

Barnes, C.R., Sass, D.B. & Poplawski, M.L.S., 1973. Conodont Ultrastructure: the family Panderodontidae. *Life Sciences Contributions Royal Ontario Museum*, **90**, 1-36

Barrick, J. E., 1977. Multielement simple-cone conodonts from the Clarita Formation (Silurian), Arbuckle Mountains, Oklaholma. *Geologica et Palaeontologica,* **11**, 47-68

Barrick, J.E., 1977. Multielement simple-cone conodonts from the Clarita formation (Silurian), Arbuckle Mountains, Oklahoma, *Geologica et Palaeontologica,* **11**, 47-68

Barskov, I.S., Moskalenko, T.A. & Starostina, L.P., 1982. New evidence for the vertebrate nature of conodontophorid. *Palaeontology Journal,* **1982**, 82-90

Bassler, R.S., 1925. Classification and stratigraphic use of the conodonts, *Geological Society of America Bulletin*, **36**, 218-220

Bengston, S., 1976. The structure of some Middle Cambrian conodonts, and the early evolution of conodont structure and function. *Lethaia.* **9**, 185-206

Bengston, S., 1983. The early history of Conodonta. *Fossils and strata.* **15**, 5-19

Bergström, S. M., 1971. Conodont biostratigraphy of the Middle and Upper Ordovician of Europe and Eastern North America. *Geological Society of America Memoir* **127,** 83-162.

Bergström, S. M., 1990. Relations between conodont provincialism and the changing palaeogeography during the early Palaeozoic. In, *Palaeozoic Palaeogeography and Biogeography* (McKerrow, W. S. and Scotese, C. R. eds.). *Geological Society Memoir*, **12,** 105-121

Bergström, S. M., & Massa, D., 1987, Stratigraphic and Biogeographic significance of Upper Ordovician conodonts from North Western Libya, *The Geology of Libya*, **IV .**

Bergström, S.M. & Mitchell, C.E. 1992. The Ordovician Utica Shale in the eastern Midcontinent region: age, lithofacies, and regional relationships, *Oklahoma Geological Survey Bulletin*, **145**, 67-89

Bergström, S.M. & Orchard, M.J., 1985. Conodonts from the Cambrian and Ordovician systems of the British Isles, in *A Stratigraphical Index of Conodonts* (Higgins, A.C. and Austin, R.L., eds.), Ellis Horwood, Chichester. 32-68

Bergström, S.M. & Sweet, W.C., 1966. Conodonts from the Lexington Limestone (Middle Ordovician) of Kentucky and its lateral equivalents in Ohio and Indiana, *Bulletin of American Paleontology*, **50**, 271-441

Bergström, S.M., 1980. Conodonts as palaeotemperature tools in Ordovician rocks of the Caledonides and adjacent areas in Scandinavia and the British Isles. *Geologiska Foreningens I Stockholm Förhandlingar*, **102(4)**, 377-392

Bergström, S.M., 1983. Biogeography, evolutionary relationships and biostratigraphic significance of Ordovician Platform conodonts. *Fossils and Strata*, **15**, 33-58

Bergström, S.M., 1990 Biostratigraphic and Biogeographic significance of middle and Upper Ordovician conodonts in Girvan, South-West Scotland. *Courier Forsch, - Inst. Senckenberg*, **118**, 1-43

Bergström, S.M., 1964, Remarks on some Ordovician conodont faunas from Wales, *Acta Univ. Lundensis II*, **3**, 1-66

Bergström, S.M., 1973. Ordovician conodonts, in *Atlas of Palaeobiogeography* (Hallam, A. ed.), 47-58

Bergström, S.M., 1978. Middle and Upper Ordovician conodont and graptolite biostratigraphy of the Marathon, Texas graptolite zone reference standard, *Palaeontology*, **21**, 723-758

Bergström, S.M., 1981. Family Strachanognathidae, in *Treatise on Invertebrate Paleontology W (Supplement 2, Conodonta)* (Robison, R.A., ed.), University of Kansas Press.

Berry, W.B.N., Wilde, P. & Quimby-Hunt, M.S., 1987. The oceanic non-sulfidic oxygen minimum zone: a habitat for graptolites? *Bulletin of the Geological Society of Denmark*, **35**, 103-114

Beynon, A.D. & Wood, B.A., 1987. Patterns and rates of enamel growth in the molar teeth of early hominids. *Nature*, **326**, pp. 493-496

Bischoff, G. & Sannemann, D., 1958. Unterdevonische Conodonten aus dem Frankenwald. *Notizbl. Hess. L.-Amt Bodenforsch*, **86**, 87-110

Bischoff, G.C.O. & Sannemann, D., 1958. Unterdevonische conodonten aus dem Frankenwald, *Notizble. Hess. Landesamtes Bodenforsch. Wiesbaden*, **86**, 87-110

Branson, E. B. & Mehl, M. B., 1933a. Conodont studies Number 1. Introduction. *University of Missouri Studies*, **8(1)**, 5-17

Branson, E. B. & Mehl, M. B., 1933b. Conodonts from the Joachim (Middle Ordovician) of Missouri. *University of Missouri Studies*, **8(2)**, 77-100.

Branson, E.B. & Branson, C.C., 1947. Lower Silurian conodonts from Kentucky, *Journal of Paleontology*, **21**, 549-556

Branson, E.B. & Mehl, M.G., 1933c. Conodonts from the Maquoketa-Thebes (Upper Ordovician of Missouri. *Ibid.* 121-132

Branson, E.B., Mehl, M.G. & Branson, C.C., 1951. Richmond conodonts of Kentucky and Indiana, *Journal of Paleontology*, **25**, 1-17

Brenchley, P. J. & Newall, G., 1984. Late Ordovician environmental changes and their effect on faunas. In *Aspects of the Ordovician System.* (Bruton, D.L. ed.) *University of Oslo Palaeontological Contributions* 65-79

Brenchley, P.J., Marshall, J.D., Carden, G.A.F., Robertson, D.B.R., Long, D.G.F., Meidla, T., Hints, L. & Anderson, T.F., 1994. Bathymetric and isotope evidence for a short lived late Ordovician glaciation in a greenhouse period, *Geology*, **22**, 295-298

Briggs, D.E.G., Aldridge, R.J. & Smith, M.P., 1987. Conodonts are not aplacophoran molluscs. *Lethaia*, **20**, 381-382

Briggs, D.E.G., Clarkson, E.N.K. & Aldridge, R.J., 1983. The conodont animal. *Lethaia*, **16**, 1-14

Bruton, D.L and Owen, A.W. 1979. Late Caradoc - early Ashgill trilobite distribution in the central Oslo region, Norway. *Norsk Geologisk Tidsskrift*, **59**, 213-222

Bruton, D.L., Lindström, M. and Owen, A.W., 1985. The Ordovician of Scandinavia, in The Caledonide Orogen-Scandinavia and related areas (Gee, D.G. and Sturt, E.A., eds.), John Wiley, Chichester, 273-282

Bruun, A.F., 1957. Deep sea and abyssal depths. *Geological Society of America Memoir*, **67(1)**, 641-672

Campana S.E & Neilson, J.D., 1985. Microstructure of fish otoliths. *Canadian Journal of Fisheries and aquatic science*, **42**, 1014-1032

Campana, S.E., 1984. Lunar cycles of otolith growth in the juvenile starry *flounder Platichthys stellatus. Marine Biology,* **80**, 239-246

Carls, P., 1977. Could conodonts be lost and replaced? *Neues. Jahrb. Geol. Paläont. Abh.*, **155**, 18-64

Carlson, S.J., 1992. Vertebrate Dental Structures. Chapter 21 in, *Skeletal biomineralization: Patterns, Processes and Evolutionary Trends. Volume I.* (Carter, J.G. ed.) Van Nostrand Reinhold, New York

Cave, R. & Dixon, R.J., 1993. The Ordovician and Silurian of the Welshpool area, in *Geological Excursions in Powys* (Woodcock, N.H. and Bassett, M.G. eds.), University of Wales Press, National Museum of Wales, 51-84

Cave, R. & Price, D., 1978. The Ashgill Series near Welshpool, N. Wales, *Geological Magazine,* **115** 183-194

Cave, R., 1965. The Nod Glas Sediments of Caradoc Age in North Wales, *Geological Journal*, **4**, 279

Charlesworth, B., 1990. Speciation. *In* Briggs, D.E.G. & Crowther, P.R. (eds) Palaeobiology: A Synthesis. Blackwell Scientific publications, Oxford. 100-106

Clark, D. L., 1981. Classification. *In Treatise of Invertebrate Paleontology, W (Supplement 2, Conodonta), W102-103.* (Robison, R. A. ed.) Geological Society of America, University of Kansas Press.

Cocks, L.R.M & Fortey, R.A., 1998. The Lower Palaeozoic margins of Baltica. *GFF*, **120**, 173-179

Cocks, L.R.M, McKerrow, W.S. & van Staal, C.R., 1997. The margins of Avalonia. *Geol. Mag.*, **134** (5), 627 - 636

Cocks, L.R.M. and Fortey, R.A., 1990. Biogeography of Ordovician and Silurian faunas, in *Palaeozoic Palaeogeography and Biogeography*, (McKerrow, W.S. and Scotese, C.R. eds.) *Geological Society of London Memoir,* **12**, 97-104

Conway Morris, S., 1989. Conodont palaeobiology: recent progress and unsolved problems. *Terra Nova* **1**, 135-150

Cooper, A.H., Millward, D., Johnson, E.W. & Soper, N.J., 1993. The Early Palaeozoic evolution of North West England. *Geological Magazine.* **130** (5), 711-724

Cooper, B.J., 1975. Multielement conodonts from the Brassfield Limestone (Silurian) of southern Ohio. *Journal of Paleontology,* **49**, 84-108

Cooper, B.J., 1976. Multielement conodonts from the St. Clair Limestone (Silurian) of Southern Illinois. *Journal of Paleontology,* **50**, 205-217

Cooper, B.J., 1977. Toward a familial classification of Silurian conodonts. *Journal of Paleontology*, **51**, 1057-1071

Cooper, R.A. & Lindholm, K., 1990. A precise worldwide correlation of Early Ordovician graptolite sequences, *Geological Magazine*, **127**, 497-525

Cooper, R.A., 1999. Global correlation of Ordovician graptolites. *Lethaia*, **32**, 1-12

Cooper, R.A., Fortey, R.A. & Lindholm, K., 1991. Latitudinal and depth zonation of early Ordovician graptolites, *Lethaia*, **24**, 199-218

Cronin, T.M and Raymo, M.E., 1997 Orbital forcing of deep sea benthic species diversity. *Nature*, **385**, 624

Crowley, T.J. and Baum, S.K., 1991. Toward reconciliation of late Ordovician glaciation with very high CO_2 levels, *Journal of Geophysical Research*, **96**, 22,597-22,610

Deuser, W.G., 1986. Seasonal and interannual variations in deep water particle fluxes to the Sargasso Sea and their relation to surface hydrology. *Deep-Sea Research*, **33a**, 225-246

DeVries, A.L. & Eastmann, J.T., 1981. Physiology and ecology of nototheniod fishes of the Ross Sea. *Journal of the Royal Society of New Zealand*, **11(4)**, 329-340

Dickson, R.R., Gould, W.J., Griffiths, C, Medler, K.J. & Gonitrowicz, E.M., 1986. Seasonality in currents of the Rockall Channel. *Proc. Ro. Soc. Edinburgh*, **88B**, 103-125

Donoghue, P.C.J & Purnell, M.A., 1999. Growth, function, and the conodont fossil record. *Geology*, **27**, 251-254

Donoghue, P.C.J, Purnell, M.A. & Aldridge, R.J., 1998. Conodont anatomy, chordate phylogeny and vertebrate classification. *Lethaia*, **31:3**, 211-219

Donoghue, P.C.J., 1998. Growth and patterning in the conodont skeleton. *Phil. Trans. R. Soc. Lond. B.* **353**, 633-666

Donoghue, P.C.J., 1997. A technique for conodont histology. *Lethaia*, **30**, 329-330

Dresbach, R.I., 1983. Conodont biostratigraphy of the Middle and Upper Ordovician Viola Group of south-central Oklahoma Arbuckle anticline. Unpublished Msc. Thesis, Department of Geology and Mineralogy, The Ohio State University, 101 pp.

Druce, E.C., 1973. Upper Palaeozoic and Triassic conodont distribution and the recognition of biofacies, in *Conodont Palaeozoology* (Rhodes, F.H.T. ed.), *Geological Society of America Special Paper*, **141**, 191-237

Drygant, D.M., 1974. \Simple conodonts from the Silurian and Lowermost Devonian of the Volhyno-Podolia area, *Lvov Palaeont. Sb.*, **10**, 64-70

Dunham, R.J., 1962, Classification of Carbonate Rocks According to Depositional Texture, in *Classification of Carbonate Rocks,* (Ham, W.E., ed.) *American Association of Petroleum Geologists Memoir,* **1**, 108-121

Dzik, J, 1983. Relationships between Ordovician, Baltic and North American Midcontinent faunas. *Fossils and Strata,* **15**, 59-85

Dzik, J. & Drygant, D., 1986. The apparatus of panderodontid conodonts. *Lethaia* **19**, 133-141.

Dzik, J., 1994. Conodonts of the Mojcza Limestone. *Palaeontologia Polonica*, **53**, 43 – 128

Dzik, J., 1976. Remarks on the evolution of Ordovician conodonts. *Acta Palaeontologica Polonica,* **21**, 395-449

Dzik, J., 1986. Chordate affinities of conodonts. In, *Problematic Fosil Taxa.* (Hoffman, A. and Nitecki M.H. eds.) *Oxford Monographs on Geology and Geophysics* No. **5**, 240-254. Oxford University Press, New York

Epstein, A.G., Epstein, J.B. and Harris L.D., 1977. Conodont color alteration- An index to organic metamorphism, *U.S. Geological Survey Professional Paper,* **995**, 27

Ethington, R.L., 1959. Conodonts of the Ordovician Galena Formation, *Journal of Paleontology*, **33**, 257-292

Fahraeus L.E. & Nowlan G.S., 1978. Franconian (late Cambrian) to early Champlanian (Middle Ordovician) conodonts from the Cow Head Group, Western Newfoundland. *J. Paleontol,* **52**, 444-471

Fåhraeus, L.E., 1982 Allopatric speciation and lineage zonation exemplified by the *P.serra - P. anserinus. Newsl. Stratigr.*, **11(1)**, 1-7

Fåhraeus, L.E., 1996. Eustacy and Chrono-correlations facts and theories with examples from the Ordovician. *Geoscience Canada*, **23** (2), 77-84

Fåhraeus, L.E. and Nowlan, G.S., 1978. Franconian (Late Cambrian) to Early Champlainian (Middle Ordovician) conodonts from the Cow Head Group, Western Newfoundland. *Journal of Paleontology*, **52**, 444-471

Ferretti, A. & Barnes, C.R., 1997. Upper Ordovician conodonts from the Kalkbank Limestone of Thuringia, Germany. *Palaeontology*, **40**, 15-42

Finney, S.C. & Berry, W.B.N., 1997. New perspectives on graptolite distributions and their use as indicators of platform margin dynamics. *Geology*, **25**, 919-922

Finney, S.C., 1986. Graptolite biofacies and correlation of eustatic, subsidence, and tectonic events in the Middle to Upper Ordovician of North America. *Palaios*, **1**, 435-461

Finney, S.C., 1988. Middle Ordovician strata of the Arbuckle and Ouachita Mountains, Oklahoma; contrasting lithofacies and biofacies deposited in the southern Oklahoma aulacogen and Ouachita geosyncline. In *South-Central section of the Geological Society of America Centennial Field Guide* **4**. (Hayward, O.T. ed.). Boulder, Colorado, 468pp.

Fischer, A.G., 1964. The Lofer cyclothems of the Alpine Triassic, in *Symposium on Cyclic Sedimentation* (Merriam, D.F. ed.), *State Geological Survey of Kansas Bulletin,* **1**, 107-149

Fitzgerald, C.M., 1998. Do enamel microstructures have regular time dependency? Conclusions from the literature and large-scale study. *Journal of Human Evolution*, **35**, 371-386

Forey, P & Janvier, P., 1993. Agnathans and the origin of jawed vertebrates. *Nature*, **361**, 129-134

Forey, P & Janvier, P., 1994. Evolution of the early vertebrates. *American Scientist*, **82**, 554-565

Fortey, R. A., 1984. Global earlier Ordovician transgressions and regressions and their biological implications. In, *Aspects of the Ordovician System.* (Bruton, D.L. ed.) University of Oslo Palaeontological Contributions **295,** 35-50.

Fortey, R.A., Bassett, M.G., Harper, D.A.T., Hughes, R.A., Ingham, K.J., Molyneux, S.G., Owen, A.W., Owens, R.M., Rushton, A.W.A. and Sheldon, P.R., 1995. Progress and problems in the selection of the stratotypes for the bases of series on the Ordovician System. *Geological Survey of Canada*, Paper 90-***9***, 5-25

Frakes, L. A., Francis, J. E., & Syktus, J. I., 1992. *Climate modes in the Phanerozoic: the history of the earths climate over the past 600 million years.* Cambridge University Press 274pp.

Francillon-Vieillot, H., 1992. Microstructure and Mineralization of Vertebrate Skeletal Tissues. Chapter 20 in, Skeletal biomineralization: Patterns, Processes and Evolutionary Trends. Volume I. (Carter, J.G., ed.). Van Nostrand Reinhold, New York

Fukhara, T., 1959. Comparative anatomical studies of the growth lines in the enamel of mammalian teeth. *Acta Anat. Nipp.* **34,** 322-332

Furnish, W.M., 1938. Conodonts from the Prairie du Chien (lower Ordovician) beds of the Upper Mississippian Valley. *Journal of Paleontology.* **12,** 318-340

Gabbott, S.E., Aldridge, R.J. & Theron, J.N., 1995. A giant conodont with preserved muscle tissue from the Upper Ordovician of South Africa. *Nature,* **374,** 800-803

Gage J.D. & Tyler, P.A. 1984. The reproductive biology of Echinothuriid and Cnidarid sea-urchins from the deep-sea. *Marine Biology*, **80:1**, 63-74

Gage, J.D. & Tyler, P.A., 1991. *Deep-sea Biology: A natural history of organisms at the deep-sea floor.* Cambridge University Press.

Gibbons, W. 1987. Menai Strait Fault System: An early Caledonian terrane boundary in North Wales. *Geology*, **15**, 744-747.

Goldman, D. & Bergström, S.M., 1997. Late Ordovician graptolites from the North American Midcontinent. *Palaeontology*, **40**, 965-1009.

Goldman, D. & Mitchell, C., 1994. K-bentonites and Graptolite Biostratigraphy in the Middle Ordovician of New York State and Quebec: A new chronostratigraphic model. *Palaios*, **9,** 124-143

Goldreich, P., 1982. Tides and the Earth-Moon system. *Scientific American*, **226**(4), 42-52.

Gooday, A.J., 1988. A response by Foraminifera to the deposition of phytodetritus in the deep-sea. *Nature* **332**, 70-73.

Gooday, A.J., Turley, C.M. & Allen, J.A., 1990. Responses by benthic organisms to inputs of organic material to the ocean floor; a review. In, *The Deep Sea Bed: its physics, chemistry and biology.* (Charnock, H., Edmond, J.M., McNave, I.N., Rice, A.L. & Wilson, T.R.S., eds.). *Proceedings of a Royal Society Discussion Meeting,* 119-138

Gordon, J.M.D., 1979. Seasonal reproduction in deep-sea fish. In *Cyclic phenomena in Marine Plants and Animals*, (Naylor, E. & Hartnoll, R.G. eds.). Oxford: Pergamon Press, 223-229

Gordon, J.M.D., 1985. The ecology of the deep-sea benthic and benthopelagic fish on the slopes of the Rockall trough, northeastern Atlantic. *Progress in Oceanography*, **15**, 37-69.

Gordon, J.M.D., 1987. Deep-sea bottom dwelling fishes at two repeat stations at 2200m and 2900m in the Rockall Trough, northeastern Atlantic Ocean. *Marine Biology* **96**, 309-325

Gross, W., 1954. Zur Conodonten-Frage. *Senckenbergiana Lethaea* **35**, 73-85

Gross, W., 1960. Uber die basis bei den gattungen Palmatolepis und Polygnathus (Conodontida). *Paläontologische Zeitschrift*, **34**, 40-58.

Hadding, A., 1913. Undre dicellograptusskiffern I Skåne jämte några därmed ekvivalenta bildningar: *Lunds. Univ. Arsskr Adv.*, **2**, 9, 15, 1-90

Hallam, A. & Wignall, P.B., 1997. Mass extinctions and their aftermath. Oxford University Press, Oxford 319pp.

Halstead, L.B., 1974. *Vertebrate Hard Tissues.* Wykeham Publications (London) LTD, pp179

Hamar, G., 1964. The middle Ordovician of the Oslo region, Norway. 17. Conodonts from the Lower Middle Ordovician of Ringerike, *Norsk Geologisk Tidsskrift*, **44**, 243-292

Hamar, G., 1966. The middle Ordovician of the Oslo Region Norway. *Norsk Geologisk Tidsskrift*, **46**(1), 27-83

Harley, J. 1861. On the Ludlow bone-bed and its crustacean remains. *Quarterly Journal of the Geological Society, London* **17**, 542-552

Harper, D.A. T. & Owen, A.W., 1986. A shelly biofacies from the graptolitic mudstones of the lower Balclatchie Group (Lower Caradoc) near Laggan, Girvan district. *Scottish Journal of Geology,* **22(2)**, 271-283

Harper, D.A.T., Owen, A.W. & Williams, S.H., 1985. The middle Ordovician of the Oslo Region, Norway, 34. The type Nakkholmen Formation (upper Caradoc), Oslo, and its faunal significance. *Nor. Geol. Tidsskr.* **34**, 293-312

Hartnoll, R.G. & Rice, A.L., 1985. Aspects of the biology of the deep-sea spider crab. *Proceedings of the 19th European Marine Biology Symposium.* (Gibbs, P.E. ed.) Cambridge University Press, UK, 231-241

Hass, W.H, 1959. Conodonts from the Chappel Limestone, Texas, *U.S. Geological Survey Professional Paper,* **294J**, 365-400

Hass, W.H., 1941. Morphology of Conodonts. *Journal of Paleontology* **15**, 71-81

Henningsmoen, G., 1948. The *Tretaspis* series of the Kullatorp Core, *Bulletin of the Geological Institute of the University of Uppsala,* **32**, 374-432

Hennismoen, G., 1948. The Trataspis Series of the Kullatorp Core. *Bull. Geol. Inst. Univ. Uppsala,* **32**, 374-432

Hoffman, P., Dewey, J.F., & Burke, K., 1974. Aulacogens and their genetic relation to geosynclines, with a Proterozoic example from Great Slave Lake, Canada. In, *Modern and ancient geosynclinal sedimentation.* (Dott, R.H, and Shaver, R.H eds.). *Society of Economic Paleontologists and Minerologists Special Publication,* **19**, 380pp.

Holland, S.M., 1993. Sequence stratigraphy of a carbonate–clastic ramp: the Cincinnatian Series (Upper Ordovician) in its type area. *Geological Society of America Bulletin*, **105**, 306-322

Horak, J.M., Doig, R., Evans, J.A. & Gibbons, W. Avalonian magmatism and terrane linkage: new isotopic data from the Precambrian of North Wales. *Journal of the Geological Society London*, **153**, 91- 99.

Hutton, D.W.H., 1987. Strike-slip terranes and a model for the evolution of the British and Irish Caledonides. *Geological Magazine*, **124**, 405-425

Huysseune, A. & Sire, J.Y., 1998. Evolution of patterns and processes in teeth and tooth-related tissues in non-mammalian vertebrates. *European Journal of Oral Sciences*, **106**(S1), 437-481

Ingham, J.K, 1992. Girvan Foreshore, in Lawson, J.D. & Weedon, D.S. (eds) Geological excursions around Glasgow and Girvan. *Geological Society of Glasgow*, pp. 495

Ingham, J.K. & McNamara, K.J., 1978. The Coniston Limestone Group, in *The Geology of the Lake District* (Moseley, F. ed.), *Yorkshire Geological Society Occasional Publication,* **3**, 121-129

Jenkyns, H.C., 1989, Pelagic Environments, Chapter 11 In *Sedimentary Environments and Facies*, (Reading, H.G. ed.). Blackwell Scientific Publications, 343-399

Jeppsson, L., 1976. Autecology of Late Silurian Conodonts. In *Conodont Palaeoecology.* (Barnes, C.R. ed.) *Geological Association of Canada, Special Paper,* **15**, 105-118

Jeppsson, L., 1979. Conodont element function. *Lethaia*, **12**, 153-171

Jeppsson, L., 1990. An Oceanic Model for Lithological and Faunal Changes Tested on the Silurian Record, *Journal of the Geological Society of London*, **147**, 663-674

Johnson, H.D. & Baldwin, C.T., 1989. Shallow Siliciclastic Seas, in *Sedimentary Environments and Facies*, (Reading, H.G. ed.), p229-282

Jones, C. R., 1986, Ordovician Llandeilo and Caradoc Beyrichiocope Ostracoda from England and Wales (I & II), *Monograph of the Palaeontographical Society*

Jones, O.T., 1938. On the evolution of a syncline. *Quarterly Journal of the Geological Society of London*, **94**, lx-cx.

Jumars, P.A., Mayer, L.M., Deming, J.W., Baross, J.A. & Wheatcroft, R.A., 1990. Deep-sea deposit feeding strategies suggested by environmental and feeding constraints. *Philosophical Transactions of the Royal Society of London*, **A**, *331*, 85-101.

Kamyowski, D. & Zenetra, S-J, 1990. Hypoxia in the world ocean as recorded in the historical data set. *Deep-sea research*, **37**, 1861-1874

Kennedy, D.J., Barnes, C.R. & Uyeno, T.T., 1979. A Middle Ordovician Conodont faunule from the Tetagouche Group, Camel Back Mountain, New Brunswick. *Cand. J. Earth Sci.* **16**, 540-551

Kennedy, D.J., Barnes, C.R. and Uyeno, T.T., 1979. A Middle Ordovician conodont faunule from the Tetagouche group, Camel Back Mountain, New Brunswick, *Canadian Journal of Earth Sciences*, **16**, 540-551

Klapper, G. and Johnson, J.G., 1980. Endemism and dispersal of Devonian conodonts, *Journal of Paleontology*, **54**, 400-455

Kneller, B.C., Scott, R.W., Soper, N.J., Johnson, E.W. & Allen, P.M., 1994. Lithostratigraphy of the Windemere Supergroup, Northern England. *Geological Journal*, **29** 219-240

Kokelaar, B.P., 1988. Tectonic controls on the Ordovician arc and marginal basin volcanism in Wales. *Journal of the Geological Society, London*, **145**, 759-776.

Kokelaar, B.P., Howells, M.F., Bevins, R.E., Roach, R.A. and Dunkey, P.N., 1984. The Ordovician marginal basin of Wales, in Marginal Basin Geology (Kokelaar, B.P. and Howells, M.F., eds.), *Geological Society Special Publication*, **16**, 245-269

Krejsa, R.J, Bringas, P. & Slavkin, H.A., 1990. A neontological interpretation of conodont elements based on agnathan cyclosstome tooth structure, function and development. *Lethaia.* **23**, 359-378

Lampitt, R.S., 1985. Evidence for the seasonal deposition of detritus to the deep-sea floor and its subsequent resuspension. *Deep-sea Research* **32**, 885-897.

Lavoie, D. & Asselin, E., 1998. Upper Ordovician facies in the Lac Saint-Jean outlier, Quebec (eastern Canada): palaeoenvironmental significance for Late Ordovician oceanography. *Sedimentology*, **45**, 817-832

Lawrence, D.J.D, Webb, B.C., Young, B. & White, D.E., 1986. The geology of the Late Ordovician and Silurian rocks (Windermere Group) in the area around Kendal and Crook, *Report of the British Geological Survey*, **18**, no. 5

Lee, C., Wakeham, S.G. & Farrington, J.W., 1983. Variations in the composition of particulate organic matter in a time-series sediment trap. *Marine Chemistry*, **13**, 181-194

Leggett, J.K., McKerrow, W.S., Cocks, L.R.M. and Rickards, R.B., 1981, Periodicity in the early Palaeozoic marine realm. *Journal of the Royal Geological Society of London,* **138**, 167-176

Leslie, S.A. and Bergström, S.M., 1995. Element morphology and taxonomic relationships of the Ordovician conodonts *Phragmodus primus* Branson and Mehl 1933, the type species of *Phragmodus* Branson and Mehl 1933 and *Phragmodus undatus* Branson and Mehl 1933. *Journal of Paleontology*, **69:5**, 967-975

Lindström, M., 1959. Conodonts from the Crug Limestone (Ordovician, Wales). *Micropalaeontology*, **5**, 427-452

Lindström, M., 1976. Conodont provincialism and palaeoecology- a few concepts, in Conodont Paleoecology (Barnes, C.R. ed.). *Geological Association of Canada Special Paper,* **15**, 3-9

Lindström, M., 1955. Conodonts from the lowermost Ordovician strata of south-central Sweden. *Geologiske Föreningens I Stockholm Forhandlingar,* **74**, 517-603

Lindström, M., 1964. *Conodonts*, Amsterdam, Elsevier.

Lindström, M., 1970. A supragenic taxonomy of conodonts. *Lethaia*, **3**, 427-445

Lindström, M., 1971. Lower Ordovician conodonts of Europe. *Memoirs of the Geological Society of America,* **127**, 21-61

Lindström, M., 1974. The conodont apparatus as a food gathering mechanism. *Lethaia,* **3**, 427-445.

Lindström, M., 1977. *Amorphognathus; Rhodesognathus*, in Catalogue of Conodonts (Ziegler, W. ed), **3**, 21-52, 531-537

Lindström, M., McTavish, R.A. & Zeigler, W., 1972. Feinstructurelle untersuchungen an conodonten. *Geologica et Palaeontologica,* **6**, 33-43

Loomis, F.B., 1936. Are conodonts gastropods?. *Journal of Paleontology,* **10**, 663-664.

Mac Niocill, Van der Pluijm, B.A. & Van der Voo, R., 1997. Ordovician Palaeogeography and the evolution of the Iapetus Ocean. *Geology*, **25**, 159-162

MacDonald, A.G., 1975. *Physiological aspects of deep-sea biology.* Cambridge University Press.

Mantyla, A.W. & Reid, J.L., 1983. Abyssal characteristics of the worlds ocean waters. *Deep-sea Research*, **30A**, 805-833.

Matthews, S.C., 1973. Notes on open nomenclature and on synonymy lists. *Palaeontology,* **16**, 713-719

McCave, I.N., 1983. Particulate size spectra, behaviour and the origin of nepheloid layers over the Nova Scotian continental rise. *Journal of Geophysical Research,* **88**, 7647-7666.

McCracken, A. D., 1989. Preliminary report on Ordovician-Devonian conodont collections from carbonate and fine grained clastic facies of northern Yukon Terrotory and northwest District of MacKenzie, NWT. Contribution to Frontier Geoscience Program.

McCracken, A.D. & Nowlan, G.S., 1984. Conodonts from Ordovician-Silurian Boundary strata, Whittaker Formation, Avalanche Lake, Mackenzie Mountains, Northwest territories, Canada. *Geol. Soc. Am.,* **16**, 179

McCracken, A.D., 1989. *Protopanderodus* (Conodonta) from the Ordovician Road River Group, northern Yukon territory, and the evolution of the genus. *Geological Survey of Canada Bulletin,* **388**.

McCracken, A.D., 1991. Middle Ordovician conodonts from the Cordilleran Road River Group, northern Yukon Territory, Canada, in Ordovician to Triassic conodont palaeontology of the Canadian Cordillera (Orchard, M.J. and McCracken, A.D. eds.). *Geological Survey of Canada Bulletin,* **417**

McKerrow, W. S. & Cocks, L. R. M., 1976. Progressive faunal migration across the Iapetus ocean. *Nature,* **263,** 304-306.

McKerrow, W.S., 1988. The development of the Iapetus Ocean from the Arenig to the Wenlock, in *The Caledonian-Appalachian Orogen* (Harris, A.L. and Fettes, D.J. eds.) *Geological Society Special Publication,* **38**, 405-412

Menzies, R. J., George, R. Y., & Rowe, G. T., 1973. *Abyssal environment and ecology of the world oceans.* Wiley 488pp.

Menzies, R.J., 1965. Conditions for the existence of life on the sea floor. *Oceanography and Marine Biology: an Annual Review*, **3**, 195-210

Mikulic, D.G., Briggs, D.E.G. & Kluessendorf, J., 1985. A new exceptionally preserved biota from the Lower Silurian of Wisconsin, U.S.A. *Philosophical Transactions of the Royal Society of London* series, **B 311**, 78-85

Müller, K.J. & Nogami, Y., 1972. Growth and function of conodonts. *24th IGC,* **7**, 20-27

Müller, K.J., 1971. Zoolological affinities of conodonts. In, *Treatise on Invertebrate palaeontology, Part W, supplement 2, Conodonta.* (Robinson, R.A., ed.). Geological Society of America and University of Kansas Press, Lawrence, Kansas, W78-W82

Nicoll, R.S., 1985. Multielement composition of the conodont genera *Polygnathus xylus xylus* Stauffer, 1940 and *Ozarkodina brevis* (Bischoff and Ziegler, 1957) from the Upper Devonian of the Canning Basin, western Australia. *BMR Journal Australian Geology and Geophysics,* **9**, 133-147

Nicoll, R.S., 1987. Form and function of the Pa element in the conodont animal. In, Palaeobiology of conodonts. BMS Series, Ellis Horwood, Chichester, Aldridge, R.J., editor, 49-61

Nowlan, G.S. and Barnes, C.R., 1981. Late Ordovician conodonts from the Vaureal Formation, Anticosti Island, Quebec. *Geological Survey of Canada Bulletin*, **329**, 1-49

Nowlan, G.S., McCracken, A.D. & McLeod, M.J. 1997. Tectonic and palaeogeographic significance of Late Ordovician conodonts in the Canadian Appalachians. *Canadian Journal of Earth Sciences*, **34 (11)**, 1521-1537

Oberg, R., 1966. Winnepeg Conodonts from Manitoba, *Journal of Paleontology,* **40**, 130-147

Orchard, M.J., 1980. Upper Ordovician conodonts from England and Wales, *Geologica et Palaeontologica,* **14**, 9-44

Ørvig, T., 1976. The interpretation of oseodentine, with remarks on dentition in the Devonian dipnoan *Griphognathus. Zoologica Scripta*, **5**, 79-96

Ørvig, T., 1977. A survey of Odontodes ('dermal teeth') from developmental, structural, functional and phyletic points of view. in, *Problems of vertebrate evolution*, (Andrews, S.M., Miles, R.S. and Walker, A.D. eds). *Linnean Society Symposium Series* **4**, 53-75

Owen, A.W. & Ingham, J.K., 1988, The Stratigraphical Distribution and Taxonomy of the Trilobite *Onnia* in the Type Onnian Stage of the Uppermost Caradoc. *Palaeontology,* **31:3**, 829-855

Owen, A.W., 1978. The Upper Ordovician succession at Noderhov and Frognøya in Ringerike. *Norsk Geologisk Tidsskrift*, **48**, 245-258

Owen, A.W., Bruton, D.L., Bockelie, J.F. & Bockelie, T.G., 1990. The Ordovician sucessions of the Oslo Region, Norway. *Norges Geologiske Undersøkelese*, Special Publication **4**, 53pp.

Owen, A.W., Harper, D.A.T. & Clarkson, E.N.K., 1996. The trilobites and brachiopods of the Wrae Limestone conglomerate in the Southern Uplands. *Scottish Journal of Geology,* **32 (2)**, 133-149

Owens R.M, 1993. British Ordovician and Silurian Proetidae (Trilobita). *Palaeontographical Society Monograph*, London, 98pp.

Pander, C.H., 1856. Monographie der fossilen Fische des silurischen Systems der nisichbaltischen Governments. Akademie der Wissenschafen, St. Petersburg 10, 1-91

Pannella, G., 1971. Fish otoliths: Daily Layers and Periodical patterns. *Science.* **173**, 1124-1127

Pickering, K.T. & Smith, A.G., 1995. Arc and backarc basins in the Early Palaeozoic Iapetus Ocean. *The Island Arc*, **4**, 1-67

Pickering, K.T., 1987. Deep-marine foreland basin and forearc sedimentation; a comparitive study from the Lower Palaeozoic of the Northern Appalachians. In, *Marine Clastic Sedimentology.* (Leggett, J.K. and Zuffa, G.G. eds) Graham and Trotman, London, 190-211.

Pickering, K.T., Bassett, M.G. and Siveter, D.J., 1988. Late Ordovician- early Silurian destruction of the Iapetus Ocean: Newfoundland, the British Isles and Scandinavia: A discussion. *Transactions of the Royal Society of Edinburgh: Earth Sciences.* **79**, 361-382

Pietzner, H., Vahl, J. & Ziegler, W., 1968. Zur chemischen Zusammensetzung und Mikromorphologie der Conodonten. *Palaeontographica*, **128**, 115-152

Pohler, S.M.L & Barnes, C.R., 1990. Conceptual models in conodont palaeoecology, in *Papers on conodonts and Ordovician to Triassic conodont stratigraphy ECOS V* (Ziegler, W. ed.) *Courier Forschungsinstitut Senckenberg,* **118**, 409-440

Pratt, W.T., 1991. The Nod Glas decollement of the Welsh Basin. *Geological Magazine*. **128**, 279-282

Pratt, W.T., Woodhall, D.G. & Howells, M.F., 1995. Geology of the country around Cadir Idris. British Geological Survey.

Price, D. & Magor, P.M., 1984. The ecological significance of variation in the generic composition of Rawtheyan (late Ordovician) Trilobite faunas from North Wales, U.K. *Geological Journal*, **19**, 187-200

Price, D., 1973. The age and stratigraphy of the Sholeshook limestone of southwest Wales. *Geological Journal*, **8**, 225-246

Price, D., 1974. Trilobites from the Sholeshook Limestone (Ashgill) of South Wales. *Palaeontology*, **17**, 841-868

Price, D., 1977. Species of *Tretaspis* (Trilobita) from the Ashgill series in Wales. *Palaeontology*, **20**, 762-792.

Price, D., 1980. A revised age correlation for the topmost Sholeshook Limestone Formation (Ashgill) of south Wales. *Geological Magazine*, **117**, 485-489.

Price, D., 1980a. The Ordovician Trilobite fauna of the Sholeshook Limestone Formation, south Wales. *Palaeontology*, **23**, 839-887.

Price, D., 1981. *Tretaspis radialis* Lamont and allied species. *Geological Magazine*, **118**, 289-295.

Price, D., 1982. *Calymene quadrata* King 1923 and allied species of trilobites from the Ashgill series of North Wales. *Geological Magazine*, **119**, 57-66.

Pridmore, P.A., Barwick, R.E. & Nicoll, R.S., 1997. Soft anatomy and affinities of conodonts. *Lethaia*, **27**, 317-328

Purnell, M. A. & Donoghue, P. C. J., 1998. Skeletal architecture, homologies and taphonomy of ozarkodinid conodonts. *Palaeontology,* **41(1),** 57-102.

Purnell, M. A., 1993b. The *Kladognathus* apparatus (Conodonta, Carboniferous): homologies with ozarkodinids and the prioniodinid Bauplan. *Journal of Paleontology,* **67,** 875-882.

Purnell, M. A., 1995. Microwear in conodont elements and macrophagy in the first vertebrates. *Nature,* **374,** 798-800.

Purnell, M.A. & Donoghue, P.C.J., 1997. Architecture and functional morphology of the skeletal apparatus of ozarkodinid conodonts. *Philosophical Transactions of the Royal Society of London,* **B 352,** 1545-1564

Purnell, M.A., 1993a. Feeding mechanisms in conodonts and the function of the earliest vertebrate hard tissues. *Geology,* **21,** 375-377

Purnell, M.A., 1994. Skeletal ontogeny and feeding mechanisms in conodonts. *Lethaia,* **27,** 129-138

Radke R.L. & Dean, J.M., 1982. Increment formation in the embryos, larvae and juveniles of the mummichog, *Fundulus heteroclitus*; Information available from Otoliths. *Canadian Journal of fisheries and aquatic science,* **44,** 1840-1847

Rasmussen, J.A., 1998. A reinterpretation of the conodont Atlantic realm in the late Early Ordovician (Early Llanvirn). In, *Proceedings of the Sixth European conodont Symposuim (ECOS VI)* (Szaniawki E. ed.), *Palaeontologia Polonica,* **58,** 66-77

Reif, W.E., 1979. Structural convergence between enameloid of actinopterygian teeth and shark teeth. *Scanning Electron Microscopy,* 1979/**II**, 547-556

Reif, W.E., 1982. Evolution of the dermal skeleton and dentition in vertebrates. The odontode regulation theory. *Evolutionary Biology,* **15,** 287-368

Rhodes, F. H. T., 1952. A classification of Pennsylvanian conodont assemblages. *Journal of Paleontology,* **26,** 886-901.

Rhodes, F. H. T., 1953. Some British Lower Palaeozoic conodont faunas. *Philosophical Transactions of the Royal Society,* **B 237,** 261-334.

Rhodes, F.H.T., 1955. The conodont fauna of the Keisley Limestone, *Quarterly Journal of the Geological Society of London,* **111:2,** 117-142

Rhodes, F.T.H., 1962. Recognition, interpretation and taxonomic position of conodont assemblages. In, *Treatise on Invertebrate Paleontology, Part W, Miscellanea, W70-W83*, (Moore, R.C. ed.), Geological Society of America and University of Kansas Press (New York and Lawrence)

Risnes, S., 1998. Growth tracks in dental enamel. *Journal of Human Evolution*, **31**, 331-350

Rokop, F.J., 1974. Reproductive patterns of the deep-sea benthos. *Science*, **186**, 743-745

Romer, A.S. & Parsons, T.S., 1977. *The Vertebrate Body* (eds.) The W.B.Saunders Co.

Ross, J. R. P., & Ross, C. A., 1992. Ordovician sea - level fluctuations. In *Global Perspectives on Ordovician Geology*. (Webby, B. D., and Laurie, J. R., eds.), Balkema 327-336.

Rowe, G.T., 1981, The deep-sea ecosystem. In *Analysis of Marine Ecosystems*, (Longhurst, A.R. ed.), London Academic Press. Pages

Sadler, P.M., Osleger, D.A. and Montanez, P., 1993. On labelling, length and objective basis of Fischer plots. *Journal of Sedimentary Petrology*, **63**, 360-368.

Sansom, I. J., 1992. The palaeobiology of the Panderodontacea and selected other euconodonts. Ph. D. thesis. University of Durham, U.K

Sansom, I.J., 1996. *Pseudooneotodus*: a histological study of an Ordovician to Devonian vertebrate lineage. *Zoological Journal of the Linnean Society*, **119**, 47-57

Sansom, I.J., Armstrong, H.A. & Smith, M.P., 1995. The apparatus architecture of *Panderodus* and its implication for coniform conodont classification. *Palaeontology*, **37(4)**, 781-799

Sansom, I.J., Smith, M.P. & Smith, M.M., 1994. Dentine in conodonts. *Nature*, **368**, 591

Sansom, I.J., Smith, M.P., Armstrong, H.A. & Smith, M.M., 1992. Presence of the earliest vertebrate hard tissues in conodonts. *Science*, **256**, 1308-1311

Savage, N. M., & Bassett, M.G., 1985. Caradoc-Ashgill conodont faunas from Wales and the Welsh borderland. *Palaeontology*, **28(4)**, 679-713

Schoener, A., 1968. Evidence for reproductive periodicity in the deep-sea. *Ecology* **49**, 81-87

Schwab, K.W., 1965. Microstructure of some Middle Ordovician conodonts. *Journal of Paleontology*, **39**, 590-593

Scotese, C. R. & McKerrow, W. S., 1990. Revised World maps and introduction, in *Palaeozoic Palaeogeography and Biogeography*. (McKerrow, W. S. & Scotese, C. R. eds.), Geological Society Memoir **12,** 1-21

Scrutton, C.T., (1973). Periodic growth features in fossil organisms and the length of the day and month. In, *Tidal Friction and the Earth's rotation* (Broche, P & Sündermann eds). Springer-Verlag, Berlin Heidelberg New York.

Seddon, G. & Sweet, W.C., 1971. An ecologic model for conodonts. *Journal of Paleontology*, **45**, 869-880

Sellwood, B.W. Shallow marine Carbonate environments. Chapter 10, *In Sedimentary Environments and Facies*, (Reading, H.G. ed.). Blackwell Scientific Publications 283-343

Serpagli, E., 1967. Conodonti dell Ordovicano superiore (Ashgilliano) delle Alpi Carniche. *Bull. Soc.Palaeont. Italiano*, **6**, 30-111

Sheldon, P.R., 1987. Parallel gradualistic evolution of Ordovician trilobites. *Nature*, **330**, 6148, 561-563

Sheldon, P.R. 1990 Shaking up evolutionary patterns. *Nature*, **345**, p772

Sheldon, P.R. 1996 Plus ça change - a model for stasis and evolution in different environments. *Palaeogeography, Palaeocloimatology, Palaeoecology,* **127**, 209-227

Sheldon, P.R., 1993. Making sense of evolutionary patterns. Chapter 2 in *Evolutionary patterns and processes*, Lees, D.R. & Edwards, D. (eds.). *The Linnean Society of London, Symposium*, **4,** 19-31, Academic Press, London.

Skelton, K., 1993 (ed). Chapters in *Evolution: a biological and palaeontological approach.* Addison-Wesley Publishing Company

Smith, C.R., 1986. Nekton falls, low-intensity disturbance and community structure of infaunal benthos in the deep-sea. *Journal of Marine Research,* **44**, 557-600

Smith, J.M., 1987. Darwinism stays unpunctured. *Nature*, **330**, 516

Smith, K.L. & Baldwin, M., 1984. Seasonal fluctuations in deep-sea sediment community oxygen consumption: central and eastern North Pacific. *Nature,* **307**, 624-626

Smith, M.M. & Coates, M.I., 1998. Evolutionary origins of the vertebrate dentition: phylogenetic patterns and developmental evolution. *European Journal of Oral Sciences*, **106** (suppl. 1), 482-500

Smith, M.M. & Hall, B.K., 1993. A developmental model for evolution of the vertebrate exoskeleton and teeth: the role of cranial and trunk neurocrest. *Journal of Evolutionary Biology*, **27**, 387-448

Smith, M.P., Briggs, D.E.G. & Aldridge, R.J., 1987. A conodont animal from the lower Silurian of Wisconsin, U.S.A., and the apparatus architecture of panderodontid conodonts, in *Palaeobiology of Conodonts*. (Aldridge, R.J., ed), 91-104. Chichester, UK, Ellis Horwood

Somero, G.N., Siebenaller, J.F. & Hochanchka, P.W., 1983. Biochemical and physiological adaptations of deep-sea animals, in, *The Sea*, **8**. (Rowe, G.T., ed.), 331-370. New York: John Wiley.

Soper, N.J., 1988. Timing and geometry of collision, terrane accretion and sinistral strike-slip events in the British Caledonides, in *The Caledonian-Appalachian orogen*. (Harris, A.J. and Fettes, D.J. eds.) *Geological Society, London, Special Publication*, **38**, 481-192.

Soper, N.J., Starchan, R.A., Holdsworth, R.E., Gayer, R.A. & Greiling, R.O., 1992. Sinistral transpression and the Silurian closure of Iapetus. *Journal of the Geological Society*, London **149**, 871-880

Stauffer, C.R., 1935a. Conondonts from the Glenwood Beds, *Bulletin of the Geological Society of America*, **45**, 125-168

Stauffer, C.R., 1935b. The conodont fauna of the Decorah Shale (Ordovician), *Journal of Paleontology*, **9**, 596-620

Stauffer, C.R., 1940. Conodonts from the Devonian and associated clays of Minnesota. *Journal of Paleontology*, **14**, 417-435

Stauffer, C.R., 1940. Conodonts from the Devonian and associated clays of Minnesota, *Journal of Paleontology*, **14**, 417-435

Stockton, W.L. & Delaca, T.L., 1982. Article, In *Deep-sea Research*, **29**, 157-169

Stone, G.L. & Furnish, W.M., 1959. Bighorn conodonts from Wyoming. *Journal of Paleontology*, **33**, 211-228

Stone, G.L. & Furnish, W.M., 1959. Bighorn conodonts from Wyoming. *Journal of Palaeontology*, **33**, 211-228

Størmer, L., 1953. The Middle Ordovician of the Oslo Region. *Norsk Geologisk Tidsskrift,* **31**, 37-141

Størmer, L., 1967. Some aspects of the Caledonian geosyncline and foreland west of the Baltic Shield. *Quarterly Journal of the Geological Society of London*, **123**, 183-214.

Stouge, S. & Rasmussen, J.A., 1995. Upper Ordovician conodonts from Bornholm and possible migration routes in the Palaeotethys ocean. *Bulletin of the. Geological Society of Denmark*, **43**, 54-67

Stowe, K., 1996. *Exploring ocean science* (2nd Edition). John Wiley and Sons, Inc.

Sweet, W. C. & Bergström, S. M., 1974. Provincialism exhibited by Ordovician conodont faunas. *Special Publications of the Society of Economic Paleontology and Mineralogy* **21,** 189-202.

Sweet, W. C. & Bergström, S. M., 1976. Conodont biostratigraphy of the Middle and Upper Ordovician of the United States Midcontinent, in *The Ordovician System.* (Bassett, M. G. ed.) University of Wales Press and National Museum of Wales, Cardiff 121-151.

Sweet, W. C., 1988. *The Conodonta: Morphology, Taxonomy, Paleoecology and Evolutionary History of a Long-Extinct Animal Phylum.* Oxford University Press 212pp.

Sweet, W.C. & Bergström, S.M., 1984. Conodont provinces and biofacies of the Late Ordovician. *Geological Society of America Special Paper* **196,** 69-87.

Sweet, W.C. & Bergström, S.M., 1986. Conodonts and Biostratigraphic correlation. *Ann. Rev. Earth Planet. Sci.,* **14**, 85-112

Sweet, W.C. & Schönlaub, H.P., 1975. Conodonts of the genus *Oulodus* Branson & Mehl 1933. *Geologica et Palaeontologica*, **9**, 41-59

Sweet, W.C. *et al.*, 1975. Studies in Stratigraphy. Part I. Conodont stratigraphy of the Cape Limestone (Maysvillian) of eastern Missouri. Report of Investigations. *Missouri Geological Survey*, **57**, 5-58.

Sweet, W.C., 1979a. Conodonts and conodont biostratigraphy of post-Tyrone Ordovician rocks of the Cincinnati Region. *United States Geological Survey Professional Paper,* **1066-G**, G1-G26

Sweet, W.C., 1979b. Late Ordovician conodonts and biostratigraphy of the Western Midcontinent Province. *Brigham Young University Geology Studies*, **26**, 45-86.

Sweet, W.C., 1981a. Genus *Phragmodus* Branson and Mehl 1933. In, *Catalogue of Conodonts* **IV** (Zielger, W. ed.), Schweizerbart'sche Verlagsbuchanlung, 245-270

Sweet, W.C., 1982. Conodonts from the Winnipeg formation (Middle Ordovician) from the northern Black Hills. *Journal of Paleontology*, **56**, 1029-1049

Sweet, W.C., 1984 Graphic correlation of upper middle and upper Ordovicain rocks, North American Midcontinient Province, USA. In, *Aspects of the Ordovician system 23-25.* (Bruton, D.L. ed.) *Palaeontology contributions from the University of Ohio.*

Sweet, W.C., Ethington, R.L. & Barnes, C.R., 1971. North American Middle and Upper Ordovician conodont faunas. *Geological Society of America Memoirs,* **127**, 163-193

Sweet, W.C., Turco, C.A., Warner, E.Jr. & Wilkie, L.C., 1959. The American Upper Ordovician Standard. I. Eden Conodonts from the Cincinnati Region of Ohio and Kentucky. *Journal of Paleontology*, **33**, 1029-1068

Szaniawski, H. & Bengtson, S., 1993. Origin of Euconodont elements. *J. Paleont.*, **67**(4), 640-654

Szaniawski, H., 1982. Chaetognath grasping spines recognised among Cambrian protoconodonts. *Journal of Paleontology,* **56**, 806-810.

Szaniawski, H., 1987. Preliminary structural comparisons of protoconodont, paraconodont and euconodont elements, in *Palaeobiology of conodonts.* BMS series, Ellis Horwood, Chichester, Aldridge, R.J (ed), 35-47

Temple, J.T. & Cave, R., 1992. Preliminary report on the geochemistry and mineralogy of the Nod Glas and related sediments (Ordovician) of Wales. *Geological Magazine,* **129**, 589-594

Ten Cate, A.R., 1989. *Oral Histology: development structure and function.* The C.V. Mosby Company, St. Louis, 466p

Theil, H., 1989. Phytodetritus on the deep-sea floor in a central ocean region of the northeast Atlantic Ocean. *Biological Oceanogaphy*, **6**, 203-239

Theil, H., 1975. The size structure of deep-sea benthos. *International Revue des Gesamten Hydrobiologie*, **60**, 575-606

Thompson, T.L. & Satterfield, I.R., 1975. Stratigraphy and conodont biostratigraphy of strata contiguous to the Ordovician-Silurian boundary in eastern Missouri, *Rep. Invest. Mo. geol. Surv*, **57**, 67-108

Thorpe, S.A. & White, M., 1988. A deep intermediate nepheloid layer. *Deep-sea Research,* **35**, 1665-1671

Torsvik, T.H., 1998. Palaeozoic palaeogeography: A North Atlantic Viewpoint. *GFF*, **120**, 109-118

Trench, A. & Torsvik, T.H., 1991. A revised Palaeozoic apparent polar wander path for Baltica: Palaeomagnetic data from the Silurian Limestones of Gotland, Sweden, *Geophysical Journal International*, **104**, 373-379

Trench, A. & Torsvik, T.H., 1995. The closure of the Iapetus Ocean and Tornquist Sea: new palaeomagnetic constraints. *Journal of the Geological Society London*, **149**, 867-870

Tucker, R.D., Krogh, T.E., Ross, R.J. JR. & Williams, S.H., 1996. Time-scale calibration by high precision U-Pb zircon dating of interstratified volcanic ashes in the Ordovician and Lower Silurian stratotypes of Britain. *Earth and Planetary Science letters*, **1000**, 51-58

Tyler, P.A. & Gage, J.D., 1979. In, Cyclic phenomena in marine plants and Animals. *Proc. 13th Europ. Mar. Biol. Symp.* Naylor, E. & Hartnoll, R.G (eds) Pergamon Press, Oxford, 215-222

Tyler, P.A., 1988. Seasonality in the deep-sea. *Oceanography and Marine Biology: an Annual Review*, **26**, 227-258

Tyler, P.A., 1995. Conditions for the existence of life at the deep-sea floor: an update. *Oceanography and Marine Biology: an Annual Review*, **33**, 221-244

Van-Praet, M., 1983. Nutrition of sea anemones. In, *Proceedings of the 17th European Marine Biology Symposium., Oceanologia. Acta Special Volume*, 197-200.

Viira, V., 1974. Ordovician conodonts of the Baltic region, Tallin, USSR ("Valgus"). 142pp

Wilde, P. & Berry, B.N., 1984. Destabilization of the oceanic density structure and its significance to marine "extintion" events. *Palaeogeography, Palaeoclimatology and Palaeoecology*, **48**, 143 – 162

Wilde, P., Berry, W. B. N., 1978. Progressive ventilation of the oceans - an explanation for the distribution of the Lower Paleozoic black shales. *American Journal of Science* **278**, 257-275.

Williams, A., Strachan, I., Bassett, D.A., Dean, W.T., Ingham, J.K. Wright, A.D. & Whittington, H.B., 1972. A correlation of Ordovician rocks in the British Isles. *Geological Society of London Special Report*, **3**, 1-74

Williams, S.H. & Bruton, D.L., 1983. The Caradoc-Ashgill boundary in the central Oslo region and associated graptolite faunas. *Norsk Geologisk Tidsskrift*, **2:3**, 147-191

Wilson, G.D.F. & Hessler, R.R., 1987. Deep sea Speciation. In, *Annual review of Ecology and systematics*, **18**, 185-207

Witzke, B.J. & Kolata, D.R., 1988. Changing structural and depositional patterns, Ordovician Champlainian and Cincinnatian Series of Iowa-Illinois, in *New perspectives on the Palaeozoic history of the upper Mississippi Valley*. (Ludvigson, G.A. and Bunker, B.J., eds.), *Iowa Department of Natural Resources, Geological Survey Bureau, Guidebook*, **8**, 1-77.

Woodcock, N.H. & Gibbons, W., 1988. Is the Welsh Borderland Fault System a terrane boundary? *Journal of the Geological Society of London*, **145**, 915-923.

Woodcock, N.H., 1990. Sequence stratigraphy of the Palaeozoic Welsh Basin. *Journal of the Geological Society of London*, **147**, 537-547

Worsley, D., Aarhus, N., Bassett, M.G., Howe, M.P.A., Mørk, A. & Olausson, S., 1983. The Silurian succession of the Oslo region, *Nord. Geol. Unders. Bull.*, **384**, 1-57

Wright, J., Conca, J.L., Repetski, J.E. & Clark, J., 1990. Microgeochemistry of some Lower Ordovician Cordylodans from Jilin, China. *Courier Forschungsinstitut Senckenberg*, **118**, 307-332

Wright, P.J., Mosegaard, H., Morales-Nin, B. & Geffen, A., 1997. The regulation of otolith formation and its significance to age determination, size back-calculation and elemental composition. Proceedings of a workshop, ORSTROM, France, *European Fish Ageing Network* (EFAN), **1-98**, 4-21

Wright, P.J., Rowe, D. & Thorpe, J.E., 1991. Otolith calcification in Atlantic Salmon parr, *Salmosalar L.* and its relation to photoperiod and calcium metabolism. *Journal of Fish Biology*, **40**, 779-790.

Young, C.M & Tyler, P.A., 1993. Embryos of the deep-sea echinoid *Echinus affinis* require high pressure for development. *Limnology and Oceanography*, **38**, 178-181.

Zalasiewicz, J.A., Rushton, A.W.O. & Owen, A.W., 1995. Late Caradoc graptolitic faunal gradients across the Iapetus ocean. *Geological Magazine* **132**, 611-617

Zezina, O.N., 1975. On some deep-sea Brachiopods from the Gay Head – Bermuda transect. *Deep-sea Research* **22**, 903-12

Zhang, S., Aldridge, R.J. & Donoghue, P.C.J., 1997. An Early Triassic conodont with periodic growth? *Journal of Micropalaeontology*, **16**, 65-72

Appendix 2A

A glossary of terms used in (Part II) Chapter 3 is provided below (adapted from Huysseune and Sire, 1998, Table 1. p. 439).

Odontode – An isolated, hard, superficial structure of the skin. The composition and growth of odontodes is discussed in the main body of the text.

Odontocomplex – a cluster or agglomeration of odontodes forming directly upon, or beside, one another during successive stages of growth.

Odontode derivatives – tissues which are derived from tissues of the ancestral odontocomplexes (ganoine or dentine) but have been modified during evolution in such a way that their homology is difficult to infer.

Placoid Scales – small dermal denticles (odontodes) in the skin of chondrichthyans (e.g. sharks). They have an enameloid layer surrounding a dentine crown and pulpar cavity. They form like teeth and are replaced when shed.

Scales – mineralised elements which form in the upper part of the dermis (excludes epidermal scales of bird and reptiles). Scales show polymorphism for example, placoid scales (chondrichthyans) are small tooth shaped units and elasmoid scales (teleosts) are thin lamellar plates.

Elasmoid Scales – thin, lamellar, imbricated plates with a thick, partially mineralised lamellar basal layer (elasmodin) covered by a thin, well mineralised ornamented external layer which is generally covered itself by an outer limiting layer in regions close to the epidermis.

Keratinous toothlets – ectodermal structure resembling teeth but made up of keratin, such as found in the buccal cavity of extant agnathans.